NTNU – Trondheim
Norwegian University of
Science and Technology

Modeling and Simulation of Transient Performance and Emission of Diesel Engine

Pseudo Bond Graph Approach to Modelling
the Thermodynamic Process

Kevin Koosup Yum

Marine Technology
Submission date: November 2012
Supervisor: Eilif Pedersen, IMT

Norwegian University of Science and Technology
Department of Marine Technology

Abstract

Internal combustion engines have been very successful as power producers in the marine applicaiton due to their simplicity of construction, high efficiency and long track of proven technology. However, as the environmental foot print of industry is gaining more and more attention, the emission from the engine must be reduced. The main emission from the diesel engines are namely nitrogen oxide(NO_x) and particulate matter(PM). Sulfur oxide(SO_x) and carbon dioxide emission(CO_2). In the marine industry, the transient emission has not been brought to the table of discussion when it comes down to the regulations. However, the assessment and improvement in the transient emission will gain more attention.

In order to predict the emission from the diesel engine in the generic manner, the dynamic engine model should be developed. This model must be able to capture the in-cylinder process during the combustion in cylcle-to-cycle resolution. Transient load would put more challenges to the prediction as the in-cylinder states are far from the steady-state conditions. In the thesis, the dynamic simulation model of the diesel engine is developed in order to predict the emission. Firstly, the emission from the diesel engine, with special focus on NO_x formation, is reviewed in general. Then overall process of the development of the mathmatical model of the diesel engine is described. Bond graph model was used as the framework of modeling approach. Finally the simulation result is compared with the test result from the laboratory and recommendations for further development are presented.

The main contributions of the thesis are:

- A overall process of building the engine model of was reviewed and implemented. It covers most of the building blocks from the thermodynamic calculation to the calculation of states of the components of the diesel engine.
- The model developed in the project has significant improvement in terms of computational efficiency. Implementing Grill's method for the calculation of the equilibrium composition of the combustion gas was the key to this success.
- The bond graph model based on the multi-component gases in the combustion gases was constructed and it founded a ground for adaptation of the emission reduction strategy such as exhaust gas recirculation.
- The overall model was built with component libraries which can be reused in the future project. Full description of the components libraries is given so that potential users may have the easy access.
- A mathmatical model for NO_x is coupled with the dynamic engine model together with the two-zone model approach. The calculation of the two-zone model in the absence of the pressure profile was achieved with an effective method so that calculation time has not increased significantly from the single zone model.

Acknowledgements

The work has been done as a part of the master program in the Department of Marine Technology, NTNU. This work has been carried out under the supervision of Associate Professor Eilif Pedersen. The greatest thanks to God who led me to Norway and helped in everyday in every way. Also the same magnitude of thanks is given to my wife, Suhyun, who patiently accepted my decision to come to Norway. Also to my children, Seonah and Seongyu, who have given the unlimited support and affection. Also great thanks to Eilif Pedersen, my supervisor, for timely and helpful guidance and also for giving me the opportunity to continue my study at NTNU.

Contents

List of Tables

List of Figures

Nomenclature

NO_x	Nitrogen oxides
PM	Particulate Matter
SO_x	Sulfur oxides
p	Pressuer
T	Temperature
$\mathbf{x}$	A vector column containing the mole fractions of the gas species
m	Mass
m_f	Mass of fuel
N	A vector column containing the number of moles of the gas species
U	Internal energy
V	Volume
F	Fuel-air equivalent ratio
f_s	Stoichiometic fuel-air ratio
R	Gas constant of a specific gas
R_0	Universal gas constant
M	Molecular weight of the gas specie
u	Specific Internal energy
h	Specific enthalpy
s	Specific entropy
g	Specific Gibbs free energy
C_p	Specific heat capacity at constant pressure
C_v	Specific heat capacity at constant volume
W	Work done by the control volume
u	Specific Internal energy
$BMEP$	Brake mean effective pressure
$BSFC$	Brake specific fuel consumption
P_e	Brake power
φ	Crank angle in degree
RPM	Revolution per minute
ω	Engine speed in radian per second
Tq	Torque
$\dot{x}$	Flow of variable x

IMO	International Maritime Organization
ISO	International Organization for Standardization
LHV	Lower heating value
MGO	Marine gas oil
NIST	National Institute of Standards and Technology
NASA	National Aeronautics and Space Administration
JANAF	Joint Army, Navy, Air Force
ROHR	Rate of heat release

Chapter 1

Introduction

1.1 Background

Internal combustion engine has been very successful as a power producer in wide range of application. The primary benefits of the diesels engines are their simplicity of construction, high efficiency and long track of proven technology and reliability. However, as the environmental foot print of industry is gaining more and more attention, these engines have a big huddle to overcome to prolong its existence, the gas pollution from its process. Special attention is given to the diesel engines, since they are used in the area where larger power unit is required such as power plants and marine application. The main emission from the diesel engines are namely nitrogen oxide(NO_{x}) and particulate matter(PM). Sulfur oxide(SO_{x}) and carbon dioxide emission is more closely related to the type and quality of the fuel.

The marine industry has always favored using diesel engines for its benefits mentioned. Recently strong regulation has entered into force in attempt to reduce the emission of NO_{x} and SO_{x} by IMO. However, the regulation is still revolving around the benefits of the players in the industry and is lagging behind other industries. Especially, emission from transient load conditions are not yet on the table of discussion yet but it is obvious to predict that it is the matter of time in a relatively short term that more strict legislation will come into force to parallelize with other industries.

In this project, the special interest is given to the gas emission from the diesel in marine application. The object is to overview the characteristics of the operation of marine application and gas emission from it, to present the mathmatical model to simulate the performance and emission from the engine in connection with the process of the power production in the engine.

1.2 Operation and Load Characteristics

Steady state performance of the engines has been well verified and improved by the various test programs from the industry and theoretical studies. However, transient load and the emission from it is still in question when it comes to optimization of the design. Transient operation is defined as change of load of the engine from one to the other in a manner that the performance and the emission formation characteristics significantly deviate from the steady state ones. The challenge of the transient load from the diesel engines are the rotational inertia of the turbocharger which is the property responsible for the so called turbo-lag when the power demand is increased. When more power is demanded from the engine, the turbine and compressor needs time accelerate its rotational speed and air flow to match the demand.[27]

The challenge extends more in diesel engine which should operate in air excess condition. When power demand is increased due to environmental variation, air excess will suffer from injecting more fuel to meet the demand. The engine is running at minimum air access as far as the combustion can allow. In time, the fuel-air ratio will reach its desirable point as the turbocharging system catches up the change of operating point but during this transition higher formation of soot and NO_{x} is expected.

In marine operation, the situation is more complex. The operation and load characteristics differ widely depending on the type of the operation and the configuration of power plants. Most international freights will spend most of its time in steady state regime when vessel is in a voyage at constant speed over long time. Port operation or lightering service may cause a certain degree of the transient load situation but the interest in such operation is low at the moment. Coast liners and short-voyage supply vessel will have greater extent of transient operation.

Among various operation modes, dynamic positioning(DP) will be the key interest with regard to the transient load. In DP vessels, the power plants are normally configured with multiple prime movers. However, it is quite common to operate each unit or groups of the units separately which may cause a higher degree of inefficiency and transient load for the engine. In this regards, transient emission and performance is gaining greater interest in this type of operation.

1.3 Challenges of Transient Emission

In order to design the engine optimized for the transient emission, there exists several challenges doing so. Firstly, it is much more complicated to determine the operational input to the design. In the steady state operation, mostly only speed and load are main parameters as design inputs. However, the transient load is inherently dynamic system where not only the speed and load matter but also the time and related states from the previous engine cycle have major influence on the performance. In this regards, systematic

testing of the engine can be extremely time consuming due to the very high number of combinations of conditions and control settings.[27]

Another challenge is the measurement techniques in transient operation. Generally, very fast response is required for the measurement to be valid. High accuracy is also demanded at the same time. Meeting those two contracting characteristics, the sensors may not exist or highly uneconomical.

Also transient phenomena inherently requires higher level of complication in the mathmatical modeling. One may have to have full predictive model including three dimensional fluid motion model in the cylinder together with detailed spray formation model. Empirical formulation used for the steady state regimes may not be valid any more in the transient regime.

In this regards, there are great potential for proper modeling of the transient operation which can be universally used for study and verification of the engines. It will save tremendous time and brings a greater understanding of the physical process of the engine.

1.4 Thesis

1.4.1 Objectives and Scope of Work

In this thesis, the special interest is given to the gas emission from the diesel and gas engines in transient operation. The object is to overview the characteristics of the operation of marine application and gas emission from it, to present the mathematical model to predict the emission from the engine in connection with the process of the power production in the engine. The scope of work will include :

1. Review the current and upcoming emission legislation for diesel engines with special focus on transient operation,
2. Perform a literature review on the state-of-art emission models used for emission predictions in transient mode,
3. Review the engine system models available at the Department of Marine Technology, NTNU, and bring possible improvements to a more general and complete level,
4. Perform the measurement of performance and emission from the available engine and compare it with the simulation result.

1.4.2 Thesis structure

The thesis consists of six chapters including introduction. In the chapter 2, the emission from the diesel is discussed in regard to the identification of main emission, rules and

regulations for marine engines and its mechanism. In particular the chapter gives more attention to the mechanism of formation of NO_x and its prediction model. In the chapter 3, mathmatical model of the diesel engine and is introduced and explained. It covers description of the state of the art and the methods implemented in the thesis. In the chapter 4, the prediction model for NO_x is presented in a couple with combustion model of the engine. It presents the multi-zone approach and validation of it. In the chapter 5, it discusses the engine test performed in the laboratory and the results are compared to the simulations output from the mathmatical model. The last chapter is the conclusion where the thesis is summarized and area of further research is addressed.

Chapter 2

Emission from the Engine

2.1 Introduction

Gas emission from the combustion process of the engines is inevitable byproducts. The main concerned emission from the engines are carbon dioxides(CO_2), nitrogen oxides(NO_x), sulfur oxide(SO_x)volatile organic compounds(VOC) and particulate matter(PM). The adverse effect of gas emission from combustion is schematically shown in the figure 2.1[3].

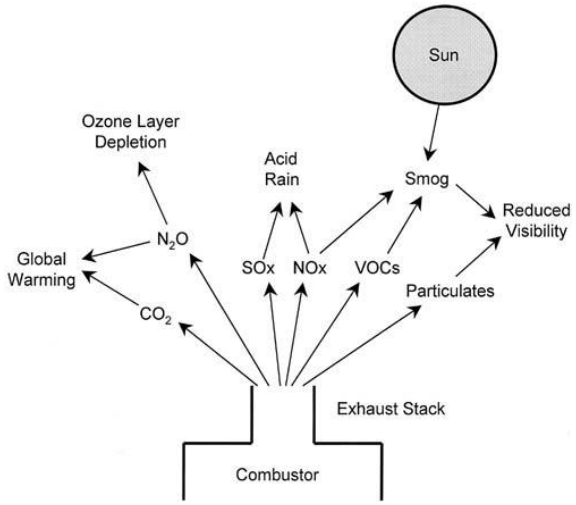

Figure 2.1: Diagram of atmospheric pollution

After being aware of the negative effect of the emission on human health, ecological system and global warming, the trend of technological development of the has shifted to environmental friendly performance of the engine.

In this chapter, the main emission from the diesel or gas engine in aspects of their adversary effect, formation mechanism and the possible model for simulation will be reviewed

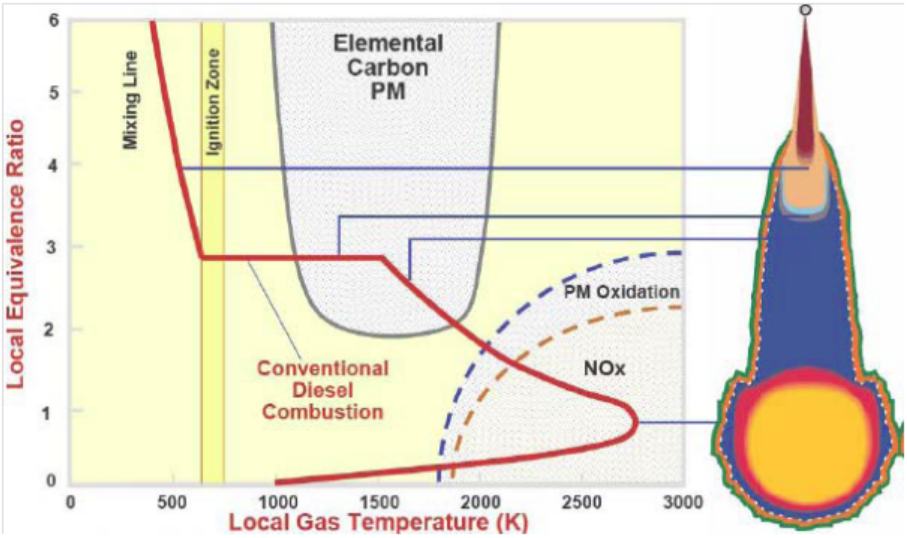

Figure 2.2: Typical mixing line and emission formation in the F-T plane

and discussed. In particular, NO_x and PM are the prime interest for the diesel engine.

2.2 Emission from the diesel engine

The diesel engine is widely used in the marine application due to high power density, efficiency, reliability and maturity in technology. However, in order for the diesel engine to prosper for the future, emission control from the engine must be improved. Due to its heterogeneous combustion characteristics, high emission of NO_x and particulate is inevitable. The engine development in the past has been focused on the power output and the efficiency. Improvement of efficiency in general can reduce the emission due to reduction of fuel consumption. However, it has a certain degree of adversary effect on the emission also.

In general, NO_x and particulate emission is closely related to the fuel-air ratio(F) and the temperature of the combustion. In the diesel engine where the fuel is injected after compression and the combustion locally takes place with high F value and accordingly high temperature , it is inevitable to avoid the formation of a relatively larger amount NO_x and particulate in form of soot. According to the investigation of the flame structure by laser-sheet imaging, the combustion of the diesel engine is conceptually modeled to explain this physical phenomenum.[9]. A common representation for emission formation is F-T plot which show under what conditions soot and NO_x are formed. The figure 2.2 shows an example together with Dec's model[27].

It shows the area where the F-T coordinate favors the formation of emission. The red line is called mixing line which shows the typical F-T coordinates of the gas mixture in the flame during the diesel combustion. As shown, the mixing line both trespasses both areas

Tier	Tier	NO_x limit, g/kWh		
		n < 130	130 $\leq$ n < 2000	n $\geq$ 2000
Tier I	2000	17.0	$45 \cdot n^{-0.2}$	9.8
Tier II	2011	14.4	$44 \cdot n^{-0.23}$	7.7
Tier III	2016	3.4	$9 \cdot n^{-0.2}$	1.96

Table 2.1: MARPOL Annex VI NOx Emission Limits

of PM and NO_x formation. This F-T diagram also suggests that which strategy to take for reduction of certain emission. For example, lowering the temperature of flame would reduce the formation of NO_x but also it would reduce the oxidation of PM increasing the total amount of PM to be increased. Therefore, one should be able to achieve the leaner mixture together with reduced temperature in order to achieve both emissions to be reduced.

2.3 Legislations for Emission in Marine Engines

Marine transportation is considered to be the most environmental friendly when the specific pollutant per ton-mile is concerned. In this regards, the regulation on the emission in the marine application has lagged behind others. Especially, the transient emission has not been brought on the table up to this date. This may be rationalized by the fact that there exists a great number of variations in the characteristics of operation of the vessel. Many commercial vessels engaged in the international transportation spend most of time under a steady load. Coast liners or DP operation vessels will be more characterized by the transient load. Therefore, it would be quite difficult to apply a unified regulation to those having different operating characteristics.

The current regulation with regard to the NO_x emission and particulate matter emission is established by IMO. The regulation is underlined in MARPOL Annex 73/78 Annex VI which calls for NO_x emission reduction of 20% by 2010 and 80% by 2016 and limits the sulfur content of the fuel. The requirement of regulation is shown in the figure 2.3 and the table 2.1 [10].

It should be noted that the Tier III criteria is only required in the emission control areas(ECA) including Baltic Sea, North Sea, North America ECA including most of US and Canadian coast and US Caribbean ECA including Puerto Rico and the US Virgin Islands.

For the verification of compliance with the regulation, the engine is tested on the standard condition. It would be not feasible to test the emission level directly from the vessel in

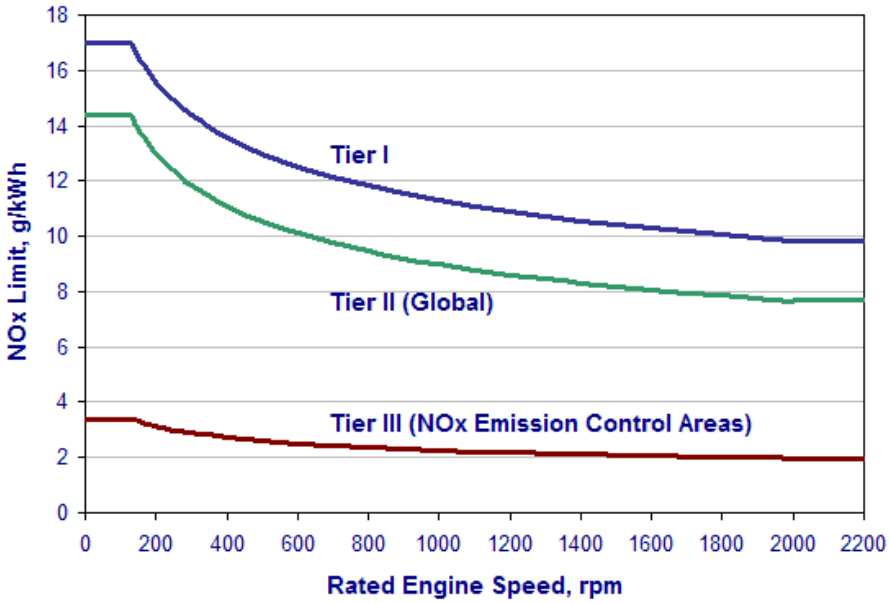

Figure 2.3: MARPOL Annex VI NOx Emission Limits

operation because of the cost and duration. The engines are tested according to ISO 8178. The ISO 8178 is an international standard designed for a number of non-road engine applications[10]. The ISO 8178 is actually a collection of many steady-state test cycles (type C1, C2, D1, etc.) designed for different classes of engines and equipment. Each of these cycles represents a sequence of several steady-state modes with different weighting factors. Therefore, it can not truly represent the emission in the transient load. Depending the application of the engine, the test cycle would be differently applied as following[16].

1. Constant speed marine diesel engines for ship main propulsion (electric propulsion, controllable pitch propeller) : E2

2. Propeller law operated main and propeller law operated auxiliary engines : E3

3. Constant speed auxiliary engines : D2

4. Variable-speed, variable-load auxiliary engine : C1

The table 2.2 shows the operating modes and the weighting factors for the relevant cycle[10].

For the particulate matter, there is no international regulation as of today. In some countries, smoke from the ship is regulated. However, the IMO regulation on the sulfur content in the fuel will reduce the particulate emission by a small degree since the sulfate formed after combustion from the sulfur in the fuel constituents a small fraction of particulates.

Mode number	1	2	3	4	5	6	7	8	9
Torque (%)	100	75	50	25	10	100	75	50	0
Speed	Rated					Intermediate			idle
C1	0.15	0.15	0.15	-	0.1	0.1	0.1	0.1	0.15
D2	0.05	0.25	0.30	0.30	0.10	-	-	-	-
E2	0.20	0.50	0.15	0.15	-	-	-	-	-
Propeller law operated engines									
E3 - Speed (%)	100	91	80	63	-	-	-	-	-
E3 - Factor	0.20	0.50	0.15	0.15	-	-	-	-	-

Table 2.2: Test Cycle with Weighting Factors

2.4 NO_x Emission

NO_x generally include nitrogen monoxide or nitric oxide (NO) and nitrogen dioxide (NO_2). In the broader term, nitrous oxide (N_2O), known as laughing gas, and as well as other less common combinations of nitrogen and oxygen such as nitrogen tetroxide (N_2O_4) and nitrogen pentoxide (N_2O_5) can be included in this category[3]. In the thesis, it will be focused on the first two compounds which are dominantly emitted from marine internal combustion engines.

NO_x emission is a primary concerned emission especially for the diesel combustion process which leads to the fact that it is the main emission from shipping since the diesel engines are most widely used in this industry. NO_x Emissions from shipping represent about 15% of global anthropogenic NOx emissions and around 40% of global NOx emissions from transport of freight.[13]

2.4.1 Source of nitrogen

The primary source of nitrogen which is key ingredient for the formation of NO_x during the combustion process of marine engines are:

1. Oxidizer : Air which is the most common oxidizer for the internal combustion engine contains 79 vol% of nitrogen as inert gas.

2. Fuel : Certain fuels classified as dirty product contains a certain amount of nitrogen atom chemically bound to the molecules. Heavy fuel oil contains a significant amount of nitrogen. The typical average nitrogen content is distillate fuels are 1.4 wt% for heavy distillates and 2.3 wt% for asphaltenes.[4] For the heavy fuel oil, the value would lie between these two distillates. Cleaner fuel such as light oils and natural gas may contain some content but often in a very small constituent.

2.4.2 Formation mechanism

The formation of NO_x in the marine engines can be described by three different mechanisms:

1. Thermal NO_x : The formation occurs by the high temperature reaction between N_2 and O_2 according to the Zeldovich mechanism. The process is highly dependent on the temperature
2. Prompt NO_x : The formation occurs at relatively low temperature when the reaction occurs between N_2, O_2 and hydrocarbon radicals produced during combustion process. The name describes the nature of the reaction rate. It is of less importance in the combustion in marine engines dominated by high temperature. It may become more significant in case of fuel rich condition at low load where concentration of hydrocarbon increases at lower temperature.
3. Fuel NO_x : The formation occurs when the nitrogen chemically bound to the fuel molecule reacts with the oxygen in the air. Where heavy fuel oil is used for main fuel, this mechanism may contribute a significant amount in total formation according to the content of nitrogen in the fuel.

In this thesis, only thermal NO_x will be considered for developing an emission model since it consists vast majority of total NO_x produced from the marine engines and for it well-defined models. This assumption is valid as long as the exhaust gas recirculation rate is moderate [28].

For the thermal NO_x, it is assumed that NO is the predominant oxide of nitrogen in the engine cylinder [15]. Zeldovich model which describes the reaction of formation of NO can be used to describe the process of formation of NO_x. This is widely used model for prediction of NO_x. There are three chemical reactions in the model given as:

$$\begin{aligned} O + N_2 &\leftrightarrow NO + N \\ N + O_2 &\leftrightarrow NO + O \\ N + OH &\leftrightarrow NO + H \end{aligned} \tag{2.1}$$

Based on the equation 2.1, the rate of formation of NO can be written as:

$$\begin{aligned} \frac{d[NO]}{dt} =& k_1^+ [O][N_2] + k_2^+ [N][O_2] + k_3^+ [N][OH] \\ & - k_1^- [NO][N] + k_2^- [NO][O] - k_3^- [NO][H] \end{aligned} \tag{2.2}$$

where,

$[\,]$: Species concentration in moles per cm^3
k_i^+: Forward rate constant of the reaction
k_i^-: Reverse rate constant of the reaction

Reaction	Rate constant ($cm^3/mol \cdot s$)	Temperature range (K)
(1) $O + N_2 \rightarrow NO + N$	$7.6 \times 10^{13} \exp[-38000/T]$	2000-5000
(-1) $N + NO \rightarrow N_2 + O$	1.6×10^{13}	300-5000
(2) $N + O_2 \rightarrow NO + O$	$6.4 \times 10^{9} T \exp[-3150/T]$	300-3000
(-2) $O + NO \rightarrow O_2 + N$	$1.5 \times 10^{9} T \exp[-19500/T]$	1000-3000
(3) $N + OH \rightarrow NO + H$	4.1×10^{13}	300-2500
(-3) $H + NO \rightarrow OH + N$	$2.0 \times 10^{13} \exp[-23500/T]$	2200-4500

Table 2.3: Rate constant for NO formation mechanism

The rate constants are given as in the table 2.3.

In the internal combustion engine, the combustion occurs at high pressure so the flame reaction zone is extremely thin (about 0.1mm) and, therefore, the residence time in the zone is very short. Also as the burned gas is compressed during the early stage of combustion, the temperature rises further. Therefore, the NO formation in the burned gas zone is predominant to one from the flame front zone. This fact enables to assume that the combustion and NO formation processes are decouples and to assume the concentration of the species concerned to be their equilibrium value at the corresponding pressure and temperature[15]. By this assumption, the equation 2.2 can be simplified to

$$\frac{d[NO]}{dt} = \frac{2R_1 \left\{1 - \left([NO] / [NO]_e\right)^2\right\}}{1 + \left([NO] [NO]_e\right) R_1 / \left(R_2 + R_3\right)} \tag{2.3}$$

where

$R_1 = k_1^+ [O]_e [N_2]_e = k_1^- [NO]_e [N]_e$
$R_2 = k_2^+ [N]_e [O_2]_e = k_2^- [NO]_e [O]_e$
$R_3 = k_3^+ [N]_e [OH2]_e = k_3^- [NO]_e [H]_e$

[ ]: Species equilibrium concentration for the one-way equilibrium rate for reaction 2.1

2.4.3 Factors affecting the formation

The rate of formation has a very strong dependency on the temperature in the exponential term. Therefore, the temperature is the key driver of the concentration of NO. As the rate constant increases exponentially with temperature, more NO is expected to be produced at higher temperature. Together with the rate of formation, the resident time in the corresponding temperature affect the total amount. Finally the concentration of the species has a direct influence on the rate of formation.

There are several factors affecting NO_x formation. The first one to mention is the oxygen content of oxidizer. As the oxygen content in the oxidizer increases, it increases the flame temperature due to higher reaction rate and also reduced mass of air required. Therefore,

NO formation rate will increase. Reduced concentration of N_2 in the oxidizer will result in reduction in the formation rate. Since the temperature increase has much higher dominant effect, the amount of NO production will increase when the oxygen content enlarged from the standard air. However, as it replaces most of the nitrogen, the temperature will saturate and the nitrogen content plays a more important role from a certain point. Thus, the amount of NO formed will decrease beyond this point. In contrast, reduction of oxygen content would decrease the flame temperature as well as the concentration of the oxygen for NO mechanism. Therefore, the amount of NO will decrease.

Besides, the specific heat capacity of the oxidizer has a great influence on the cylinder temperature. Reduced temperature in the cylinder is expected when the oxidizer has a larger value of the specific heat capacity. The specific heat capacity can be controlled by water content in the oxidizer or fuel and amount of exhaust gas recycled.

Air-fuel equivalent ratio has also direct influence on the cylinder temperature in case of homogeneous charge combustion. Increased air-fuel equivalent ratio will result in the reduced cylinder temperature as the there will be more gas to be heated for the same amount of heat released. Therefore, lean burn spark ignition engine can result in relatively low NO emission. In addition, fuel quality or composition may affect the formation of NO due to its affect on the flame temperature or nitrogen content it itself.

2.5 PM Emission

The negative effect of the diesel engine combustion process is that it produces highly carbonaceous material known as soot or, in more general term, particulate matter(PM). There are two types of PM emission from the diesel engine. The first one which constitutes the majority of the emission is known as soot. The other one is nuclei mode particles which consist mainly of condensed hydrocarbon and sulphates. In this project, the focus will be put on the soot. Diesel engines are high emitters of particulate emissions: about 0.2-0.5% of the fuel mass is emitted as small particulates[15].

2.5.1 Adverse effect of PM emission

The finer particles formed during combustion will be suspended in ambient air. They are responsible for increased respiratory disease. They are believed to have adverse effects, both short term and long-term, on human health. In earlier times, it was believed that PM10 of particle diameter less than 10 μm has an close association with chronic lung disease, lung cancer, influenza, asthma, and increases in daily mortality. Recent researches suggest that these correlations are more closely associated with finer particulates such as PM2.5 of diameter less than 2.5 μm and ultra-fine particulates PM0.1, because the fine and ultra-fine particulates can easily penetrate deep into the lungs[31].

Element	C	H	N	O	S
Virgin soot	83.5	1.04	0.24	10.5	1.13
De-gassed soot	83.8	0.85	0.22	10.7	0.10

Table 2.4: Elemental composition of diesel soot particulates

Furthermore, the soot has a significant effect on the global warming depending on the size, concentration, and optical properties of carbonaceous soot aerosols in the atmosphere. Soot has a direct warming effect on the climate by absorbing solar radiation in the atmosphere and converting it to heat radiation. Also reduced reflection on the snow and ice by deposition of soot in arctic region contributes to the global warming. In addition, the deposited soot on ice may cause the ice to melt causing the sea level to rise[13].

In addition, the soot formations in diesel engines can also have influence on engine performance and have feedback effects on in-cylinder combustion and other emission formation processes. The radiation heat transfer from soot to in-cylinder engine walls account for a significant portion of the heat loss in a diesel engine, and a lowering of flame temperature by radiation heat transfer from soot, which will in turn affect NOx formation[31].

2.5.2 Characteristics of Soot

Composition of soot

The composition of typical diesel soot is composed of carbon, hydrogen, nitrogen, oxygen and sulfur. The composition of it is shown is the table 2.4. Where carbon, hydrogen, nitrogen and oxygen are strongly bonded together, sulfur is present as compounds absorbed onto the surface. Other element such as zinc, phosphorus, calcium, iron, silicon and chromium are also present as minor compound.

Structure of Soot

The soot is referred as necklace-like agglomerates in terms of its structure. These agglomerates can be broken down into smaller, basic partide units that are normally in form of a near sphere called spherules. The size of the spherules in diameter is distributed in the range of 10 to 90 μm, but most lies between 15-50 mum.(Walker 1966) The surface of the spherules are consisted of adhering hydrocarbon and inorganic material which is mainly sulfate. These spherules are called p̈rimary soot particlesẅhere as the agglomerates are called s̈econdary soot particles.ẅhich are made of several tens or hundreds of primary soot particles. The figure 2.4 shows the microscopic view of th partides containing the agglomerates of spherules.

The even finer resolution of the figure by transmission electron microscopy suggests that the spherules are composed of laminations with surface steps which are again made of a number of concentric crystallites. The basic unit of the crystallites is called platelet which is a hexagonal face-centered arrays of the carbon atoms. The mean space between

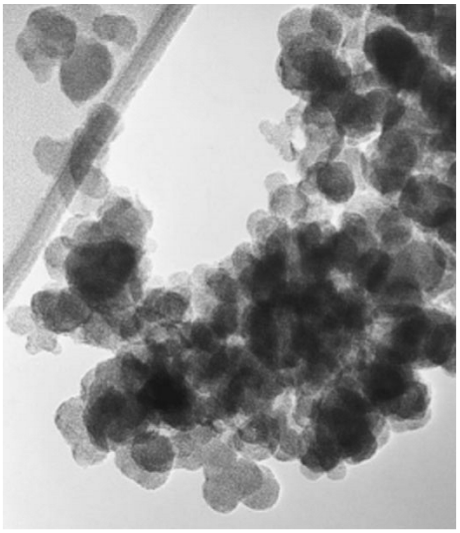

Figure 2.4: Micrograph of diesel soot

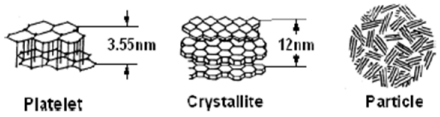

Figure 2.5: TEM view of the soot

the platelets is approximately 3.55 nm. The thickness of the crystallites is about 12 nm and one spherules normally contains about 100 crystallites. The figure 2.5 presents the graphical view of the units of the structure.

Also the finer resolution TEM image shows that the two distinct parts are identified in the spherules: an outer shell and inner core as shown in the figure 2.7.

The platelet model mentioned above applies to the outer shell. In contrast, the inner core contains fine partides with a spherical nucleus surrounded by carbon networks. It indicates that the outer part of the spherule is rigid structure while the inner core is chemically and structurally less stable.

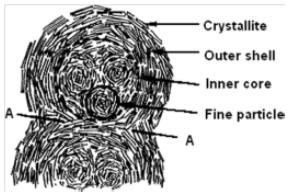

Figure 2.6: TEM view of the particle with finer resolution

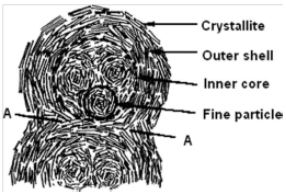

Figure 2.7: TEM view of the particle with finer resolution

2.5.3 Formation of Soot

Soot is produced during the high temperature pyrolysis which means combustion in lack of oxidation agent or combustion of hydrocarbons, which is mostly carbon. Other elements such as hydrogen and oxygen are usually present in small amounts. A soluble organic fraction (SOF) is frequently found in the soot whose constituents include aromatic compounds as well as various other unburned hydrocarbons. The formed soot is also oxidated at high temperature in the burned zone of the cylinder and exhaust gas. The net emission of the soot is determined by the competition between soot formation and oxidation[31].

Observing the structure of the soot, it can be inferred that the formation of the soot deals various processes which are chemically and physically different to others. They are represented by steps such as formation and growth of large aromatic hydrocarbons and their transition to particles, the coagulation of primary particles to larger aggregates, and the growth of solid particles by adhering growth components from the gas phase.

During the combustion, the hydrocarbon fuel is degraded into small hydrocarbon radicals. The radicals are added together and it forms aromatic rings when the size of the radical hydrocarbon reaches a certain point. The formation of the aromatic rings occur by the addition of acetylene(C_2H_2) within the molecular length scale. This is shown in the figure 2.7

The formed aromatic structure quickly coagulate and contribute the growth of the partide simultaneously picking up molecules from the gas phase for the surface growth. The surface growth directly contributes to determining the concentration of PM in the emission while coagulation determines the distribution of the size of PM. The details of the each process remains the challenges for the researchers but the general features of them are in considerable agreement. They can be summarized as following[31].

1. Formation of molecular precursors of soot
2. Nucleation or inception of particles from heavy polycyclic aromatic hydrocarbon(PAH) molecules
3. Mass growth of particles by addition of gas phase molecules
4. Coagulation via reactive particle-particle collision
5. Carbonization of particulate material

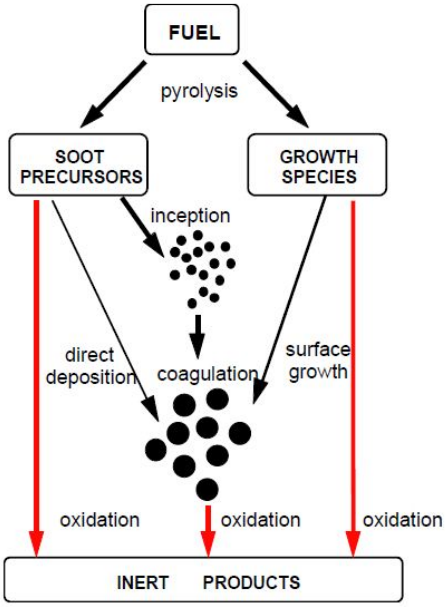

Figure 2.8: Mechanism of soot formation

6. Oxidation of PAHs and soot particles.

The process occur in stages with certain overlap and the detail will be discussed in the following sections. The figure 2.8 shows the schematic mechanism of the formation.

Chapter 3

Modeling of the Power Cycle of the Engine and the Connected Systems

3.1 Goal and the scope of the modeling

Before starting modeling of any physical system, it is important to define the goal and the scope of the model so that the characteristics of the system is well captured without sacrificing too much of the performance of the model in terms of fidelity and the speed of the calculation.

3.1.1 Objectives of the simulation model

The objectives of the model is stated as following:

1. To provide the performance and the emission prediction with reasonable accuracy under the transient load.
2. To be used for the design of the control system and/or used as the control plant in the designated controller.
3. To be used as a general template for modeling other type of engine from different manufacturers

The first objective sets the main use of the model whereas the second puts limitation in terms of calculation time. It should have reasonable fidelity with at least real time simulation. The best way to achieve the two goal will be to build a look-up table or empirical relationship between the inputs and outputs of interest through an extensive engine test. However, this would contradict the third goal that it is hardly transferable even if a single important component is replaced by a different type or even by one from a different maker. This would harm the benefit of the model in terms of generic adaptation. Therefore, the model should include the physical process as much as possible also. At

least, the in-cylinder physical process and the gas dynamics should be modeled so that the outputs are given in cycle-to-cycle resolution. The most crucial part of the model affecting this generality is the combustion process in the cylinder and the air and exhaust system with turbocharger. Having the goals in mind, one can start considering the methodology to be used.

3.1.2 Methodology

It is the combustion process that contributes most to the complexity and fidelity of the model of the diesel engine process and emission formation model is highly dependent on it. Therefore, in this section, methodology will be considered mainly related to the combustion process and emission model. The emission model can be classified by the two different aspects.[28] The first aspect is how to formulate the chemical reaction of the formation processes relevant to the combustion process. In this aspect, either equilibrium assumption can be taken for the chemical reactions or full kinetics of the reaction can be modeled. For NO_x formation mechanism, it is appropriate assumption that the reaction is in equilibrium since majority of formation takes place under the high temperature and high pressure. However, this would not be true as the combustion gas cools down. The most simple and reasonably accurate way to reflect this kinetics is to freeze the composition of the combustion gas under certain temperature [15] .

The second aspect is how to define the control volume with regard to spatial resolution. There exist the models from 0-D approach where any space resolution is ignored to 3-D approach which is also called CFRD (computational fluid and reaction dynamics). Also some authors proposed 1-D approach where one considers the spatial resolution in a limited dimension for only a certain phenomenon such as spray of fuel. CFRD would be only used for study of dimensional parameters of the engine design or verification of the other methods. Also the division of cylinder control volumes into a number of zones according to the local fuel-air equivalent ratio will enhance the prediction of emission formation.

In terms of calculation efficiency, Albrecht [1] and Westlund [28] showed an overview of the calculation time versus the complexity of the model as in the figure 3.1.

For the real time application, the best fidelity can be acquired by 0-D phenomenological model where only equilibrium chemistry is considered. However, it doesn't discourage to construct the model with more complexity since it would enable the modeler to verify the simpler model and provides better insight into the physical process. In the thesis, as the first step of development process, 0-D phenomenological model with two-zone will be used for the modeling approach together with equilibrium assumption.

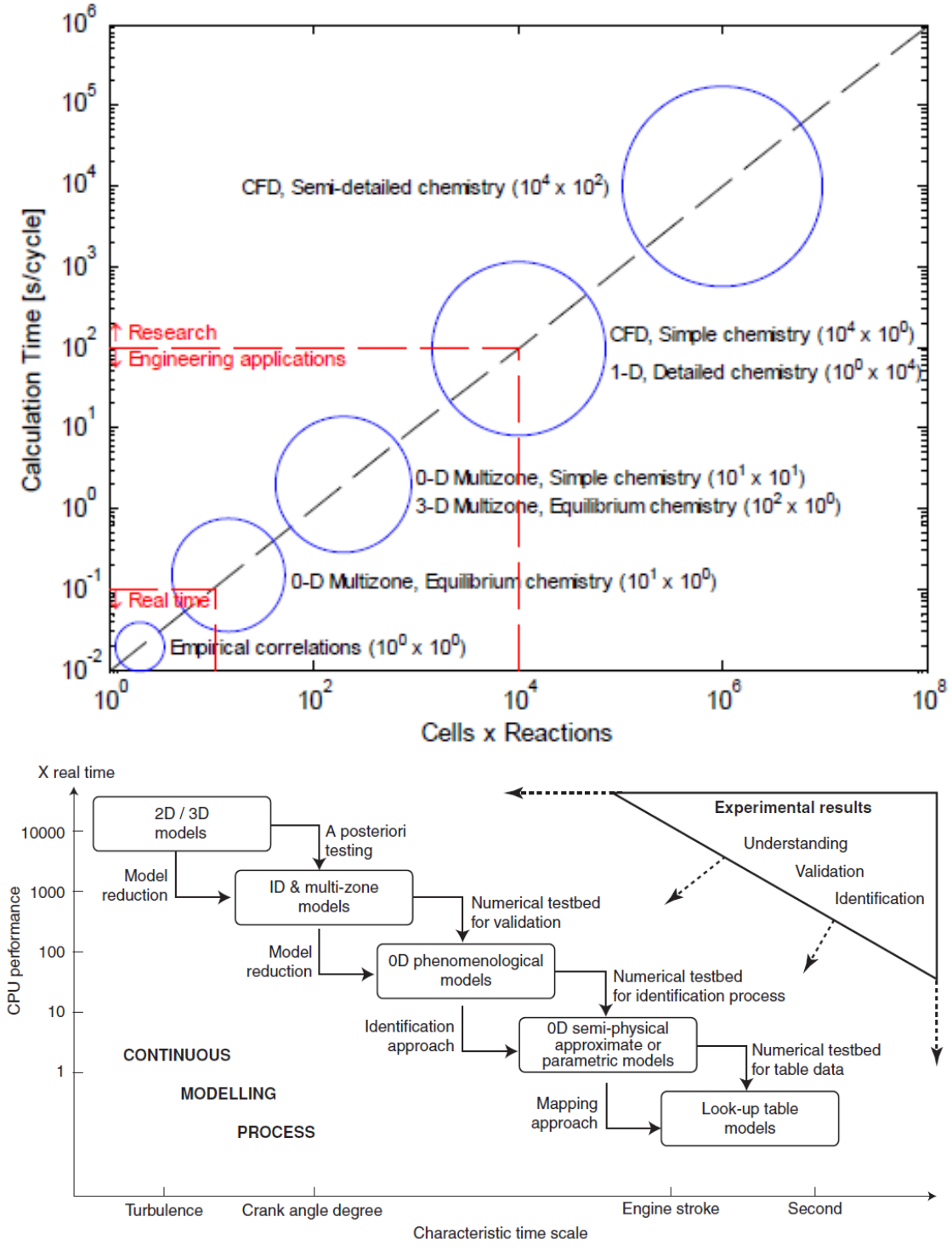

Figure 3.1: Computation time vs. Complexity of the model

3.1.3 Scope of modeling

In the thesis, the scope is defined with the objective of the model in mind. It should contain the cylinders including the intake and exhaust valves and combustion model as the core part. As the turbocharger plays an important role in the transient cases, this should be also included in the dynamic model. The intercooler is also modeled as a part of turbocharging system. Pipes connecting the components should be modeled also in order to achieve the integrity of the model but to a minimum complexity. Mechanical part of the engine can be also simply modeled as a single rotating mass excluding the complexity of the dynamics of crank mechanism. The load on the crank shaft can be included to capture the dynamics and it can be defined depending on the application cases. The governor plays an important role in the dynamics of the system but it is out of scope of the research in the thesis and, therefore, a simple PI controller can be implemented.

3.2 Modeling framework

In the thesis, the bond graph method is used to construct the framework of the model. This approach enables to construct the model in component-wise with a constant system of implementation and also the structure of the model presents the physical connection of the components and therefore provide the modeler more intuitive implementation and interpretation of the model. Firstly the bond graph method is summarized in general in the next section.

3.2.1 Bond graph approach in general

Bond graph is a methodology to build a dynamic system of different energy domain. The beauty of this approach is that it uses the common element for the components in different energy domain and deals with energy flow from one port to the other, which means that the systems of different energy domains are easily connected. The terms used in the bond graph are explained following:

- State Variables : The variables used for bond graph approach can be either power variables and energy variables. The power variables are effort and flow and denoted as e and f respectively. In the basic bond graph application, the product of the power variables is power transmitted from one to the other entity. The energy variables are momentum and displacement and can be obtained from integration of the power variables. They are denoted as p and q in general. The physical interpretation of the state variables are given in the table 3.1
- Power port : A port is an interface point on the element or junction where energy flows in or out. Ports are connected by the power bond and there may be one or multiple ports on one element or junction.

- Power bond : Power bond connects the port from one element to the other. Through the power bond, power is instantaneously transfered from one to the other without loss
- Element : Elements are Representation of physical element or transformation of the energy from one domain to the other. In the basic bond graph, C, R, and I element are commonly used as representation of capacitor, resistor and inertia respectively. These mentioned elements are 1-port element. For transformation of the energy from one domain to the other, TF, and GY element are commonly used as representation of transformer and gyrator respectively. These are two elements. MTF or MGY may be used when the module for the transformation is a function of other variable. The physical meaning of the elements in the different physical domains are presented in the table 3.2.1 as well as the constitutive laws of the element.
- Junction : The junction is the representation of balance of energy, mass or speed. These are multiports elements. 1-junction is used where the flow is equal to all connected port and the sum of the efforts is zero. 1-port is commonly used for the balance of force, moment, pressure and voltage. 0-junction is used where the effort is equal to all connected port and the sum of the flow is zero. It is used for the balance of mass and energy or used for kinematic relationship.
- Field : Elements with multiple ports are called the field. The basic constitutive laws are the same but only with multiple inputs and outputs.
- Causality : Causality determines the input and output for the constitutive laws for the element. Causality is preferred in the way that the output is the function of integration of the output where it is applicable by the constitutive law as in C and I element.

From the bond graph representation, the state equations can be driven by the systematic way to form the state-space equations. Then this equations can be solved either analytically or by numerical method. In short, the bond graph is the representation of the state equation to be solved for the dynamic simulation with an aid of graphically standardized way to enhance the convenience of the modeling process and the understanding of the model.

3.2.2 Word bond graph model

Before developing the detailed bond graph model for the engine, it is worthwhile to make a draft version of the model, called word bond-graph model. The word bond graph model for the intended model is presented in the figure 3.2.

The word bond graph is useful in three aspects. Firstly it clearly defines the scope of the model. As discussed in the section 3.1.3, it contains the necessary components to achieve the goal of the model. Secondly, it is convenient at this level of model to define the components to be built as library. The component library will be built in the way that it can

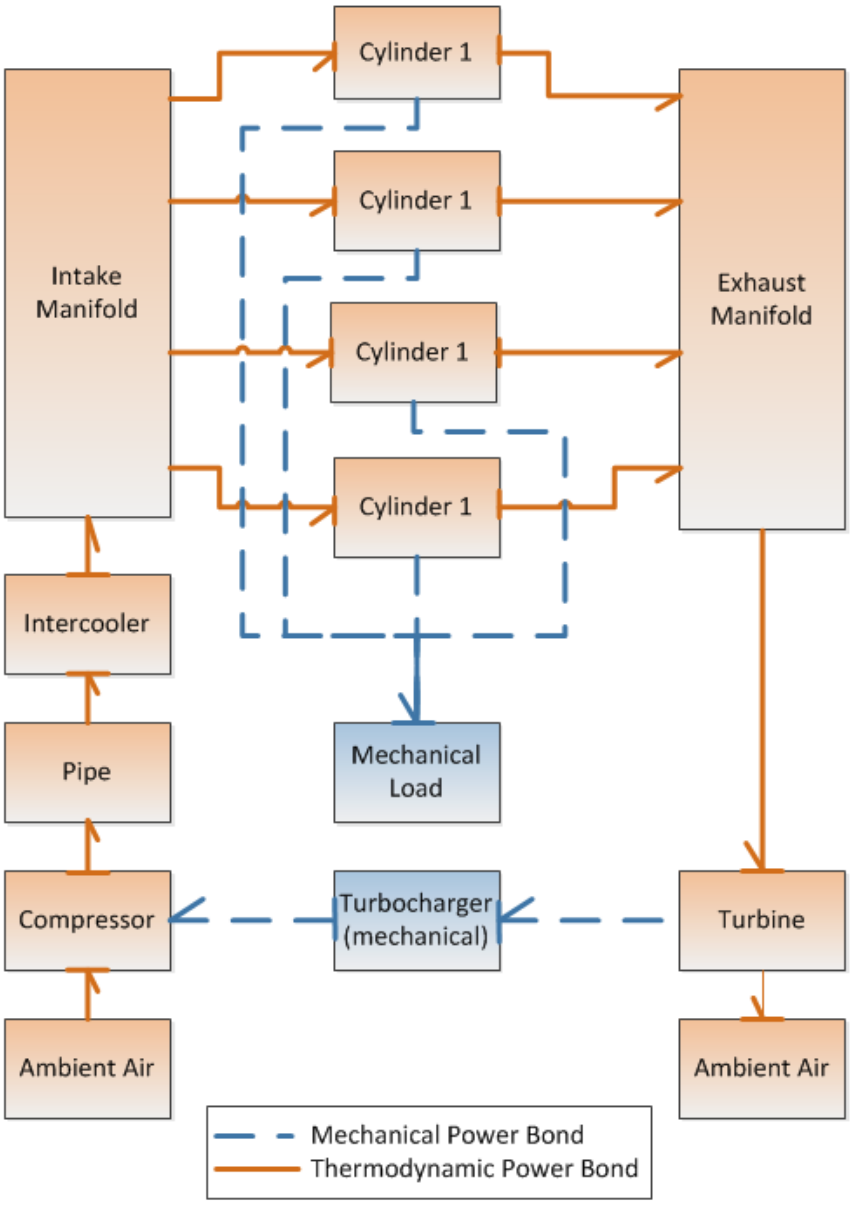

Figure 3.2: Word Bond Graph of the Engine System Model

	Power		Energy	
	Effort, e	Flow, f	Momentum, p	Displacement, s
Mechanical translation	Force (N)	Speed (m/s)	Momentum (Ns)	Displacement (m)
Mechanical rotation	Torque (Nm)	Angular speed (rad/s)	Angular momentum (Nm s)	Angular displacement (rad)
Hydraulic	Pressure (Pa)	Volume flow (m3/s)	Pressure momentum (Pa s)	Volume (m3)
Electric	Voltage (V)	Current (A)	Flux linkage variable (V s)	Charge (C)
Thermal	Temperature (K)	Entropy flow (J/K s)	Not applicable	Entropy

Table 3.1: State variables in bond graph and the physical meaning

	Representation	Constitutive law	Physical meaning
C element	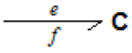	$e = \Phi(q)$	Spring, Reservoir, Cylinder, Electrical capacitor
I element	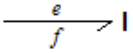	$f = \Phi(p)$	Inertia, fluid inertance, electrical inductance
R element	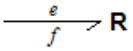	$e = \Phi(f)$	Friction, Electric resistance, heat transfer
TF element	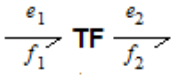	$e_1 = me_2$ $mf_1 = f_2$	Rotation, transformation of energy
GY element	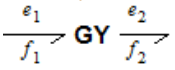	$e_1 = rf_2$ $ff_1 = e_2 2$	Transformation of energy as in the electric motor

Table 3.2: Bond graph elements and the constitutive laws

be reused for other system modeling. In this regard, causality information is important so that input and output is well defined for the library. This causality information can be also shown in the word bond graph as in the figure. Lastly, it is easy to follow the energy flow in the system and, therefore, the user can acquire the intuitive interpretation of the model easily. This word bond graph can be converted to more formal model where equation of state can be extracted. Before going to that stage, bond graph in thermodynamics will be reviewed and suitable state variables are selected for modeling.

3.2.3 Bond graph for thermodynamic system and gas mixture modeling

Pseudo bond graph and multi-component approach for gas mixture modeling

In the classical bond graph model, a single bond graph is used to connect elements or junctions. This can be applied in the same manner with the thermodynamic system where

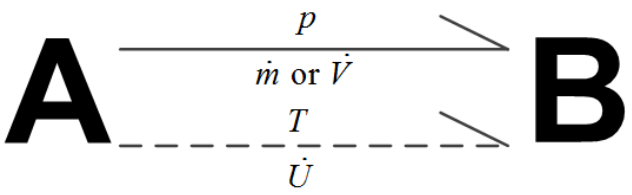

Figure 3.3: Pseudo bond graph of the thermal system

effort represents the temperature and flow, entropy flow. However, this is a bit theological and difficult to grasp in the sense of engineering application. We are more used to the thermodynamic property such as pressure, temperature as effort and mass flow and internal energy flow as flow and would like to use these variable for modeling. Hence, pseudo-bond concept was proposed by Karnopp [18] and uses two bonds, one with pressure as effort variable and mass or volume flow as flow variable and the other with temperature as effort and internal energy flow as flow as shown in the figure 3.3. The disadvantage of this approach would be it loses the concept of the original bond graph where the product of the effort and power equals the energy flow between two elements or junctions. However, the rest of the concept for the standard element and junctions is still valid and, thus, uniformity in modeling approach is not ruined.

For modeling of the thermodynamic system where the fluid is mixture of the gas and/or liquid and it the composition changes dynamically, Karnopp [17] and Pedersen [21] proposed the additional pseudo bonds to determine the thermodynamic state of the fluid. The number of independent intensive variables necessary to determine the thermodynamic state of the fluid in equilibrium is given by the Gibbs phase rule as in the equation 3.1.

$$FN = 2 + N - P \tag{3.1}$$

where,

FN : Necessary independent intensive properties to determine the thermodynamic state
N : Number of constituents of the fluid
P : Number of phases in the fluid

In the gas system as in the internal combustion engine, assuming N compositions of gases would imply that it is necessary to have at least $N + 1$ intensive properties to determine the state [21]. Implication of the Gibbs phase rule is that additional $N - 1$ bonds to the pseudo-bonds having the effort as the intensive properties would be desirable to fully describe the thermodynamic system in general. And for the gas system, it is convenient to choose the mole fraction or partial pressure as those intensive properties and, therefore, the effort of the additional bonds. Mass or mole flow of each constituent of the gas would be natural choice for the flows of those additional bonds. Even though the $N - 1$ is

the minimum number of bonds describing the mixture, N bonds are added to the basic pseudo-bond for the convenience of the calculation and representation.

The effort and flow variables for the engine model with this multi-component approach are summarized as below:

- Effort(e)

  p : Pressure of the system (Pa)
  $\mathbf{x}$: A column vector of mole fractions of the constituents (x_i) where $\mathbf{x} = [x_1, x_2, ..., x_N]^T$
  T: Temperature of the system (K)

- Flow(f)

  $\dot{m}$: mass flow of the system (kg/s)
  $\dot{\mathbf{n}}$: A column vector of mole flows of the constituents ($\dot{n}_i$ in $kmol/s$) where $\dot{\mathbf{n}} = [\dot{n}_1, \dot{n}_2, ..., \dot{n}_N]^T$
  $\dot{U}$: Energy flow of the system (K)
  $\dot{V}$: Volume flow of the system (m^3/s)

Having set up the variables as above, the constitutive laws of the C and R field of the bond graph can be generally formulated as in the equation 3.2 and 3.3 respectively. $\dot{V}$ is only taken into account when there is a volume change with time in the control volume of interest. The detailed calculation routine including thermodynamic calculation will be explained in the description of the modeling libraries and thermodynamic calculation. Hereafter, this method is called pTN approach.

Fuel-air equivalent ratio approach for gas mixture modeling

In the combustion system, fuel-air equivalent ratio can be used to determine the thermodynamic state instead of specifying the composition of the fluid. This can be done with the aid of knowledge of the chemical reaction equation for fixed air and fuel composition and fuel-air equivalent ratio. This approach has been described by Pedersen [22].

The fuel-air equivalent ratio (F) is given as

$$F = \frac{m_b}{m_{air} f_s} = \frac{m_b}{(m - m_b)\, f_s} \tag{3.6}$$

where f_s is the stoichiometric fuel-air ratio and m_b is the burned fuel mixed with air. The composition of the gas and the thermodynamic properties of the gas accordingly can be calculated by the assumption of equilibrium for the chemical reaction of the combustion and/or complete reaction scheme. The detailed method will be shown in the section 3.3.2.

The effort and flow variables in this method are summarized as below:

	Field	Constitutive laws
pTN	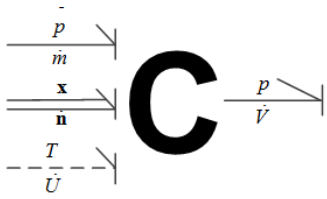	$p = \Phi_p(m, \mathbf{n}, U, V)$ $\mathbf{x} = \Phi_{\mathbf{x}}(m, \mathbf{n}, U, V)$ (3.2) $T = \Phi_T(m, \mathbf{n}, U, V)$
		$\dot{m} = \Phi_{\dot{m}}(p_1, p_2, \mathbf{x}_1, \mathbf{x}_2, T_1, T_2)$ $\dot{\mathbf{n}} = \Phi_{\dot{\mathbf{n}}}(p_1, p_2, \mathbf{x}_1, \mathbf{x}_2, T_1, T_2)$ (3.3) $\dot{U} = \Phi_{\dot{U}}(p_1, p_2, \mathbf{x}_1, \mathbf{x}_2, T_1, T_2)$
pTF	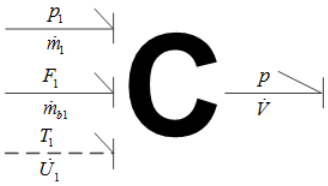	$p = \Phi_p(m, \mathbf{n}, U, V)$ $F = \Phi_F(m, \mathbf{n}, U, V)$ (3.4) $T = \Phi_T(m, \mathbf{n}, U, V)$
		$\dot{m} = \Phi_{\dot{m}}(p_1, p_2, F_1, F_2, T_1, T_2)$ $\dot{m}_b = \Phi_{\dot{m}_b}(p_1, p_2, F_1, F_2, T_1, T_2)$ (3.5) $\dot{U} = \Phi_{\dot{U}}(p_1, p_2, F_1, F_2, T_1, T_2)$

Table 3.3: Constitutive Laws of C and R-Field

- Effort(e)

  p : Pressure of the system (Pa)
  F : Fuel-air equivalent ratio
  T: Temperature of the system (K)

- Flow(f)

  $\dot{m}$: mass flow of the system (kg/s)
  $\dot{m}_b$: Mass flow of the burned fuel (kg/s)
  $\dot{U}$: Energy flow of the system (K)
  $\dot{V}$: Volume flow of the system (m^3/s)

From the state variables defined above, the constitutive laws of the C and R field of the bond graph can be generally formulated as in the equation 3.4 and 3.5. The detailed calculation routine including thermodynamic calculation will be explained in the description of the modeling libraries and thermodynamic calculation. Hereafter, this method is called

PTF approach.

Comparison of pNT and pTF approach

pTF is an efficient way of modeling because the number of state variables are reduced significantly compared to the other. In the study of internal combustion engines, number of constituents of gas species in the combustion gas ranges from nine to twenty one. [14] This means one needs 11 to 23 variables for each effort and flow. In contrast, pTF approach only requires three variables for each flow and effort. Especially when coupled with Zacharias' model for calculation of the thermodynamic properties, it provides robust and very fast calculation scheme.

The disadvantage of the pTF method is that the composition of the gas should be recalculated even in case that chemical reaction is negligible in order to calculate the thermodynamic properties. Also it is not straight forward when applying with varying composition of the air which happens in case of exhaust gas recirculation. This may lead to a significant barrier in the study of the emission reduction technology. Also the bond graph model of the engine systems based on this approach is well described by Pedersen and Engja[22]. Therefore, the thesis will concentrate on development of pNT based model.

3.3 Calculation of Thermodynamic Properties

As the physical process of internal combustion engine is mainly thermal process, calculation of thermodynamic properties of the system is main routines in the model. With pressure(p), temperature(T) and the composition of the gas as in mole fraction($\mathbf{x}$) or the fuel-air equivalent ratio (F) known, thermodynamic properties of the gas can be calculated or vice versa. The properties of interest are shown in the table 3.3. They are all intensive properties which is not affected by the dimension of the system. The extensive properties of the system can be calculated by multiplying the mass.

	Property	Unit
R	Gas constant	J/kgK
Cp	Specific heat capacity at constant pressure	J/kgK
Cv	Specific heat capacity at constant volume	J/kgK
u	Specific internal energy	J/kg
h	Specific enthalpy	J/kg
s	Specific entropy	J/kgK
g	Specific Gibbs free energy	J/kg

Table 3.4: Add caption

The general approach to calculate the properties of the mixture of the gases is, first, to calculate the composition of the gas in mole fraction and the properties of each constituent and then to sum the product of the each property and the mole fraction. This scheme can be expressed in the vector form as in the equation 3.7.

$$\begin{aligned} R &= \frac{R_0}{M} & M &= \mathbf{M}^T\mathbf{x} \\ C_p &= \frac{\mathbf{C_p}^T \cdot \mathbf{x}}{M} & C_v &= C_p - R \\ h &= \frac{\mathbf{h}^T \cdot \mathbf{x}}{M} & u &= h - RT \end{aligned} \tag{3.7}$$

where,

$$\mathbf{x} = [x_1, x_2, ..., x_N]^T \qquad \mathbf{M} = [M_1, M_2, ..., M_N]^T$$
$$\mathbf{C_p} = [C_{p1}, C_{p2}, ..., C_{pN}]^T \qquad \mathbf{h} = [h_1, h_2, ..., h_N]^T$$

x_i : mole fraction of the gas specie

M_i : Molecular weight of the gas specie (kg/mol)

C_{pi} : Specific heat capacity at constant pressure of the gas specie (J/kgK)

h_i : Specific molar enthalpy of the gas specie (J/kg)

For calculation of the specific internal energy, the gas is assumed to be ideal gas ($pv = RT$). For all calculation of thermodynamic properties and the state in the thesis, the gas will be assumed to be ideal. This is appropriate since the pressure in the cylinder is expected to be under 200 bar and the gas is not any close to critical conditions. If the pressure is getting too high as in large two-stroke engines where compression ratio is up to 22:1, real gas property may be considered partly. However, this would be out of scope in the thesis.

One can also use Zacharias' method for calculation of the properties. The properties of interest above as well as other properties can be determined by given p, T and F. It is a highly empirical formulation fitting to the specific composition of fuel. However, it is very fast and robust calculation scheme so that it is widely used for the thermodynamic calculation in conjunction with combustion. First, general method is explained. Comparison of the two methods will be given in the section 3.3.3.

3.3.1 Calculation of thermodynamic properties based on mole fraction of the mixture

The molecular weight of a gas specie can be obtained from various sources. In the thesis, the NIST on-line database was used[8]. Specific heat capacity can be calculated from the JANAF table [6] or NASA 7 polynomials. NASA polynomial is a mean to present the

thermodynamic properties as function of temperature. It is a compact way of presentation compared to the bulky tables of numbers as in JANAF table. It can be used for the temperature range from $50K$ to $6000K$ depending on the order of polynomials. 7-term polynomial can predict the properties from $150K$ with confidence in the fourth and fifth digits. For the lower temperature application, 9-term can be used [5].

7-term polynomial for the property calculation is given in the equation 3.8.

$$\frac{C_p}{R} = a_1 + a_2T + a_3T^2 + a_4T^3 + a_5T^4 \tag{3.8}$$

$$\frac{h_T^o}{RT} = a_1 + \frac{a_2T}{2} + \frac{a_3T^2}{3} + \frac{a_4T^3}{4} + \frac{a_5T^4}{5} + \frac{a_6}{T} \tag{3.9}$$

$$\frac{s_T^o}{R} = a_1 \ln T + a_2T + \frac{a_3T^2}{2} + \frac{a_4T^3}{3} + \frac{a_5T^4}{4} + a_7 \tag{3.10}$$

$$\frac{g}{RT} = a_1 (1 - \ln T) - \frac{a_2T}{2} - \frac{a_3T^2}{6} - \frac{a_4T^3}{12} - \frac{a_5T^4}{20} + \frac{a_6}{T} - a_7 \tag{3.11}$$

It should be noted that the both sides of the equations are dimensionless so that it can be used for both mole and weight based calculation. Also, the enthalpy obtained from the polynomial is the "engineering enthalpy" defined as

$$h_T^o = \Delta_f h_{298}^\circ + \int_{298}^{T} C_p^\circ dT \tag{3.12}$$

In the thesis, it was found that it makes more sense using absolute values since the value of the specific internal energy is preferred to be positive all the time. Then the absolute enthalpy is given

$$h = h_T^\circ - \Delta_f h^\circ 298 + h_{0\to298} \tag{3.13}$$

$\Delta_f h_{298}^\circ$ for a molecule is found in the table of NASA polynomial table from Burcat [5] and $h_{0\to298}$ is found from JANAF table available on online web page of NIST [7]. The coefficients available for a specie actually contains 15 coefficients. The first seven coefficients are used for the temperature range from $1000K$ to $6000K$. Then the next seven coefficients can be used for lower temperature range. The last coefficient provides the value of $\Delta_f h_{298}^\circ / R$ which can be used to calculate the absolute enthalpy.

For calculation of the properties of a mixture, it is a efficient way to find a single set of coefficients of the polynomials for the mixture rather than the general way presented in the section 3.3. This can be easily done by knowing the mole fraction of the constituent gases, $\mathbf{x}$. In the matrix formulation, this can be done as

$$\mathbf{A}_{mix} = \mathbf{A}\mathbf{x} \tag{3.14}$$

where,

$\mathbf{A}_{mix}$: a column vector of the coefficients of mixture where,

$$\mathbf{A}_{mix} = [a_{mix,1}, a_{mix,2}, ..., a_{mix,7}]^T$$

$\mathbf{A}$: a matrix containing the coefficients of each constituent where,

$$\mathbf{A} = \begin{bmatrix} a_{11} & a_{12} & ... & a_{17} \\ a_{21} & a_{22} & ... & a_{27} \\ \vdots & \vdots & \vdots & \vdots \\ a_{N1} & a_{N2} & ... & a_{N7} \end{bmatrix}$$

N : A number of constituents in the mixture

3.3.2 Calculation of the composition of the gas

The composition of the gas is an important intensive state to determine the thermodynamic properties of the system. Before going into the calculation, the basic constituents of the combustion gas must be defined. The kind of gas species and the number can vary depending on the purpose of application. For example, it would not require more than up to nine constituents in the combustion if the purpose of the model is to predict the thermodynamic properties of the gas according to Grill [14]. In studies of NO_x formation, the number of constituents may increase up to 12 as proposed by Olikara and Bowman [20]. Grill presented a summary table to show the different basic compositions assumed in various authors' model as in the table 3.3.2.

	CO	H2O	OH	H	O	CO2	O2	H2	N2	N	NO	NO2	N2O	HCN	CN	CH	NH	C2	C	Ar	CH4	O3	NH3	HNO3
Zacharias	x	x	x	x	x	x	x	x	x	x	x	x	x	x	x	x	x	x	x	x				
de Jaegher	x	x	x	x	x	x	x	x	x	x	x	x		x					x	x	x	x	x	x
Hohlbaum	x	x	x	x	x	x	x	x	x	x	x	x	x											
Berner / Choidi	x	x	x	x	x	x	x	x	x	x	x													
Grill	x	x	x	x	x	x	x	x	x		x													
Olikara	x	x	x	x	x	x	x	x	x	x	x									x				

Table 3.5: Basic Composition of the Combustion Gas

In this thesis, 12 composition proposed by Olikara is used for basic components in the combustion gas mixture since NO plays an important rule in the prediction of NO_x emission and Ar is has an significant constitute in air composition.

In case of non-reactive system as in the air receiver of the engine or other pipe element in the air system, the composition can be algebraically calculated by balancing the molar or mass flow in and out of the control volume. Provided the molar flow is the input to the control volume as in C-field presented in the table 3.2.3, composition is simply obtained

by

$$\mathbf{n} = \int \dot{\mathbf{n}} \mathrm{d}t \qquad \mathbf{x} = \frac{\mathbf{n}}{\sum_i n_i} \tag{3.15}$$

However, in the reactive system as in the cylinder during combustion and part of exhaust system, the composition changes with pressure, temperature and the mass of fuel burned. Firstly the base equation for the combustion reaction should be set up. On the side of reactants, air and fuel are placed and combustion gas comes on the product side. The combustion gas is assumed to have 12 gas species namely, H, O, N, H_2, OH, CO, NO, O_2, H_2O, CO_2, N_2 and Ar. Air can be mixed combustion gas before combustion in case of mixing with residual gas in the cylinder or by exhaust gas recirculation. Therefore, air also consists of twelve species of molecules. Fuel is assumed to consists of C, H, O and N. Then the chemical reaction becomes

$$\begin{aligned} x_{13}\Big[C_nH_mO_lN_k + \frac{N_L}{F}(O_2 + b_1N_2 + b_2Ar + b_3CO + b_4CO_2 + b_5H_2O \\ + b_6H_2 + b_7H + b_8O + b_9N + b_{10}OH + b_{11}NO)\Big] \\ \leftrightarrow x_1H + x_2O + x_3N + x_4H_2 + x_5OH + x_6CO + x_7NO + x_8O_2 \\ + x_9H_2O + x_{10}CO_2 + x_{11}N_2 + x_{12}Ar \end{aligned} \tag{3.16}$$

where,

$$N_L = \frac{4n + m - 2l}{4 - 2b_3 - 2b_6 - b_7 + 2b_8 + b_{10} + 2b_{11}}$$

x_i : mole fraction of gas species in the combustion gas for $i = 1, 2, ..., 12$

x_{13} : number of moles of the fuel to produce one mole of combustion gas

The combustion products to be considered varies with the combustion temperature. In the lower temperature region below 2200K, the combustion is said to be in complete combustion scheme where the main products are CO_2, CO, H_2O, H_2, O_2, N_2 and Ar. As the temperature rises above the temperature these main products dissociates and react to form other species in a considerable amount[15]. In this region, the composition of the combustion gas is close to equilibrium state since the reaction of the dissociation and reformation is much faster than the combustion process. As the gas cools down in the expansion cycle and the exhaust system, the reaction rate becomes so low that the composition is frozen from the previous state. This physical process of varying composition can be modeled by having set up two combustion scheme and mix them in the transitional region of temperature. The first scheme is called non-dissociation combustion and the other dissociation combustion at equilibrium.

Non-dissociation combustion

In this scheme, the composition of the combustion gas is determined by atomic balance of the chemical equations. It is the fuel-air equivalent ratio that determines the constituents of the combustion gas mixture. This is presented in the figure 3.4 [25].

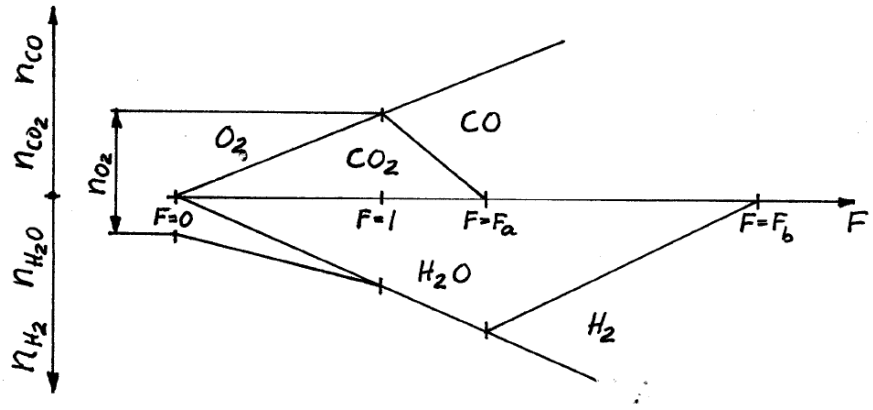

Figure 3.4: Combustion product without dissociation

The base chemical reaction to be used is given as

$$\begin{aligned} FC_nH_mO_lN_k + N_L(O_2 + b_1N_2 + b_2Ar + b_3CO + b_4CO_2 + b_5H_2O \\ +b_6H_2 + b_7H + b_8O + b_9N + b_{10}OH + b_{11}NO)\Big] \\ \leftrightarrow n_1H + n_2O + n_3N + n_4H_2 + n_5OH + n_6CO + n_7NO + n_8O_2 \\ +n_9H_2O + n_{10}CO_2 + n_{11}N_2 + n_{12}Ar \end{aligned} \tag{3.17}$$

where,

$$N_L = \frac{4n + m - 2l}{2b_8 - 2b_6 - b_7 - 2b_3 + b_{10} + 2b_{11} + 4}$$

b_i : Mole fraction of the gas specie in the air in ratio to the number of moles of oxygen

Depending on the value of F, the composition of the products varies and this can be categorized into three cases as shown in the figure 3.4:

- Lean and stoichiometric combustion : $F \leq 1$
- Rich combustion : $1 < F \leq F_a$
- Very rich combustion : $F_q < F \leq F_b$

From the base equation 3.17 and the assumption that the product composition changes linearly with F, the value of F_a and F_b can be calculated as

$$F_a = -N_L \frac{2b_4 - 2b_6 - b_7 + 2b_8 + b_{10} + 2b_{11} + 4}{2l - m - 2n} \tag{3.18}$$

$$F_b = -N_L \frac{b_4 + b_5 + b_8 + b_{10} + b_{11} + 2}{l - n}; \tag{3.19}$$

Then the composition of the product for each case can be calculated from the given F value by atomic balance of the reaction. The result is presented below.

- Lean combustion : $F \leq 1$

$$\begin{aligned}
n_{CO_2} &= nF + N_L(b_3 + b_4) \\
n_{CO} &= 0 \\
n_{H_2O} &= F\frac{m}{2} + N_L\left(b_5 + b_6 + \frac{b_7}{2} + \frac{b_{10}}{2}\right) \\
n_{H_2} &= 0 \\
n_{O_2} &= \frac{(1-F)(m - 2l + 4n)}{4} \\
n_{N_2} &= F\frac{k}{2} + N_L\left(b_1 + \frac{b_9}{2} + \frac{b_{11}}{2}\right) \\
n_{Ar} &= b_2 N_L
\end{aligned} \tag{3.20}$$

- Rich combustion : $1 < F \leq F_a$

$$\begin{aligned}
n_{CO_2} &= \{n + N_L\,(b_3 + b_4)\}\,\frac{F_a - F}{F_a - 1} \\
n_{CO} &= \frac{(F-1)(m - 2l + 4n)}{2} \\
n_{H_2O} &= F\frac{m}{2} + N_L\left(b_5 + b_6 + \frac{b_7}{2} + \frac{b_1 0}{2}\right) \\
n_{H_2} &= 0 \\
n_{O_2} &= 0 \\
n_{N_2} &= F\frac{k}{2} + N_L\left(b_1 + \frac{b_9}{2} + \frac{b_{11}}{2}\right) \\
n_{Ar} &= b_2 N_L
\end{aligned} \tag{3.21}$$

- Very rich combustion : $1 < F \leq F_a$

$$
\begin{aligned}
n_{CO_2} &= 0 \\
n_{CO} &= nF + N_L(b_3 + b_4) \\
n_{H_2O} &= \left\{ F_a \frac{m}{2} + N_L \left(b_5 + b_6 + \frac{b_7}{2} + \frac{b_{10}}{2} \right) \right\} \frac{F_b - F}{F_b - F_a} \\
n_{H_2} &= \left\{ F_b \frac{m}{2} + N_L \left(b_5 + b_6 + \frac{b_7}{2} + \frac{b_{10}}{2} \right) \right\} \frac{F - F_a}{F_b - F_a} \\
n_{O_2} &= 0 \\
n_{N_2} &= F \frac{k}{2} + N_L \left(b_1 + \frac{b_9}{2} + \frac{b_{11}}{2} \right) \\
n_{Ar} &= b_2 N_L
\end{aligned}
\tag{3.22}
$$

This calculation scheme is implemented in Matlab as the function "GetCompleteComb" where inputs are F, fuel composition (n, m, l, k) and the air composition that consists of 12 species($\mathbf{b} = [b_1, b_2, ..., b_{11}]^T$). The result of calculation for the fuel CH_2 and standard air composition is presented in the figure 3.3.2.

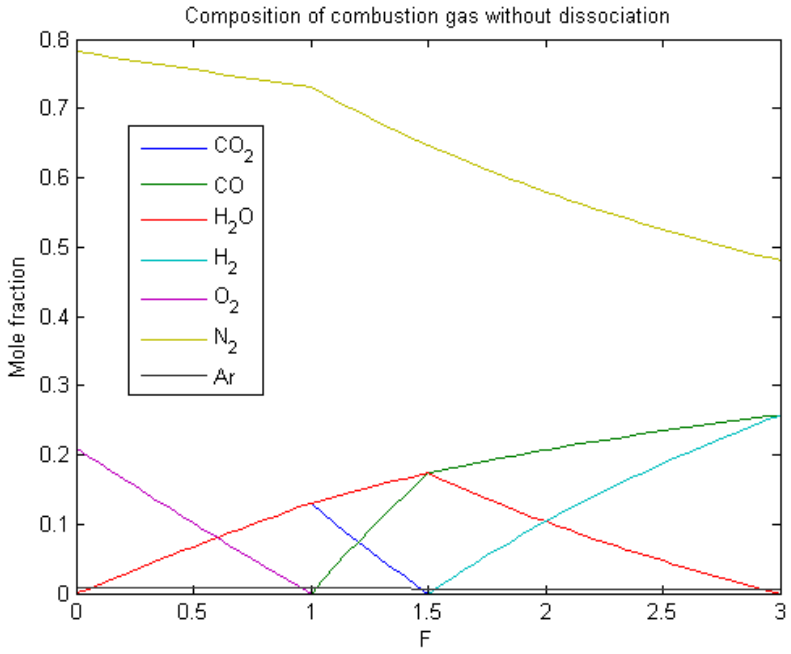

Figure 3.5: Composition of combustion gas without dissociation

Dissociation combustion at equilibrium - Olikara method

In the temperature above 2200K, the main product of combustion start to dissociate and react each other to form other gas molecules. As mentioned in the section 3.3.2, it is an appropriate assumption that these dissociation and new reactions are taking place in

equilibrium. The equilibrium calculation program was developed by Olikara and Borman and provided in the paper[20] (hereafter, called Olikara's method). This has been the basic skeleton for the further researches coming with some improvements. In the thesis, the basic method of Olikara and Borman is implemented with adaptation of combustion mixture in the air. Also Grill has presented an improved method for faster calculation [14]. This method is also implemented and compared with Olikara's method for accuracy and performance in computation.

In order to fully adapt the mixture of combustion gas in the charge air, the equation 3.16 is used for the basic combustion reaction.

The Olikara's methods assumes seven chemical reactions at equilibrium between the product of the fossil fuel combustion into account and twelve gas species arises as a result of calculations. The seven chemical reactions considered are shown in the equation 3.23.

$$\begin{aligned} {}^1\!/_2 H_2 &\rightleftarrows H \\ {}^1\!/_2 O_2 &\rightleftarrows O \\ {}^1\!/_2 N_2 &\rightleftarrows N \\ {}^1\!/_2 H_2 + {}^1\!/_2 O_2 &\rightleftarrows OH \\ {}^1\!/_2 N_2 + {}^1\!/_2 O_2 &\rightleftarrows NO \\ H_2 + {}^1\!/_2 O_2 &\rightleftarrows H_2O \\ CO + {}^1\!/_2 O_2 &\rightleftarrows CO_2 \end{aligned} \tag{3.23}$$

The left hand of the equation 3.16 can be rearranged for the convenience of the atomic balance as:

$$x_{13}\left\{r_1 C + r_2 H + r_3 O_2 + r_4 N_2 + r_5 Ar\right\} \tag{3.24}$$

where,

$$r_1 = \left[n + \frac{N_L}{F}(b_3 + b_4)\right] \qquad r_2 = \left[m + 2\frac{N_L}{F}\left(b_5 + b_6 + \frac{b_7}{2} + \frac{b_{10}}{2}\right)\right]$$
$$r_3 = \left[\frac{l}{2} + \frac{N_L}{F}\left(1 + \frac{b_3}{2} + b_4 + \frac{b_5}{2} + \frac{b_8}{2}\right)\right] \qquad r_4 = \left[\frac{k}{2} + \frac{N_L}{F}\left(b_1 + \frac{b_9}{2} + \frac{b_{11}}{2}\right)\right]$$
$$r_5 = \left[\frac{N_L}{F} b_2\right]$$

Then, the atomic balance for each element will yield the following equations.

$$\begin{aligned} \text{Carbon} &: r_1 x_{13} = x_6 + x_{10} \\ \text{Hydrogen} &: r_2 x_{13} = x_1 + 2x_4 + x_5 + 2x_9 \\ \text{Oxygen} &: r_3 x_{13} = x_2 + x_5 + x_6 + x_7 + 2x_8 + x_9 + 2x_{10} \\ \text{Nitrogen} &: 2r_4 x_{13} = x_3 + x_7 + 2x_{11} \\ \text{Argon} &: r_5 x_{13} = x_{12} \end{aligned} \tag{3.25}$$

Also as x_i represents the mole fraction of the gas specie, the sum of the total will be always equal to 1.

$$\sum_{i=1}^{12} x_i = 1 \tag{3.26}$$

In addition to the equation 3.25 and 3.26, the relation between the mole fraction can be found from the equilibrium constant of the reactions suggested in the equation 3.23. This is provided in the table 3.3.2.

Reaction	Equilibrium Constant
$^1/_2H_2 \rightleftarrows H$	$K_{p1} = x_1 p^{1/2} / {x_4}^{1/2}$
$^1/_2O_2 \rightleftarrows O$	$K_{p2} = x_2 p^{1/2} / {x_8}^{1/2}$
$^1/_2N_2 \rightleftarrows N$	$K_{p3} = x_3 p^{1/2} / {x_{11}}^{1/2}$
$^1/_2H_2 + {}^1/_2O_2 \rightleftarrows OH$	$K_{p5} = x_5 / {x_4}^{1/2} {x_8}^{1/2}$
$^1/_2N_2 + {}^1/_2O_2 \rightleftarrows NO$	$K_{p7} = x_7 / {x_8}^{1/2} {x_{11}}^{1/2}$
$H_2 + {}^1/_2O_2 \rightleftarrows H_2O$	$K_{p9} = x_9 / x_4 {x_8}^{1/2} p^{1/2}$
$CO + {}^1/_2O_2 \rightleftarrows CO_2$	$K_{p10} = x_{10} / x_6 {x_8}^{1/2} p^{1/2}$

(3.27)

Table 3.6: Equilibrium constant for the dissociation

Oilkara and Borman used the equilibrium constants found in JANAF Thermochemical Tables in 1971 and they curve-fitted the data and suggested the function in temperature as in the equation 3.28. The coefficient of each term is provided in the table 3.3.2.

$$\log K_p = A \ln T + \frac{B}{T} + C + DT + ET^2 \tag{3.28}$$

Constant	A	B	C	C	E
K_{p1}	4.3217e-1	-1.1246e+1	2.6727e+0	-7.4574e-2	2.4248e-3
K_{p2}	3.1081e-1	-1.2954e+1	3.2178e+0	-7.3834e-2	3.4465e-3
K_{p3}	3.8972e-1	-2.4583e+1	3.1451e+0	-9.6373e-2	5.8564e-3
K_{p5}	-1.4178e-1	-2.1331e+0	8.5346e-1	3.5502e-2	-3.1023e-3
K_{p7}	1.5088e-2	-4.7096e+0	6.4610e-1	2.7281e-3	-1.5444e-3
K_{p9}	-7.5236e-1	1.2421e+1	-2.6029e+0	2.5956e-1	-1.6269e-2
K_{p10}	-4.1530e-3	1.4863e+1	-4.7575e+0	1.2470e-1	-9.0023e-3

Table 3.7: Coefficient of the curve fitted for equilibrium constants

In the thesis, the function has been updated by using NASA 7 polynomials because it is based on more up-to-date data and it is convenient to modify when the basic composition

of the composition is varied. The function is given in the equation from Burcat as [5]:

$$\ln K_p = a_1(1 - \ln T) - a_2\left(\frac{T}{2}\right) - a_3\left(\frac{T^2}{6}\right) - a_4\left(\frac{T^3}{12}\right) - a_5\left(\frac{T^4}{20}\right) + a_6\left(\frac{1}{T}\right) - a_7 \tag{3.29}$$

The coefficients for each reaction can be algebraically calculated by the K_p constant for each molecule involved in the chemical reaction. Given a chemical reaction,

$$\alpha X1 + \beta X2 \rightleftarrows \gamma Y1 + \omega Y2$$

and the polynomial coefficients for each molecule in the reaction as in a column vector form ($\mathbf{a}_{X1}$, $\mathbf{a}_{X2}$, $\mathbf{a}_{Y1}$, $\mathbf{a}_{Y2}$), the coefficient for the equilibrium constants are calculated as

$$\mathbf{a}_{reaction} = \alpha\mathbf{a}_{X1} + \beta\mathbf{a}_{X2} - (\gamma\mathbf{a}_{Y1} + \omega\mathbf{a}_{Y2}) \tag{3.30}$$

The calculated values are provided in the table 3.3.2.

Constant	a_1	a_2	a_3	a_4	a_5	a_6	a_7
K_{p1}	-1.034e+0	4.133e-4	-7.320e-8	7.705e-12	-3.444e-16	-2.588e+4	-6.548E-2
K_{p2}	-7.132e-1	3.555e-4	-6.638e-8	5.335e-12	-1.700e-16	-2.983e+4	-3.215e+0
K_{p3}	-9.397e-1	5.236e-4	-1.273e-7	9.074e-12	-2.677e-16	-5.660e+4	-1.714e+0
K_{p5}	4.584e-1	-3.659e-4	1.502e-7	-2.408e-11	1.429e-15	-4.712e+3	-4.649e+0
K_{p7}	4.606e-2	-1.644e-4	1.122e-7	-1.986e-11	1.080e-15	-1.099e+4	-1.725e+0
K_{p9}	2.086e+0	-1.818e-3	5.568e-7	-6.873e-11	2.931e-15	2.846e+4	-6.199e+0
K_{p10}	2.425e-1	-1.062e-3	4.395e-7	-7.124e-11	3.814e-15	3.415e+4	9.660e+0

Table 3.8: Coefficient of the curve fitted for equilibrium constants

The difference in K_p values from equation 3.28 and 3.29 for the chemical reactions is shown in the figure 3.3.2. In the range of interest, some values are noticeably different. As the equation 3.29 is based on more update information, it is recommended to use it.

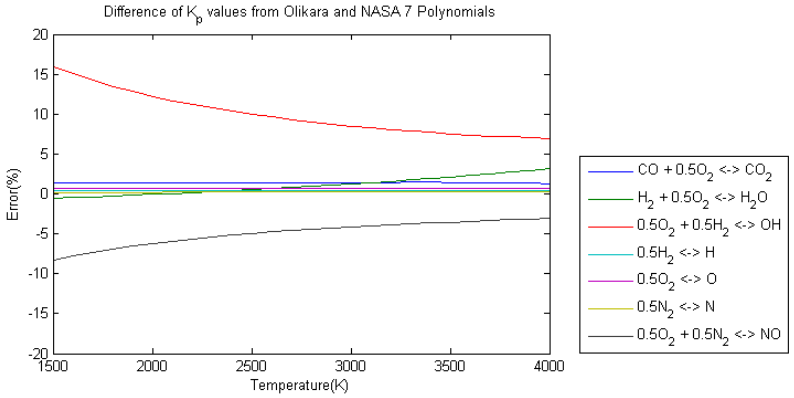

Figure 3.6: Differece of K_p values from Olikara to NASA 7 polynomials

From the equations 3.25, 3.26 and 3.27, a system of nonlinear equations can be set up with twelve equations and twelve mole fractions as unknowns. This can be solved by

linearizing the equations and solving it in the iterative manner until the change of the solution is minimal. One should be careful in the iterative method because the step to the next temporary solution may lead to the negative value for the slope of the path to the solution is very stiff near the true solution. There should be a limit to the length of the step in the iteration in order to avoid such a problem. Also the challenge is to determine the initial point but this also is well described in the paper by Olikara and Borman.

This calculation scheme is implemented in Matlab as the function "GetEquilOlikara" where inputs are p, T, F, fuel composition (n, m, l, k) and the air composition that consists of 12 species($\mathbf{b} = [b_1, b_2, ..., b_1 1]^T$). The result of calculation for the fuel CH_2 and standard air composition is presented in the figure 3.3.2, 3.3.2 and 3.3.2.

The composition of the gas calculated from Olikara's method is presented in the figure 3.3.2, 3.3.2 and 3.3.2 based on the fuel composition CH_2 and standard air.

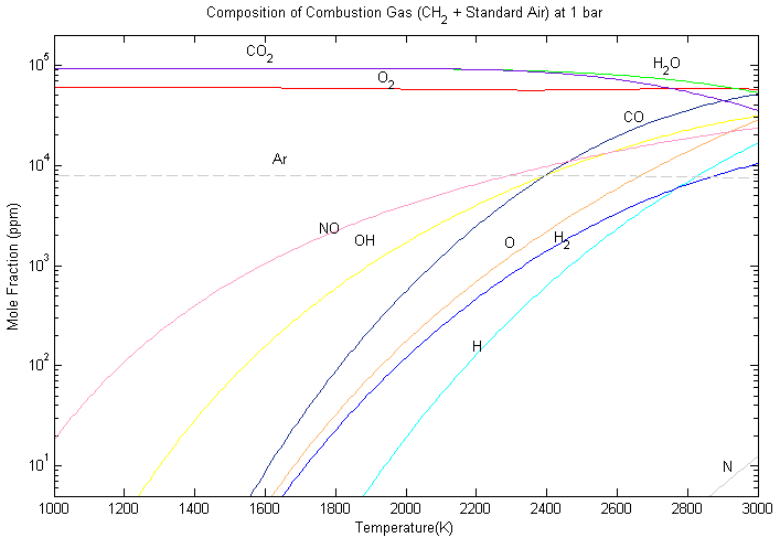

Figure 3.7: Composition of the combustion gas (CH_2 + Standard air) at $p = 1bar$ and $F = 0.7$

Dissociation combustion at equilibrium - Grill method

Grill proposed an improved method for the equilibrium calculation with a faster convergence and simpler calculation. The system of equations to be solved is expressed in the function of partial pressure of the gas species. The system of equations is also solved iterative method but only by adjusting the partial pressure of oxygen and nitrogen to satisfy the overall equations. The equations has been modified in the thesis to adapt the mixture of air with 12 component-based combustion gas. First set of equation can be obtained from the relation between the partial pressure of the gas species and the equilibrium constant, similar to the equation 3.27. Also, similarly to the equation 3.25 and 3.26, the

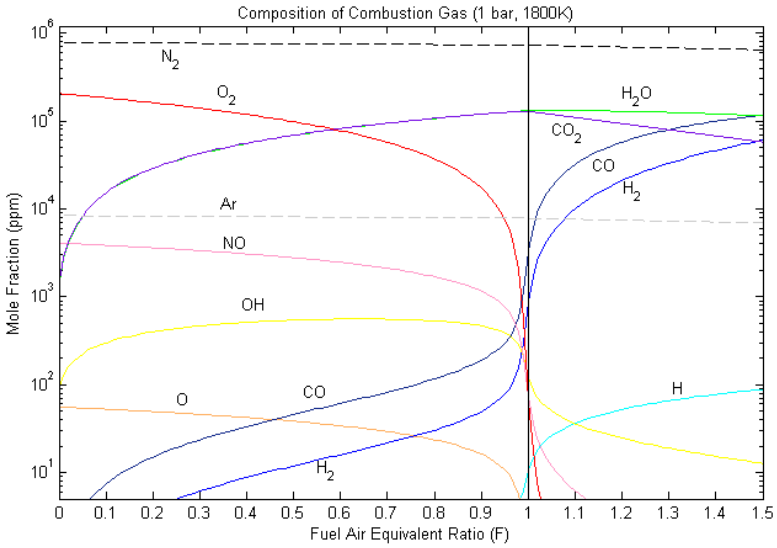

Figure 3.8: Composition of the combustion gas (CH_2 + Standard air) at $p = 1bar$ and $T = 1800K$

atomic balance of the reaction 3.16 and the sum of the partial pressure sum is expressed as

$$p = \sum_{i=1}^{12} p_i \tag{3.32}$$

$$\begin{aligned}
\frac{N_C}{N_O} &= \frac{p_{CO_2} + p_{CO}}{2p_{CO_2} + p_{CO} + 2p_{O_2} + p_{H_2O} + p_{OH} + p_O + p_{NO}} = Const. \\
\frac{N_O}{N_N} &= \frac{2p_{CO_2} + p_{CO} + 2p_{O_2} + p_{H_2O} + p_{OH} + p_O + p_{NO}}{2p_{N_2} + p_N + p_{NO}} = Const. \\
\frac{N_H}{N_O} &= \frac{2p_{H_2O} + 2p_{H_2} + p_{OH} + p_H}{2p_{CO_2} + p_{CO} + 2p_{O_2} + p_{H_2O} + p_{OH} + p_O + p_{NO}} = Const. \\
\frac{N_{Ar}}{N_C} &= \frac{p_{Ar}}{p_{CO_2} + p_{CO}} = N_{Ar/C} = Const.
\end{aligned} \tag{3.33}$$

where N_{specie1} denotes for the sum of partial pressure of constituents containing the atom specie. These ratios can be also denoted as following by the mass balance of the chemical reaction given in the equation 3.16.

$$\begin{aligned}
\frac{N_C}{N_O} &= \frac{r_1}{r_3} = N_{C/O} \qquad \frac{N_O}{N_N} &= \frac{r_3}{r_4} = N_{O/N} \\
\frac{N_H}{N_O} &= \frac{r_2}{2r_3} = N_{H/O} \qquad \frac{N_{Ar}}{N_C} &= \frac{r_5}{r_1} = N_{Ar/C}
\end{aligned} \tag{3.34}$$

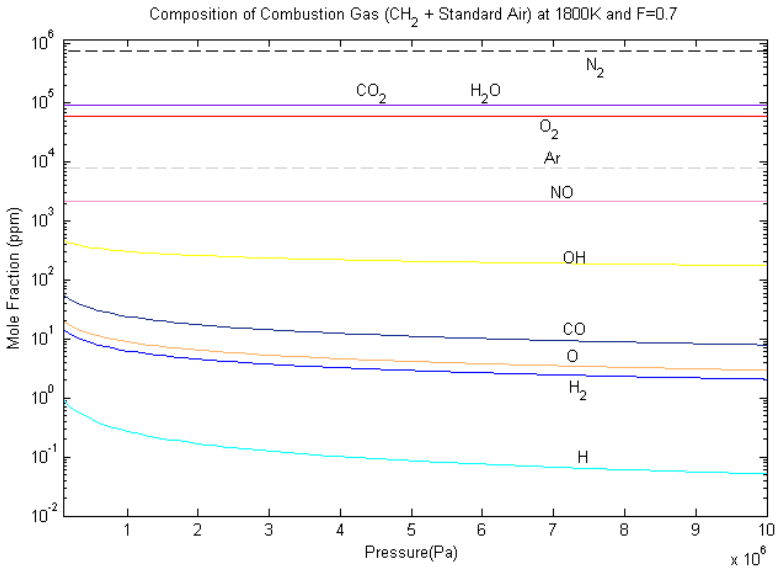

Figure 3.9: Composition of the combustion gas (CH_2 + Standard air) $T = 1800K$ and $F = 0.7$

where,

$$r_1 = \left[n + \frac{N_L}{F}(b_3 + b_4) \right] \qquad r_2 = \left[m + 2\frac{N_L}{F}\left(b_5 + b_6 + \frac{b_7}{2} + \frac{b_{10}}{2} \right) \right]$$

$$r_3 = \left[\frac{l}{2} + \frac{N_L}{F}\left(1 + \frac{b_3}{2} + b_4 + \frac{b_5}{2} + \frac{b_8}{2} \right) \right] \qquad r_4 = \left[\frac{k}{2} + \frac{N_L}{F}\left(b_1 + \frac{b_9}{2} + \frac{b_{11}}{2} \right) \right]$$

$$r_5 = \left[\frac{N_L}{F} b_2 \right].$$

Eliminating p_{Ar} from the equations, the system of 11 nonlinear equations with 11 unknowns can be found. The system of equations can be solved by linearizing each function and simply solve the linear system of equations. Finding the true solution, Newton-Raphson method is used. It requires a good guess of the initial value in order for the solution converges rapidly. Grill suggested a more simplified and faster way of solving the problem.

First one can use the initial value of N_N^* as solution to the system of equations.

- Start with $N_N^* = 0.7p$
- Start with the integration result of the last time step
- Start with

$$N_N{}^* = \begin{cases} 0.95 \dfrac{\frac{3.773 N_L}{2F}}{x + \frac{y}{2} + \frac{N_L}{2F}\left(\frac{1-F}{1} + 3.773\right)} p & \forall F < 1 \\ 0.95 \dfrac{\frac{3.773 N_L}{2F}}{x + \frac{y}{2} + \frac{N_L}{2F}(3.773)} p & \forall F \geqslant 1 \end{cases} \tag{3.35}$$

Reaction	Equilibrium Constant
$^1/_2H_2 \rightleftarrows H$	$p_H = K_{p1}\sqrt{p_{H_2}}$
$^1/_2O_2 \rightleftarrows O$	$p_O = K_{p2}\sqrt{p_{O_2}}$
$^1/_2N_2 \rightleftarrows N$	$p_N = K_{p3}\sqrt{p_{N_2}}$
$^1/_2H_2 + {}^1/_2O_2 \rightleftarrows OH$	$p_{OH} = K_{p5}\sqrt{p_{O_2}}\sqrt{p_{H_2}}$
$^1/_2N_2 + {}^1/_2O_2 \rightleftarrows NO$	$p_{NO} = K_{p7}\sqrt{p_{N_2}}\sqrt{p_{O_2}}$
$H_2 + {}^1/_2O_2 \rightleftarrows H_2O$	$p_{H_2O} = K_{p9}p_{H_2}\sqrt{p_{O_2}}$
$CO + {}^1/_2O_2 \rightleftarrows CO_2$	$p_{CO_2} = K_{P10}p_{CO}\sqrt{p_{O_2}}$

(3.31)

Table 3.9: Equilibrium constant for the dissociation in partial pressure

Having known N_N^*, the N_{atom} can be denoted as

$$N_O{}^* = N_{O/N}N_N{}^* \qquad N_H{}^* = N_{H/O}N_O{}^* \qquad N_C{}^* = N_{C/O}N_O{}^* \tag{3.36}$$

Also initial value $p^0_{O_2}.5$ is also chosen. The choice is not critical. It can be final value from the last iteration or $0.0245/F^{0.5}\ bar^{0.5}$. From the equation 3.31, 3.34 and 3.36, partial pressure of H_2, N_2, CO_2 and CO can be explicitly found.

$$\begin{aligned}
\sqrt{p_{H_2}} &= \frac{-K_{p5}\sqrt{p_{O_2}} - K_{p1} + \sqrt{\left(K_{p5}\sqrt{p_{O_2}} + K_{p1}\right)^2 + 8\left(1 + K_{p9}\sqrt{p_{O_2}}\right)N_H{}^*}}{4\left(1 + K_{p9}\sqrt{p_{O_2}}\right)} \\
\sqrt{p_{N_2}} &= -\frac{1}{4}\left(K_{p3} + K_{p7}\sqrt{p_{O_2}}\right) + \sqrt{\frac{1}{16}\left(K_{p3} + K_{p7}\sqrt{p_{O_2}}\right)^2 + \frac{1}{2}N_N^*} \\
p_{CO_2} &= N_C^*\frac{K_{p10}\sqrt{p_{O_2}}}{1 + K_{p10}\sqrt{p_{O_2}}} \\
p_{CO} &= N_C^*\left(1 - \frac{K_{p10}\sqrt{p_{O_2}}}{1 + K_{p10}\sqrt{p_{O_2}}}\right)
\end{aligned} \tag{3.37}$$

Then the new N_O^* is calculated as

$$\begin{aligned}
N_O^* &= 2p_{CO_2} + p_{CO} + 2p_{O_2} + p_{H_2O} + p_{OH} + p_O + p_{NO} \\
&= N_C^*\frac{1 + 2K_{p10}\sqrt{p_{O_2}}}{1 + K_{p10}\sqrt{p_{O_2}}} + 2p_{O_2} + K_{p9}p_{H_2}\sqrt{p_{O_2}} + K_{p5}\sqrt{p_{O_2}}\sqrt{p_{H_2}} \\
&\quad + K_{p2}\sqrt{p_{O_2}} + K_{p7}\sqrt{p_{N_2}}\sqrt{p_{O_2}}
\end{aligned} \tag{3.38}$$

The new N_O^* should be equal to the value from the equation 3.36 if p_{O_2} is chosen correctly. Unless, p_{O_2} can be found through Newton-Raphson method. When solution of p_{O_2} is found for presumed N_N^* value, the solution for other gas species can be calculated from the equation 3.31 and 3.37. Then the sum of the partial pressure should be equal to

the system pressure as in the equation 3.32. Unless, one should adjust N_N^* until the set of partial pressures satisfy the condition. This can also be done by Newton-Raphson method.

This calculation scheme is implemented in Matlab as a function "GetEquilGrill" where inputs are p, T, F, fuel composition (n, m, l, k) and the air composition that consists of 12 species($\mathbf{b} = [b_1, b_2, ..., b_{11}]^T$). In the implementation, the different criteria for convergence of the solution for Newton-Raphson method were tried because there are two iteration loops, one including the other, and error in one solution affects the performance of iteration of the other. The error is defined as following.

$$\epsilon = \left| \frac{\Delta x}{x} \right| \tag{3.39}$$

Also the smaller the error bound is, the smoother the composition change with temperature. The numerical experiments and the prediction of composition in a given temperature range is shown in the table 3.3.2 and the figure 3.3.2. The figure also compares the result of thermodynamic calculation based on equilibrium composition and Zacharias method which will be explained in the following section. In the legend, z stands for Zacharias and CE equilibrium composition. It was found that the error bound value 0.001 for both loops provide the good results.

	Case 1	Case 2	Case 3	Case 4	Case 5	Case 6
ϵ_{N_N}	< 0.01	< 0.005	<0.005	<0.001	<0.001	<0.001
$\epsilon_{\sqrt{p_{O_2}}}$	<0.01	<0.01	<0.005	<0.01	<0.005	<0.001
time(s)	0.73265	0.72301	0.75942	0.76867	0.7723	0.83446

Table 3.10: Numerical Experiment for different error bound for Grill's method (26712 cases)

Grill stated that this method is roughly 50 times faster than the procedure proposed by Olikara in the paper [14]. However, it was found that it is twice faster in most of cases. Still it is a quite significant improvement.

Transition between non-dissociation combustion to dissociation combustion at equilibrium

As explained in the section 3.3.2, the composition is calculated by the non-dissociation scheme in the lower temperature and dissociation scheme for higher. The temperature when the transition from one to the other is varying from different literature. Grill proposed 1600K for the transition and freezing the composition [14]. In the thesis, the same value will be used.

In order to prevent discontinuity of the properties and states at the transition temperature, it is recommended to use a smooth interpolation in some range of temperature near the

transition temperature. For such a purpose, an ad hoc mixing curve can be used. The curve is defined

$$z = 3q^2 - 2q^3; \tag{3.40}$$

where,

$$q = \frac{T - T_L}{T_H - T_L}$$

T_L : Low temperature limit for transition

T_H : High temperature limit for transition.

If $T_L < T < T_H$, then the composition by both schemes are calculated and the final composition is interpolated by the curve given in the equation.

$$\mathbf{x} = (1 - z)\mathbf{x}_{\text{no-diss.}} + z\mathbf{x}_{\text{diss.}} \tag{3.41}$$

The result from the calculation scheme is shown in the figure 3.3.2

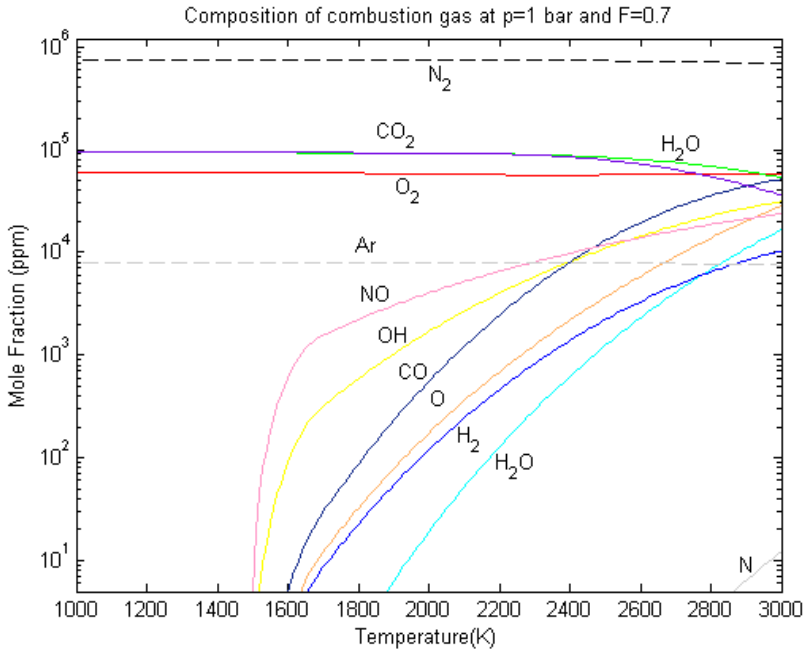

Figure 3.11: Composition of the combustion gas (CH_2 + Standard air) $T = 1800K$ and $F = 0.7$

3.3.3 Zacharias method and comparison with the composition based calculation

Apart from the general approach introduced from previous section, Zacharias' method proposed in 1967 [32] provides a fast and reliable model to calculate the thermodynamic properties of the combustion gas. It takes real gas property into account at high pressure and also dealt with dissociation in the high temperature range. The best of it is that the computation speed is incomparably faster than the general approach.

Zacharias method

In his work, Zacharias came up with mathmatical representation of enthalpy, entropy and compressibility factor of real combustion gases. The equations reflect the thermodynamic properties of burnt gases in the temperature range from 200 to 6000K and in the pressure range of 100Pa-100MPa. For the gas model, he used a modified Beattie-Bridgeman equation to take into account intermolecular forces at high pressures in the temperature range 200-1500K and in the temperature range 1500-6000 K, dissociation of up to 20 products was considered. The properties are calculated by straight forward explicit equations, therefore, without any iterative method.

The limit of the application from his work is that the coefficients to be used for the calculation is fitted only to a certain composition of the fuel. He used 85.63/14.31 for the weight ratio of carbon to hydrogen weight. This ratio can represents many common fuels available. However, if the fuel is changed to a different kind such as methane, the coefficients are not valid anymore. Therefore, it would be beneficial to use his method for only general diesel engine model with conventional fuel.

Comparison

Gas constant was calculated for comparison between the general approach and Zacharias' model. The result of calculation is shown in the figure 3.3.2. In the temperature range up to 2500K, the difference is very noticeable for high pressure above 50 bar. This is because Zacharia's model takes into account the real gas property where he used Beattie-Bridgeman equation, not ideal gas law. Also the difference is noticeable at high temperature range above 2500K. This may be caused by the different products assumed from the general approach (12 species vs. 20). For the calculation of enthalpy, the difference was not significant.

In the thesis, the general approach is used for the thermodynamic calculation in order to increase its generic capability to adapt other type of engine, especially natural gas engines in mind.

3.4 Combustion Modeling

Using the simulation model for real time or for optimization process, it is vital to have a simplified model which sufficiently fast to meet the purpose. A common way of simplification is to disregard the spatial variables is the model, that is to regard the cylinder volume as one or multiple control volumes where the states are only expressed in terms of thermodynamic properties such as pressure, temperature, mass and energy. This simplification is normally referred to 0-D model and the most common 0-D models are [28]:

- Homogeneous in-cylinder conditions
- Two zone combustion models : One zone with reactants and one zone with products.
- Multi-zone combustion models : One zone with reactants and one zone with products for each time step after the start of combustion.

In regard to the heat release rate which is prime interest from the combustion process, the one prescribed by defined net heat release rate function is usually good enough. This is called a non-predictive approach since the net heat release function is independent on the variables that may affect the combustion.[23] However, in order to simulate the combustion process variation due to the transient load, it would be valuable to have a predicted heat release model where the physical phenomena such as the charge motion in the cylinder and spray development and propagation are taken into account. This may increase the accuracy of the model with sacrifice of some simulation time.

In compromise of those two models for combustion, semi-predictive model may be considered. The correlation between the important variables, such as speed and load of the engine, and the different net heat release rate function may be found. Then a heat release function is chosen according to the operating parameters. This method is almost as fast as the non-predictive model while enhancing the accuracy of the model significantly. Therefore, semi-predictive model will be used in the thesis. Limitation is that it doesn't catch the fast transient of the heat release rate normally within the order of 20 cycles [2].

3.4.1 Rate of heat release and multi-Wiebe functions

There are several heat release rate models such as Wiebe's combustion function and Whitehouse-Way's heat release model [30]. These models are mostly empirical relation between the crank angle and the rate of heat release (ROHR). In this project, Wiebe's model will be only considered for its popularity in application and simplicity [19].

Wiebe specifies a function to describe the combustion curve for the cumulative fuel burnt as a fraction of the total fuel injected. The function is described in general:

$$x = 1 - \exp\left(-a\, y^{m+1}\right) \tag{3.42}$$

where

x : a fraction of the mass of fuel burnt relative to total mass
y : a fraction of the time realative to the duration of combustion
a, m : shape parameters

Then the rate of fuel burning can be found by differentiating the equation 3.42.

$$\frac{dx}{dy} = a\,(m+1)\, y^m\, \exp\left(-a\, y^{m+1}\right) \tag{3.43}$$

Multiplying it by the LHV and the total fuel mass will provide ROHR value. The parameter a can be found by a known combustion efficiency since x at the end of combustion is equivalent to the given combustion efficiency and it only depends on the parameter a. Then the shape of the ROHR curve depends on the parameter m. The cumulative fuel burnt and rate of fuel burnt curves are shown with different m values in the figure 3.12. The parameter a is calculated to be 6.9 assuming the combustion efficiency is 0.999.

The combustion duration is determined by defining the ignition delay and the termination of combustion. The ignition delay can be calculated according to a semi-empirical expression[15]:

$$\tau_{id} = A\, \exp\left(\frac{E_A}{RT}\right)\, p^{-n} \tag{3.44}$$

where

E_A : Apparent activation energy for the fuel autoignition process (J mol^{-1})
R : Universal gas constant (J K^{-1} mol^{-1})
T : Mean cylinder temperature (K)
p : Mean cylinder pressure (bar)
A, n : Constants dependent on the fuel

According to Wolfer[15], fuel with ceptane number greater than 50 will have $n = 1.19$, $A = 0.44$ and $E_A/R = 4650$. τ_{id} can be converted to the crank angle for further calculation and the combustion start angle will be calculated as:

$$\begin{aligned} \varphi_{id} &= \tau_{id} \cdot 180\omega/\pi \\ \varphi_{ig} &= \varphi_{inj} + \varphi_{id} \end{aligned} \tag{3.45}$$

where,

$$\omega : \text{the speed of the engine } (rad/s)$$
$$\varphi_{inj} : \text{fuel injection angle}(degree)$$

The actual point termination of combustion is irrelevant since the combustion rate decays exponentially to zero before the combustion stops. The duration of combustion can be determined by fitting the model with the actual measurement.

The single Wiebe may not be able to describe the diesel combustion well since there exits two distinct phases in the diesel combustion : the premixed part and the mixing controlled part. In addition, late combustion part which affects significantly the exhaust temperature should be accurately calculated by the function in order to predict the exhaust temperature, hence the turbine inlet condition. In this regard, three-Wiebe function is desirable to the description of the heat release rate.

In order to define the three-Wiebe function for a single combustion process, following parameters should be defined.

- Q_1 : Heat release fraction of the first Wiebe function
- Q_2 : Heat real ease fraction of the second Wiebe function
- $\Delta\varphi$: Delay of the second and third Wiebe function from the ignition in degree
- $\Delta\varphi_{\mathrm{comb}_1}$: Duration of the first Wiebe function
- $\Delta\varphi_{\mathrm{comb}_2}$: Duration of the second Wiebe function
- $\Delta\varphi_{\mathrm{comb}_3}$: Duration of the third Wiebe function
- m_1 : Shape parameter of the first Wiebe function
- m_2 : Shape parameter of the second Wiebe function
- m_3 : Shape parameter of the third Wiebe function

energy fraction and the time fraction of the premixed part should be defined as p and q. Then the equation for the total fuel burnt and the rate of fuel burnt can be expressed:

$$Q = \sum_{i=1}^{3} Q_i \left(1 - \exp\left(-a\left(y_i\right)^{m_i+1}\right)\right) \tag{3.46}$$

where,

$$Q_3 = 1 - Q_1 - Q_2$$
$$y_i = \frac{\varphi - \varphi_{\mathrm{ig}} - \Delta\varphi_i}{\Delta\varphi_{\mathrm{comb}_i}}$$
$$\Delta\varphi_1 = 0, \quad \Delta\varphi_2 = \Delta\varphi_3 = 0$$

The derivative of the equation 3.46 is

$$\frac{dQ}{dy} = \sum_{i=1}^{3} Q_i a \left(m_i + 1\right) y_i^{m_i} \exp\left(-a \left(y_i\right)^{m_i+1}\right) \tag{3.47}$$

The derivative can also be expressed with respect to time or the crank angle.

$$\begin{aligned} \frac{dQ}{d\varphi} &= \sum_{i=1}^{3} \frac{dQ}{dy_i} \frac{dy_i}{d\varphi} \\ \frac{dy_i}{d\varphi} &= \frac{1}{\Delta\varphi_{\mathrm{comb}_i}} \\ \frac{dQ}{dt} &= \frac{dQ}{d\varphi} \frac{d\varphi}{dt} = \frac{dQ}{d\varphi} 180\omega/\pi \end{aligned} \tag{3.48}$$

3.4.2 Adaptation to the specific engine model

As a ROHR curve may be unique for a specific model of the engine and a specific operating point, there's no general rules for finding the parameters for the curve given in the equation 3.46. Therefore, the specific ROHR curve for the given model and operating point has to be fitted to the measurement in this approach. The figure 3.13 shows such an manual fitting of ROHR.

There was an attempt to develop an curve-fitting tool to find the parameters using least square error method but it was not very successful as there are too many local minima for the objective function and too sensitive to the initial values. This also means that there are a number of sets of parameters for the targeted ROHR curves giving the similar results. As the parameters are not representation of the physical characteristics of the combustion, this gives difficulty of fitting.

For the intermediate operating point, the parameters may be interpolated or described by a approximate curve as the function of operating conditions may be found. The input of such a function may be the load(torque), the speed, the manifold pressure, mass of fuel injected or the fuel equivalent ratio. In the thesis, it was attempted to find the curves of the parameters in the function of the load and the speed for the test engine in the lab (Scania DC1102) but the errors of fit were not within the accuracy expected. In this regards, interpolation approach would serve better for finding the parameters for the intermediate points. The figure 3.14 shows the result of curve fitting of one parameter (Q_1) in the function of the speed(RPM) and torque(Nm) using cubic interpolation.

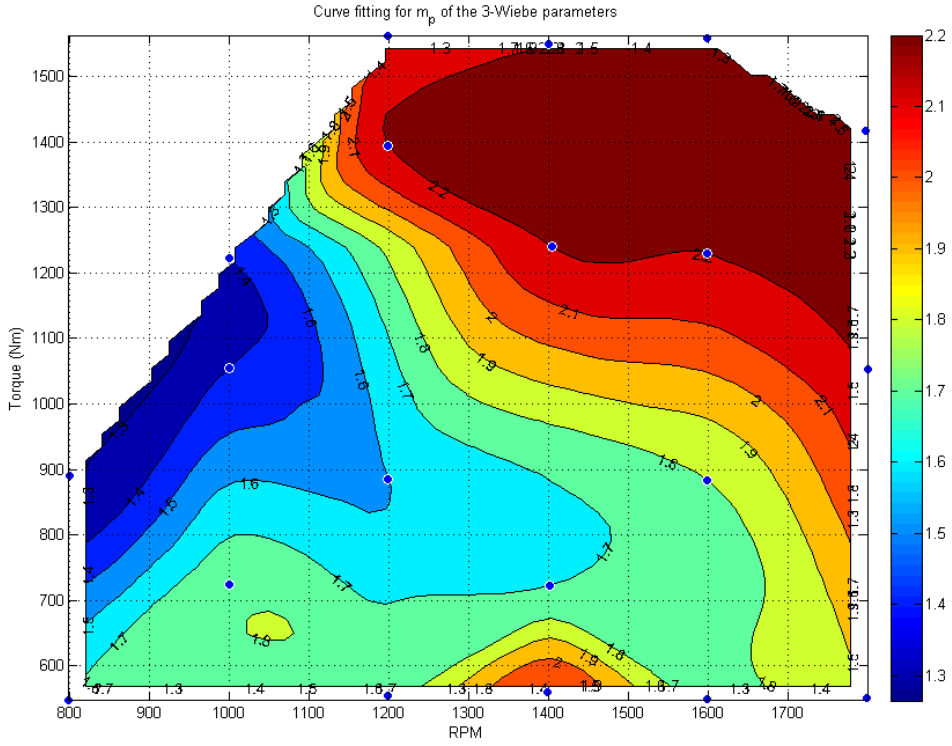

Figure 3.14: Curve fitting of m_p

3.5 Component Modeling

Based on the word bond graph shown in the figure 3.2, each component is modeled independently with clear definition of input, output and parameters as libraries. This approach will enable each model library to be used easily for other application. In the following sections, the model libraries are described with the definition of input, output and parameters, the governing laws and the calculation scheme.

3.5.1 Engine cylinder model

The cylinder model library contains the intake and exhaust valves as flow restriction into the cylinder, the control volume of the gas in the cylinder, and heat loss and power output as flow source of the energy. The model calculates the thermodynamic states of the cylinder. The input, output and parameters are defined below.

- Input : p_{in}, p_{exh}, T_{in}, T_{exh}, $\mathbf{x}_{\text{in}}$, $\mathbf{x}_{\text{exh}}$, $\dot{V}_{\text{Cyl}}$
- Output : m_{cyl}, p_{cyl}, T_{cyl}, x_{cyl}

- Parameters : Refer to the submodel description

The control volume of the cylinder model is defined as in the figure 3.16. The main assumption to be used here is that all intensive thermodynamic properties are uniform in the volume. This is called a single zone model and it is appropriate approximation for the purpose of performance prediction.

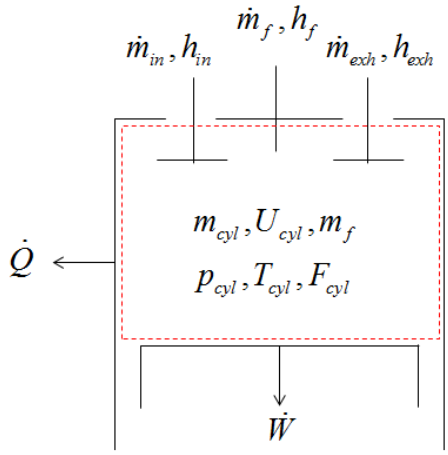

Figure 3.15: Engine Cylinder Control Volume

This can be modeled into the bond graph representation as shown in the figure 3.16.

The governing laws for the model is the conservation of mass and the first law of thermodynamics expressed respectively as:

$$\dot{m}_{cyl} = \dot{m}_{in} + \dot{m}_f - \dot{m}_{exh} \tag{3.49}$$

$$\dot{U}_{cyl} = \dot{Q} + \dot{W} + \dot{m}_{in}h_{in} + \dot{m}_f h_f - \dot{m}_{exh}h_{exh} \tag{3.50}$$

The balance of the mass and energy in the equation 3.49 and 3.50 is represented by 0-junction where the sum of the flow (energy and mass) is zero. Then the C-field element describing the cylinder chamber is used to calculate the state of the cylinder. The ROHR block is modeled to provide the mass of fuel and enthalpy from burning the fuel at the specific crank angle during the combustion. Heat loss to the environment and the work done by the control volume is modeled using the flow source to the energy of the system. The detailed description of the submodels follows below.

Intake and exhaust valve model

The valve model calculates the flow from one control volume to the other. This can be modeled as R-field in the thermodynamic bond graph. It has effort inputs from both sides and flow outputs. The inputs, outputs and model parameters are defined below.

- Input : p_1, p_2, T_1, T_2, $\mathbf{x}_1$, $\mathbf{x}_2$, φ
- Output : $\dot{m}_1$, $\dot{m}_2$, $\dot{H}_1$, $\dot{H}_2$, $\dot{\mathbf{n}}_1$, $\dot{\mathbf{n}}_2$
- Parameters : Valve profile, A_{max}

The governing law of the model is the equation for compressible flow through a flow restriction [15]. The representation is a bit altered for enhanced computation as shown below.

$$\dot{m} = \frac{A_{\text{eff}} p_{\text{in}}}{R_{\text{in}} T_{\text{in}}} k \tag{3.51}$$

where

$$k = \begin{cases} 1000\,(p_r - 1)\,\sqrt{\dfrac{2\gamma_{in}}{\gamma_{in}-1} \cdot \left(1.001^{\frac{-2}{\gamma_{in}}} - 1.001^{\frac{-\gamma_{in}-1}{\gamma_{in}}}\right)} & \text{if } p_r \leq 1.001 \\ \sqrt{\gamma_{in}\left(\dfrac{2}{\gamma_{in}+1}\right)^{\frac{\gamma_{in}+1}{\gamma_{in}-1}}} & \text{if } p_r > c \\ \sqrt{\dfrac{2\gamma_{in}}{\gamma_{in}-1}\left(p_r{}^{\frac{-2}{\gamma_{in}}} - p_r{}^{\frac{-\gamma_{in}-1}{-\gamma_{in}-1}}\right)} & \text{otherwise} \end{cases}$$

$$c = 1/p_c$$

$$p_c = (2\gamma_{in}+1)^{\frac{\gamma_{in}}{\gamma_{in}-1}}$$

A_{eff} can be obtained from the valve profile given as an external source. Typical valve profile information consists of two column where the first one denotes the crank angle and the other valve lift in mm. Given the valve profile, the A_{eff} of intake and exhaust valves can be calculated from the equation 3.52 and 3.53 respectively.

$$\begin{aligned} L_{Valve} &= \max(1.29\,L_{CAM} - 0.5, 0) && [mm] \\ C_D &= \begin{cases} 1 + 0.0825 L_{Valve} & L_{Valve} \leq 2 \\ 1.05 + 0.0575(L_{Valve} - 2) & 2 < L_{Valve} \leq 4 \\ 1.165 - 0.020625(L_{Valve} - 4) & L_{Valve} > 4 \end{cases} \\ A_{eff} &= 2 \cdot 257.106\,C_D\,L_{Valve} \times 10^{-6} && [m^2] \end{aligned} \tag{3.52}$$

$$
\begin{aligned}
L_{Valve} &= \max(1.29\, L_{CAM} - 0.7, 0) && [mm] \\
C_D &= \begin{cases} 5.1\, L_{Valve}/105, & L_{Valve} \leq 10.5 \\ 0.51 + 4.8(L_{Valve}/105 - 0.1) & 10.5 < L_{Valve} \leq 13.125 \\ 0.63 + 2.8(L_{Valve}/105 - 0.125) & 13.125 < L_{Valve} \leq 26.25 \\ 0.98 + 1.6(L_{Valve}/105 - 0.25) & 26.25 < L_{Valve} \end{cases} \\
A_{eff} &= 8659 C_D \times 10^{-6} && [m^2]
\end{aligned}
\tag{3.53}
$$

The two equations above are highly empirical fit for a specific model. In the thesis, the same equations were adapted but with adjustment of the maximum valve area. This is done by comparing the actual port area to the given value from the equation. A_R is the parameter defining the ratio. This ratio can be used for tuning the mass flow into and out of the engine as well as the valve profile.

Calculation of in-cylinder states

The states of in-cylinder system is calculated in the C-field in the thermodynamic bond graph. The inputs, outputs and parameters for the model is given below:

- Input : $\dot{m}$, $\dot{\mathbf{n}}$, $\dot{U}$, $\dot{V}$
- Output : m, $\mathbf{n}$, U, p_{Cyl}, T_{Cyl}, $\mathbf{x}_{\text{Cyl}}$
- Parameters : Cylinder number (i_{Cyl}), S, D, $\lambda_{r/S}$, compression ratio(ϵ_{comp}), $\mathbf{n}_{\text{air}}$, $\mathbf{M}_{mw}$, composition of fuel(**fc**), T_L, T_H

The integration of the input variables give states to be used for the general constitutive law expressed as

$$
\begin{aligned}
p &= \Phi_p\,(m, \mathbf{n}, E, V) \\
\mathbf{x} &= \Phi_{\mathbf{x}}\,(m, \mathbf{n}, E, V) \\
T &= \Phi_T\,(m, \mathbf{n}, E, V)
\end{aligned}
\tag{3.54}
$$

In case of no combustion, $\mathbf{x}$ can be determined from the equation 3.15. Also knowing U and m allows to find the temperature. First the specific internal energy is calculated.

$$
u = \frac{U}{m} \tag{3.55}
$$

u is explicitly expressed as a function of T as shown in the equation 3.7 and 3.8. The inverse can be also found using the Newton-Raphson method. As the function is monotonically increasing, the iteration converges fast. Having found T, p can be found from the equation of state. As the gas is assumed ideal,

$$
p = \frac{mRT}{V} \tag{3.56}
$$

In case of combustion taking place, the approach differs for finding $\mathbf{x}$. At the start of the injection when the ignition has not been started, the composition ($\mathbf{x}_{\text{air}}$) and the mass (m_{air}) of the gas are stored in the separate variables. Also the stoichiometric fuel-air ratio (f_s) is calculated based on the composition of the gas before combustion and the fuel composition. For the chemical reaction considered in the equation 3.16, it is given :

$$f_s = \frac{M_{fuel}}{N_L M_{air}} = \frac{12.0107n + 1.00794m + 15.9994l + 14.0067k}{N_L \ (\mathbf{x}^T \cdot \mathbf{M})} \tag{3.57}$$

$\mathbf{x}_{\text{air}}$, m_{air} and f_s values will not change during the cycle. When the combustion starts, the composition of the combustion gas (x_b) should be calculated with input of p, T and F (the fuel-air equivalent ratio) as variable inputs.

$$\mathbf{x}_b = \Phi_{\mathbf{x}} \left(p, T, F \right) \tag{3.58}$$

This may be a bit troublesome since p and T are output of the field. For the initial calculation, p and T from the previous time step can be used. F can be calculated as

$$F = \frac{m - m_{air}}{f_s m_{air}} \tag{3.59}$$

After temporary $\mathbf{x}_b$ is calculated, the rest of calculation is the same as in non-combustion case. However the first calculation may be inaccurate since the $\mathbf{x}_b$ is calculated from the p and T in the previous time step. $\mathbf{x}_b$ can be recalculated with new input of p and T and the updated composition can be used to calculate new p and T. This can be repeated in the iterative method until the change in the composition in the consecutive iteration is sufficiently small. In the thesis, error bound 0.001 was used for both error of p and T defined as

$$\epsilon = \frac{\Delta x}{x} \tag{3.60}$$

Rate of heat release model

The rate of heat calculates the mass flow of the fuel injected into the cylinder and the heat released from the fuel burnt. It is assumed that the fuel is burnt simultaneously as it is injected. The input, output and parameters are defined below.

- Input : p_{Cyl},T_{Cyl}, m_{air}, ω, φ, $in_{control}$
- Output : $\dot{m}_f$, $\dot{H}_f$
- Parameter : φ_{inj}, $m_{f_{max}}$, Fuel composition($\mathbf{FC}$)

At the beginning of the injection, the ignition delay is calculated as in the equation 3.44. Also the mass of fuel to be injected for the cycle is calculated as the product of the $m_{f_{max}}$ and the control input ($in_{control}$) and the Wiebe parameters for the ROHR is determined

according to the operation conditions at the same time. If the crank angle input is larger than the injection angle plus the ignition delay, then the mass of fuel is obtained from the prescribed ROHR curve.

Heat loss model

The heat loss model calculates the heat transfer from the gas in the cylinder to the cylinder wall. The input, output and parameters are defined below.

- Input : p_{Cyl},T_{Cyl}, V_{Cyl}, ω
- Output : $\dot{Q}_{\text{Loss}}$
- Parameter : $S, D, \alpha_{HT}, T_{\text{Top}}, T_{\text{Liner}}, T_{\text{Piston}}$

α_{HT} is the empirical correlating factor for heat transfer coefficient. The thesis uses a basic convective model where heat transfer equation is presented below.

$$\dot{Q}_{\text{Loss}} = hA(T_{\text{gas}} - T_{\text{w}}) \tag{3.61}$$

where h is the heat transfer coefficient and A is area of heat transfer and T_{gas} and T_{w} are temperature of the gas in the cylinder and the wall in contact respectively.

For the calculation of heat transfer coefficient, the equation is derived from the what is originally proposed by Eichelberg [12]. It is calculated as

$$h = \alpha_{HT} C_m^{1/3} \left(p_{\text{Cyl}} T_{\text{Cyl}}\right)^{1/2} \tag{3.62}$$

α_{HT} is used as an correlation factor to the specific application. Assuming that the wall temperatures of cylinder can be zoned into the cylinder head, liner and piston and the temperature of each zone is uniform, the total heat transfer can be approximated by the sum of each heat transfer rate by the equation 3.61. The liner area can be simply calculated by

$$A_{\text{Liner}} = V_{\text{Cyl}}/D \tag{3.63}$$

The model is presented bond graph method as shown in the figure 3.17

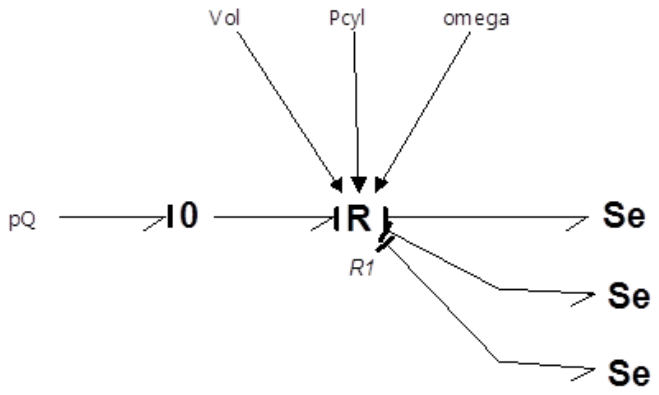

Figure 3.17: Bond Graph of Instantaneous Heat Transfer of Cylinder

3.5.2 Piping model

Piping connecting the components and manifolds are modeled as C-field similar to what's used in the cylinder model. The difference is that the volume is invariable as the pipes are assumed to be rigid and there is no combustion in the volume. It calculates the integrated states and the effort variables (m, $\mathbf{n}$, U, p, T, F) from the input of flow variables ($\dot{m}$, $\dot{\mathbf{n}}$, $\dot{U}$).

- Input : $\dot{m}$, $\mathbf{n}_dot$, $\dot{U}$
- Output : m, $\mathbf{n}$, U, p, T, $\mathbf{x}$
- Parameters : Volume (V),

The calculation scheme is identical to that of the cylinder model in non-combustion condition.

3.5.3 Turbocharger system model

Turbocharger system is used to increase the power density of the diesel engine by compressing the charge air using expanding energy of the exhaust gas. It is combination of a compressor, mostly radial type, at the end of the single shaft connected to a turbine of the radial or axial type. In order to model the compressor and turbine, performance maps provided by the manufacturer is used.

The model consists of the thermal part for each compressor and turbine and the mechanical part connecting the two parts. The calculation scheme for thermal part is identical for both compressor and turbine.

Thermal part of the turbocharger

The thesis uses the given performance map of the compressor and turbine with input of the pressure ratio, the temperature and composition of the upstream gas and rotation speed to calculate the flows through the compressor and turbine. This can be modeled by R-field in the thermodynamic domain.

- Input : p_u, p_d, T_u, $\mathbf{x}_u$, ω_{TC}
- Output : $\dot{m}$, $\dot{\mathbf{n}}$, $\dot{U}_u$, $\dot{U}_d$, Torque(Tq)
- Parameters : Turbine performance map

The performance map consists of the curves at certain corrected rotational speed (n_{298}) with horizontal coordinate of the corrected volume flow($\dot{V}_{298}$) and the vertical coordinate of the pressure ratio(p_r). It also contains the contour of the isentropic efficiency (η_{is}) and surge points. Provided with the rotational speed and pressure ratio across the turbomachinery, the mass flow and the isentropic efficiency can be found. Corrected variables are used to compensate the temperature of the upstream gas. The relation can be expressed as

$$\begin{aligned} n_{298} &= \frac{\omega_{TC}}{2\pi}\sqrt{\frac{298}{T_u}} \\ p_r &= p_d/p_r \\ \dot{V}_{298} &= \Phi_{\dot{V}}\left(n_{298}, p_r\right) \\ \eta_{is} &= \Phi_{\eta_{is}}\left(n_{298}, p_r\right) \end{aligned} \tag{3.64}$$

Having the corrected volume flow, the mass flow and molar flow can be calculated as

$$\begin{aligned} \dot{m} &= \frac{\dot{V}_{298,u}}{\sqrt{298\,T_u}}\ \frac{p_u}{R_u} \\ \dot{\mathbf{n}} &= \frac{\dot{m}}{\mathbf{M}\mathbf{x}^T}\mathbf{x} \end{aligned} \tag{3.65}$$

The change in specific enthalpy can be calculated from the isentropic efficiency as

$$\begin{aligned} T_{is} &= T_u p_r^{\frac{\gamma_u - 1}{\gamma_u}} \\ \Delta h &= \frac{\left(h_{is}(p_d\mathbf{x}_d, T_{is}) - h_u(p_u, F_u, T_u)\right)}{\eta_{is}} \end{aligned} \tag{3.66}$$

Then the specific enthalpy of the gas flowing to the downstream is calculated as

$$h_d = h_u + \Delta h \tag{3.67}$$

Energy flow from the upstream ($\dot{U}_u$) and to the downstream ($\dot{U}_d$) can be found respectively,

$$\dot{U}_u = \dot{m}h_u \qquad \dot{U}_d = \dot{m}h_d \tag{3.68}$$

The torque required or produced for the process is

$$Tq = \frac{\dot{m}\Delta h}{\omega_{TC}} \tag{3.69}$$

Mechanical part of the turbocharger

The mechanical part of the turbocharger can be modeled from the classical method in the bond graph. where 1 junction is assigned to the distinct speed and one connects the I element representing the inertial force and R element for the friction. The input of the system is Tq_{comp}, Tq_{Turb} and the output is ω_{TC}. The parameters required is the moment of inertia of the rotor and the friction parameters.

Normally, mechanical efficiency is given together with the performance map as contours on the map. This means the mechanical efficiency is found in the same manner as the isentropic efficiency of the process. Then R-element can be constructed in the way that the friction torque is proportional to the shaft torque from the turbine with coefficient of the mechanical efficiency.

$$Tq_{\text{fric}} = \eta_m Tq_{\text{Turb}} \tag{3.70}$$

Combining the thermal and mechanical part of the turbocharger, the bond graph model of the turbocharger is given in the figure 3.18.

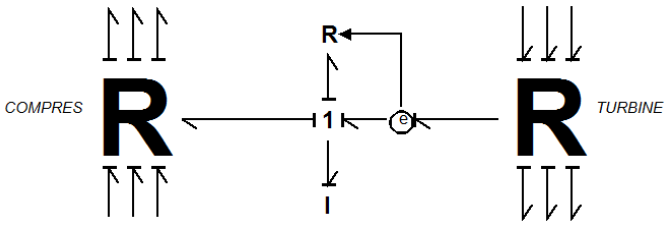

Figure 3.18: Turbocharger model

3.5.4 Mechanical model for crank shaft

The mechanical model for crank angle transforms the pressure and volume flow from the cylinder model into torque and the speed of the engine respectively or vice and versa. Also it brings the individual crank mechanism for each cylinder into single mechanical shaft. Also it contains the friction of the engine.

Crank mechanism

Firstly, the pressure in the cylinder has to be converted to the relative pressure to the crank case. This can be done by connecting the effort source to the 1-junction connected to the cylinder. Then there are two transformers that converts the pressure and volume into the torque and speed. First transformer is used to convert pressure and volume in the cylinder

into the force and the translational speed of the piston. The transformational modulus (m_1) is simply the area of the piston calculated as:

$$m_1 = \frac{\pi D^2}{4} \tag{3.71}$$

where D is the diameter of the cylinder. The second transformer is used to convert the translational force and speed into the torque and rotational speed. From the crank mechanism of the engine, the transformational modulus (m_2) can be calculated as :

$$m_2 = \frac{S}{2}\left(\sin(\varphi) + \frac{\lambda_{r/S}\sin(\varphi)\cos(\varphi)}{\sqrt{1-\left(\lambda_{r/S}\sin(\varphi)\right)^2}}\right) \tag{3.72}$$

where,

S : stroke length

φ : crank angle

$\lambda_{r/S}$: the ratio of crank rod length to the stroke length

m_2 can be calculated with the input of the crank angle which varies with the simulation. This is MTF element as explained in the section 3.2.1.

Friction

The friction of the engine is a modeled by the quadratic function of the engine speed. In the model, it contains mechanical friction of the bearings of the engines and between the piston and the liner and also parasitic work of auxiliary system. The equation used in the thesis is a rather ad hoc function which can be fitted to the real engine empirically. The quadratic function is set to be convex with the value 1 at zero speed and 0.9 at the maximum speed. The equation is given as

$$\eta_m = 1 - (1-c)\bar{\omega} - \frac{a}{1-b}\left(\bar{\omega} - b\right)\bar{\omega} \tag{3.73}$$

This quadratic model can be fitted to the measured friction from the real engine by adjusting the parameters a, b and c.

3.6 Implementation of the model

The overall model is constructed by connecting the components properly in 20-Sim software. An example of 6-cylinder engine with turbocharger is shown in the figure 3.19.

There are some additional features to the model for ease of running the simulation. Firstly, the engine governor for the speed control of the engine is modeled as a simple PI controller where input is the set point of the engine speed and measurement from the model and

output is the value between 0.2 and 1.1. The output is connected to the ROHR submodel in the cylinder model and multiplied by the maximum mass of fuel injection to determine the injected fuel for the cycle. The controller should be tuned to the specific engine model in order to achieve stable outcome.

The other feature added was the measurement unit where the performance and emission parameters as outcome of the simulation is monitored. For each signal from the simulation, a moving average is applied to fine the average value over a number of cycles. In the thesis, the period for the moving average was set to be 10 seconds to achieve the stable output for the steady state outputs.

The calculation routines for thermodynamic properties, composition of the combustion gas, the constitutive laws for the C-fields and fuel flow from ROHR curve are programmed using Matlab and converted to c++ code. Dynamic library link (dll) file is made out of the code so that routines are callable from the 20-Sim model.

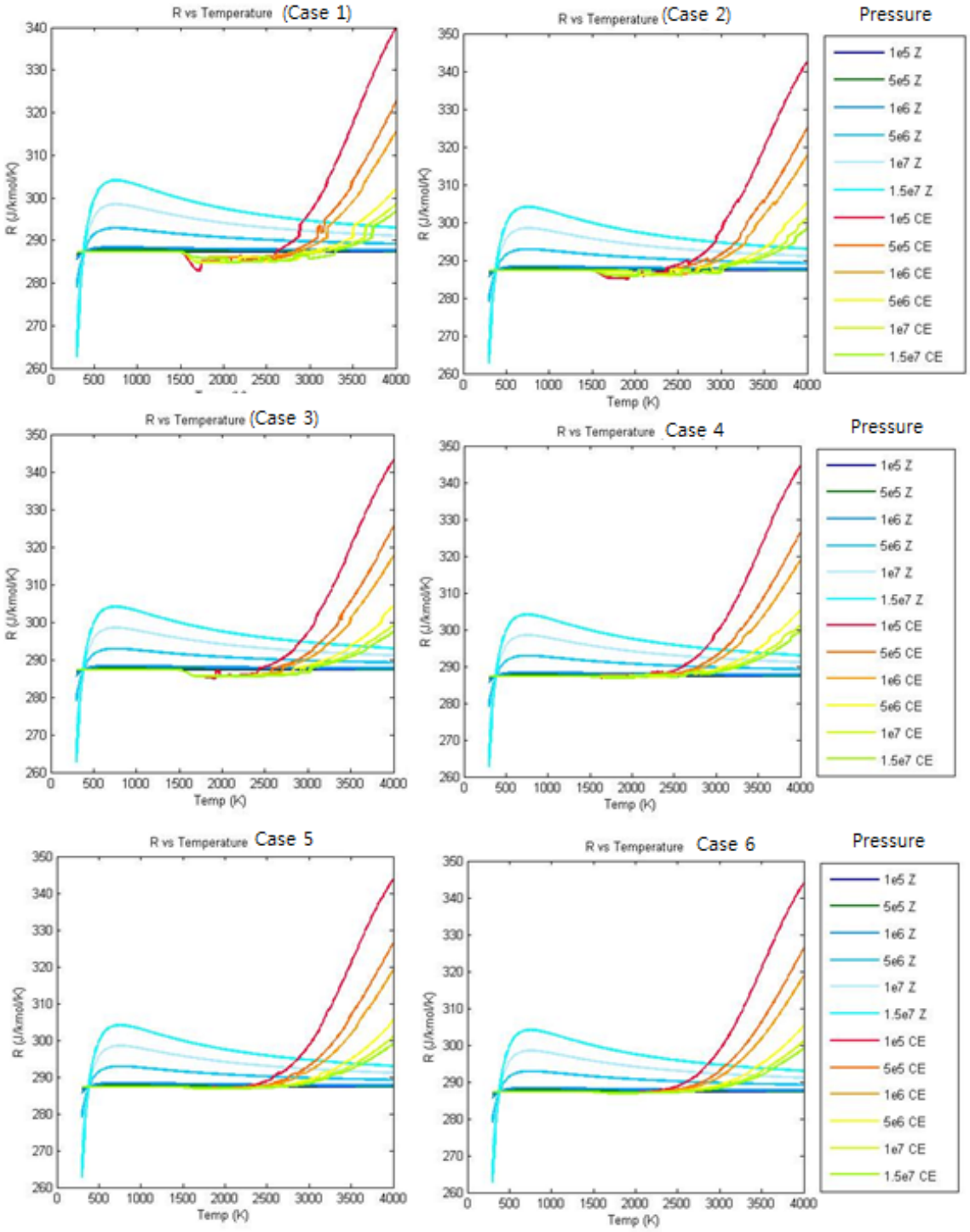

Figure 3.10: Composition of the combustion gas (CH_2 + Standard air) $T = 1800K$ and $F = 0.7$

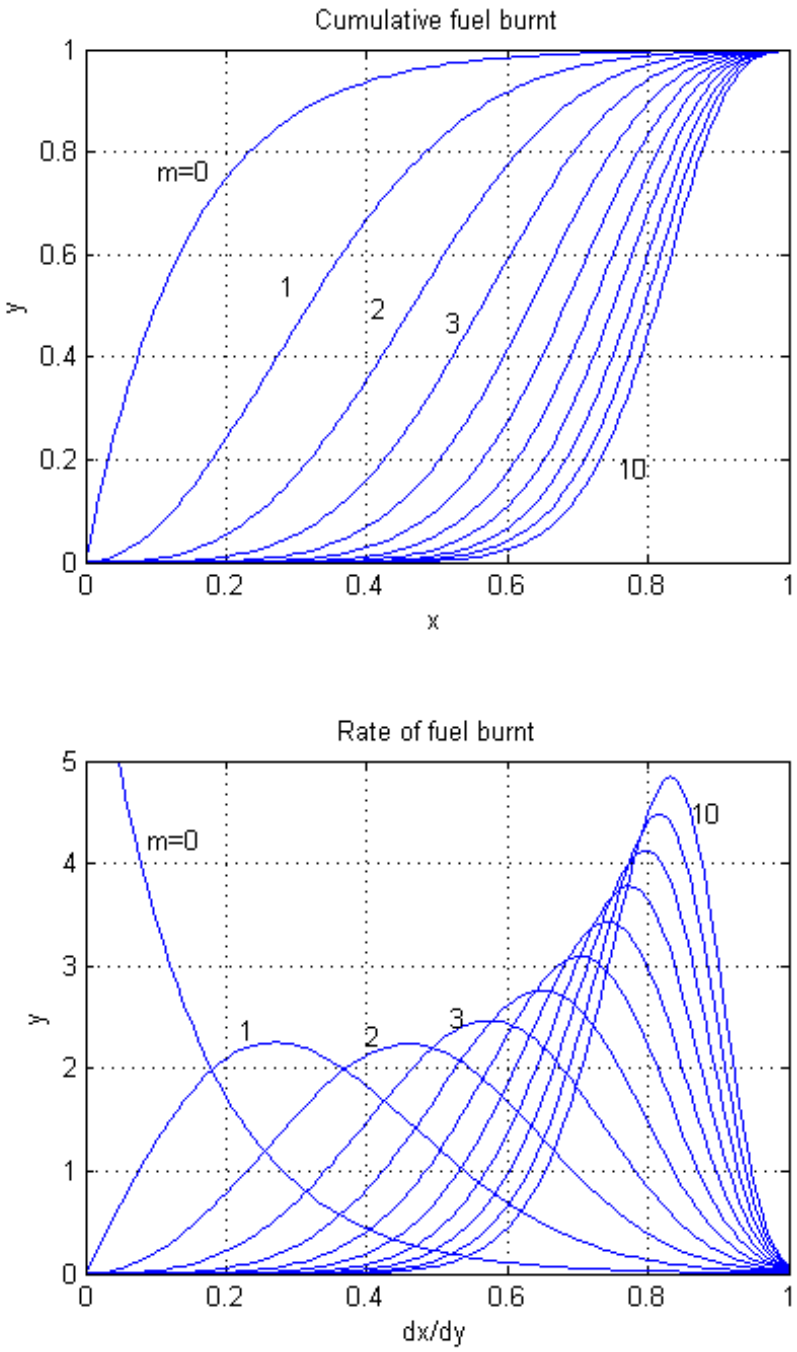

Figure 3.12: Wiebe functions for m=0,1,...,10

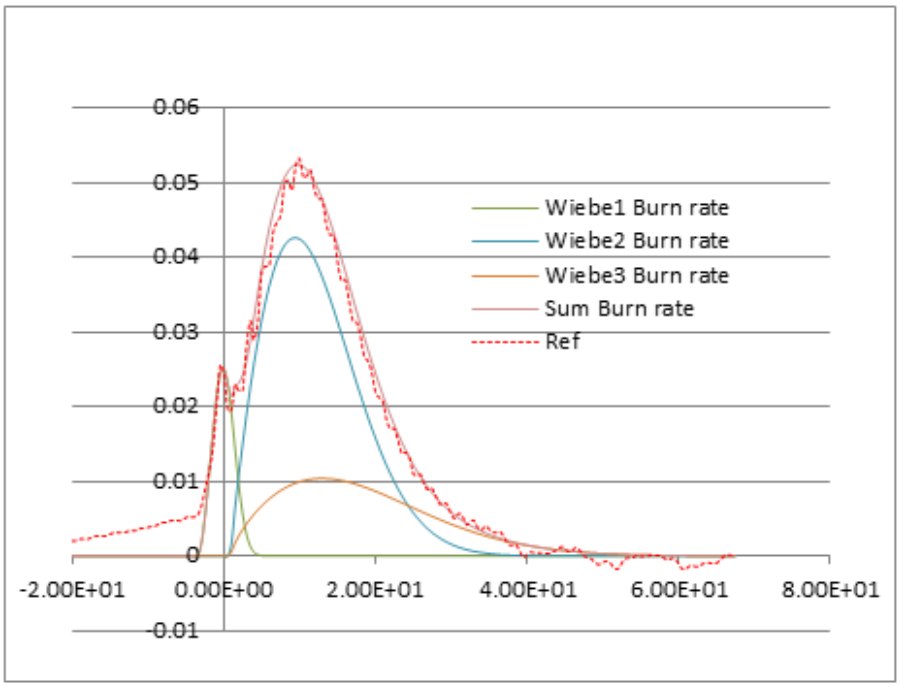

	Wiebe1	Wiebe2	Wiebe3
Fuel fraction	0.09	0.65	**0.26**
Start angle	-3.5	0.86	**0.86**
Duration	7.9	35	60
Shape parameter	1.8	0.9	0.74

Figure 3.13: Curve fitting of 3-Wiebe function to the measured ROHR

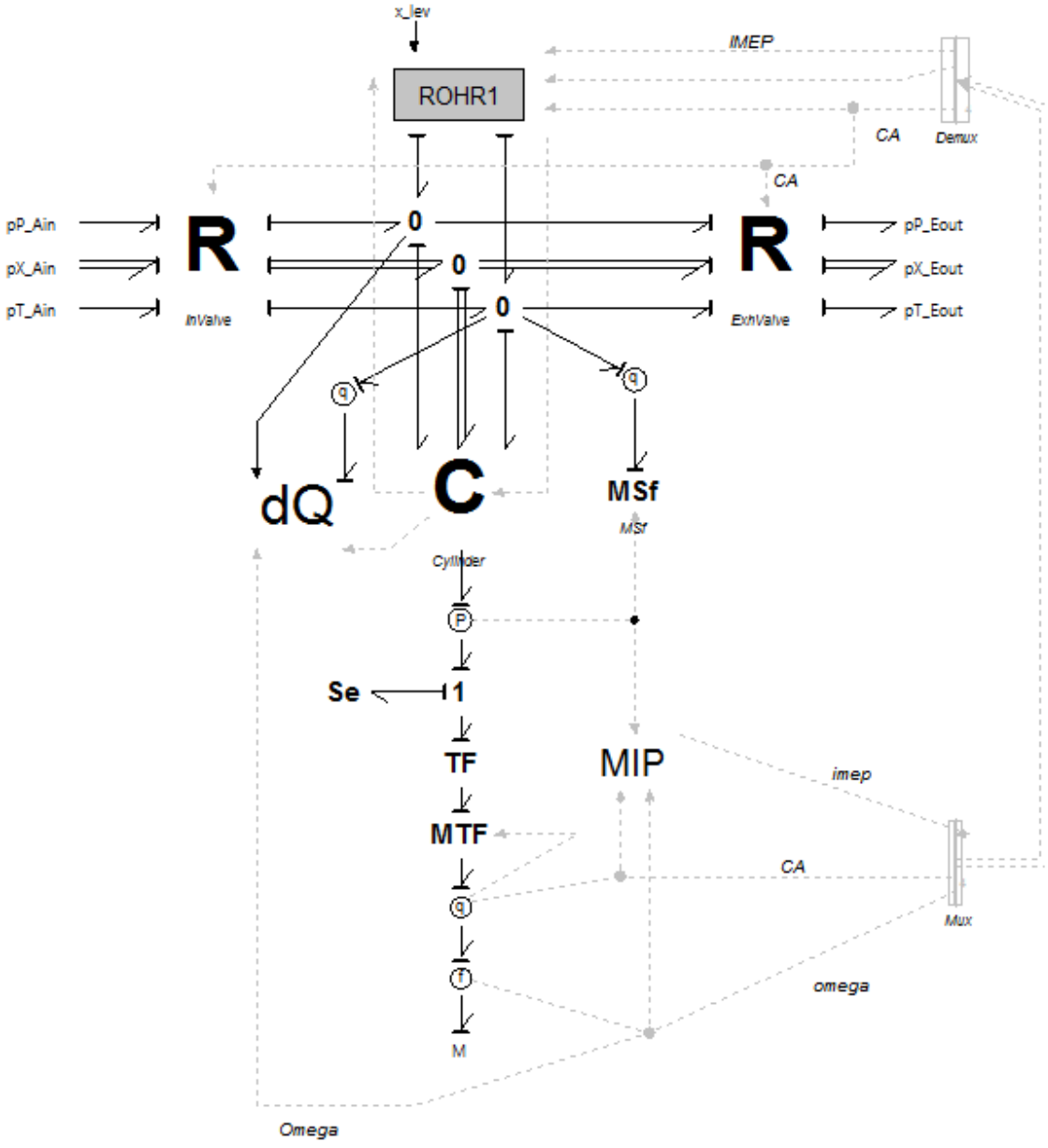

Figure 3.16: Engine Cylinder Bond Graph Model

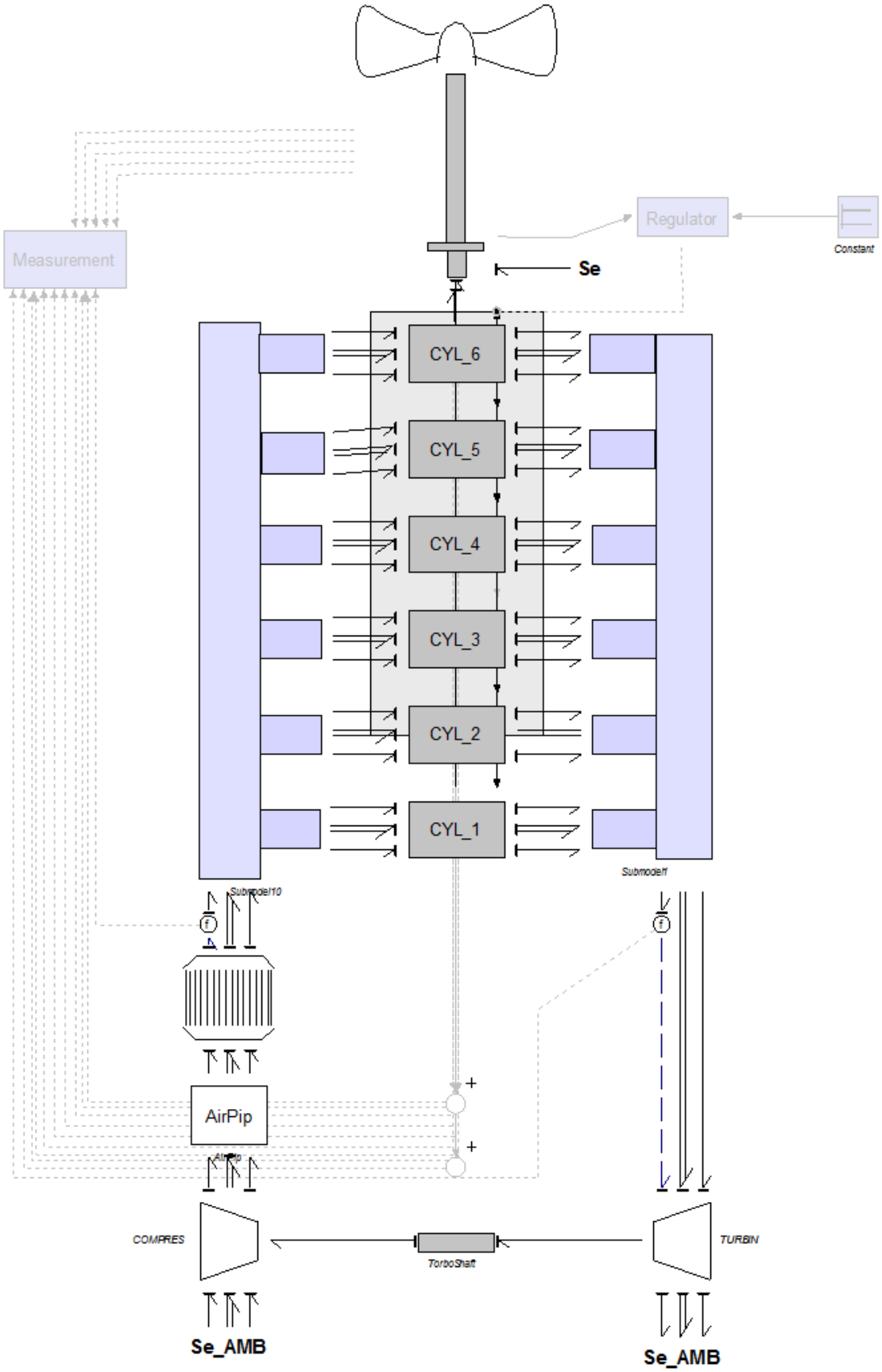

Figure 3.19: The overall model of the engine system

Chapter 4

Modeling of the NO_x emission from the engine

4.1 Modeling approach

Modeling of NO_x formation model will be based on only thermal NO_x where Zeldovich mechanism will be used. Principle of Zeldovich mechanism is explained in the chapter 2. Equilibrium assumption will be applied to simplify the formulation. When the equilibrium assumed, the rate of formation can be expressed as:

$$\frac{d[NO]}{dt} = \frac{2R_1\left\{1-\left([NO]/[NO]_e\right)^2\right\}}{1+\left([NO][NO]_e\right)R_1/\left(R_2+R_e\right)} \tag{4.1}$$

where

$R_1 = k_1^+ [O]_e [N_2]_e = k_1^- [NO]_e [N]_e$
$R_2 = k_2^+ [N]_e [O_2]_e = k_2^- [NO]_e [O]_e$
$R_3 = k_3^+ [N]_e [OH2]_e = k_3^- [NO]_e [H]_e$
[ ]: Species equilibrium concentration for the one-way equilibrium rate for reaction 2.1

Because the volume of the cylinder varies in time, the concentration is not a good choice for the state variable. It will be better to use the number of mole of NO (N_{NO}) as the state variable. Then the equation 4.1 can be expressed in the state equations with state $x = N_{NO}$ and output of the system y which is specific NO_x in g/kWh.

$$\dot{x} = V_{cyl} \cdot \frac{2R_1\left\{1-\left(x/\left(V_{cyl}\cdot[NO]_e\right)\right)^2\right\}}{1+\left(x/\left(V_{cyl}[NO]_e\right)\right)R_1/\left(R_2+R_3\right)} \tag{4.2}$$

$$y == 3600 \cdot \frac{x \cdot M_{NO}}{W_{cyl}} \tag{4.3}$$

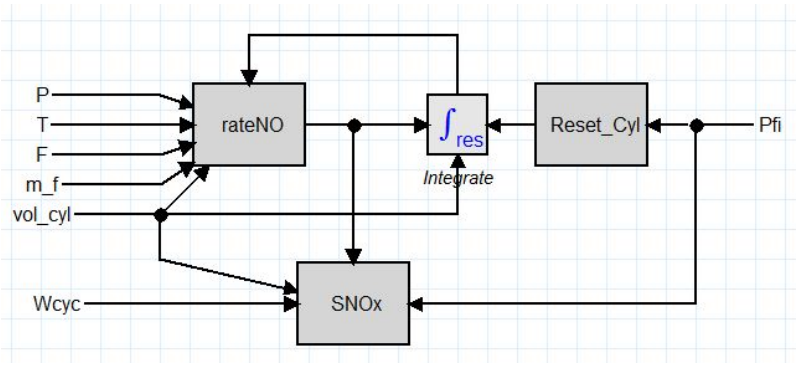

Figure 4.1: Block Diagram of NOx Calculation

where

V_{cyl}: Volume of the cylinder at time (m^3)
M_{NO}: Molar weight of NO (g/mol)
W_{cyl}: Break work of the cylinder per cycle (kJ)

The right hand side of system equation is ultimately the function of P, T, F, V_{cyl}, m_f and φ because the equilibrium concentration of a specie is given in the function of p, T, F and m_f. The calculation of the equilibrium concentration will be discussed in the next section. In this regards, the calculation of the NO_x in the cylinder is highly related to the combustion model. The block diagram of the system is shown as in the figure 4.1.

The crank angle information is necessary to reset the state after a cycle is completed since the NO formed during the combustion will be blown out with exhaust gas.

4.2 Combustion and cylinder model modification

As the thermal NO_x heavily depends on the temperature of the gas, it is crucial to determine the temperature correctly. Especially during the combustion stage, this task is a great challenge since various physical processes, such as compression or expansion, mixing of fuel with the charge air and burned gas with unburned gas, simultaneously progresses. The local temperature would vary across the cylinder volume. It is expected to observe the highest temperature in the middle of combustion zone and lowest in the volume nearest to the cylinder wall. The single zone model as explained in the section would be too rough for the estimation of the correct temperature for prediction of NO_x formation. Therefore, one easily turns to their attention to the multi-zone approach.

In the multi-zone model, the post flames zones are divided into the multiple zones. The volume of the flame front can be ignored as the residence time in the flame from is very short and the flame front is very thin in the compressed cylinder[15]. Then the simplest

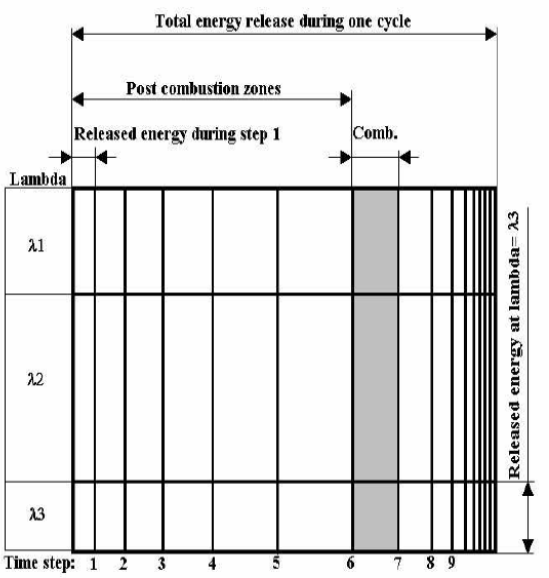

Figure 4.2: Definition of time and lambda zone

approach will be dividing the cylinder control volume into the unburned zone and burned zone. The burned zone can be further divided into the selected number of zones according to the prescribed fuel-air equivalent ratio. Egnell[11] proposed the multi-zone model where the burned gas created at each time interval of the simulation is assigned to a zone, called time zone. The new post flame zone will be created at each time interval after combustion has started. Each time zone is again divided into the multiple zones, called lambda zone, where each zone is assumed to have distinctive preset fuel-air equivalent ratio (F) or lambda. The number of distinctive F can be varied from 2 to many but three seems to lead to good accuracy according to Egnell[11]. The scheme of the division of the zone is presented in the figure 4.2

The procedure of multiple zone calculation according to Egnell[11] is presented below:

1. Determine the energy released at each time step
2. Calculate the corresponding mass of fuel being burned
3. Split the mass in different lambda zones and calculate the corresponding charge of air, residual gases, and EGR. Determine the volume of the zone and the temperature.
4. Calculate the temperature and composition of the combustion products of each lambda zone.
5. Calculate the number of NO moles formed at the combustion of each zone.
6. Update the temperature and content of old lambda zones. And calculate the number of NO moles formed during the present time step in these zones.
7. Keep the record of the total number of moles, the number of NO moles, the volumes, temperatures and species of all combusted zones and the temperature, moles

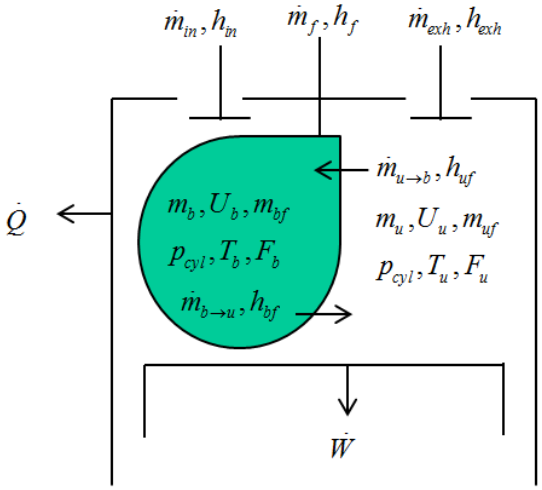

Figure 4.3: The control volume of the two-zone model

and volume of the unburned charge.

In the thesis, simple two zone model is considered and implemented in conjunction with the bond graph approach. The following section explains the challenges of such an approach and present the method for calculation.

4.2.1 Dynamic two-zone model

The control volume of the two zone can be defined as in the figure 4.3.

The following assumptions have been made to simplify the calculation without losing so much accuracy in the prediction of performance and emission.

1. The pressure is uniform for both zones.
2. The fuel is mixed and combusted instantaneously with the charge in the cylinder and produces combustion gas at the constant equivalent ratio.
3. There is no heat exchange between zones.
4. The gases are ideal.
5. The gas in the burned zone will eventually mix with the unburned gas before the opening of the exhaust valve.
6. The mass flow in and out of the cylinder only affects the mass change in the unburned zone.

The second assumption may pose some arguments since the rate of injection and the rate of heat release would not be the same physically. However, at this phase, the main interest is in building the diagnostic dynamic model adapting the two- or multi-zones and,

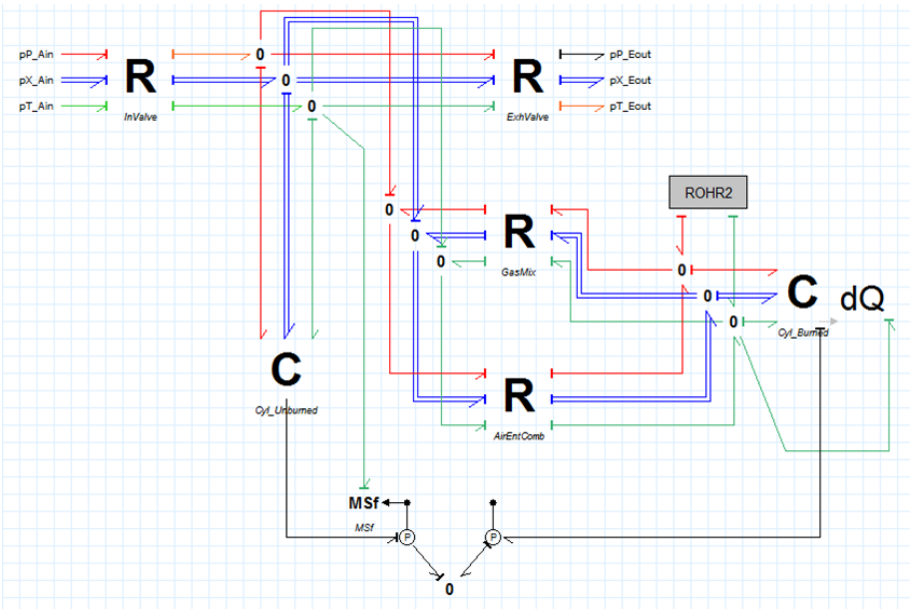

Figure 4.4: Bond graph model of 2-zone combustion

therefore, the fuel injection is assumed to be exactly same as the rate of heat release. In many literatures [11] [26], the separate mathematical models for multi-zones were built for the different stage of engine cycle, namely compression/expansion, combustion, gas exchange or only the combustion process is analyzed separately. However, in the dynamic model developed in the thesis, this transition of different model may harm the robustness of the simulation model. Therefore, the unified model for all stages of engine cycle is developed.

In order not to lose the consistency and modularity, it would be desirable to develop the two-zone modeling with bond graph approach. In this approach, each control volume of the zone is described as separate C-element. The cylinder model can be modified as in the figure 4.4 . What is particular here is that C-field of the either zone should take a pressure input, which is output of the other C-field, and the volume flow output. This is rather a relation of I element where the flow output is a function of the integration of effort. However, in the gas system within the confined volume, it is not so clear how the inertance can be defined and calculated and the physical correlation is vague. Therefore, the method is not developed further. Another approach is to have a single C-field as in the single zone model and calculate the state of the two zones within it. The states are calculated based on the assumptions and the governing equations.

Governing equations

The control volume in the cylinder is considered as C-element in the bond graph language, and therefore follows the general constitutive law:

$$[p, \mathbf{x}, T] = \Phi_{p\mathbf{x}T}\left(m, \mathbf{n}, U, V\right) \tag{4.4}$$

This can be further extended to the two-zone models.

$$[p, \mathbf{x}_u, \mathbf{x}_b, T_u, T_b] = \Phi_{2Zone}\left(m_u, m_b, \mathbf{n}_u, \mathbf{n}_b, U_u, U_b, V_u, V_b\right) \tag{4.5}$$

The challenge with the equation 4.5 is that the equation is implicit form and should be solved by the iterative method. In this method, the first law of thermodynamics, the mass conservation law and the ideal gas law are used as the governing equations. All the equations are written in the finite difference form. For any variable x, the finite difference can be expressed

$$dx = x_{k+1} - x_k \tag{4.6}$$

where k is the step number.

The mass conservation law for the zones can be expressed

$$\begin{aligned} dm_u &= dm_{in} - dm_{out} - dm_{u\to b} + dm_{b\to u} \\ dm_b &= dm_{u\to b} - dm_{b\to u} + dm_f \\ dm_{Cyl} &= dm_u + dm_b \end{aligned} \tag{4.7}$$

where,

dm_u : Change in mass of unburned gas
dm_b : Change in mass of burned gas
dm_{in} : Change in mass due to induced air
dm_{out} : Change in mass due to exhausted gas
$dm_{u\to b}$: Change in mass of unburned gas transferred to the burned zone due to combustion
$dm_{b\to u}$: Change in mass of burned gas transferred to the unburned zone due to mixing
dm_{Cyl} : Change in mass of the total gas in the cylinder

$dm_{u\to b}$ can be calculated using the assumption 2 with input of m_f as defined as

$$dm_{u\to b} = \frac{dm_f}{F f_s} \tag{4.8}$$

According to the assumption 5, mixing will be described as mass transfer of burned gas ($m_{b\to u}$) to the unburned zone. This mass transfer can be specified by the pre-defined function of the crank angle.

$$\begin{aligned} m_{b\to u} &= m_{b\to u,0}(3q^2 - 2q^3) \\ q &= \frac{\varphi - \varphi_{start}}{\varphi_{end} - \varphi_{start}} \end{aligned} \tag{4.9}$$

This is the same curve as used in the calculation of the composition in transition between non-dissociation scheme to dissociation one. This is rather an ad-hoc approach without physical meaning inside. However, the result shows that it is acceptable to use it. This mixing curve can be used for tuning parameters later when fitting to the experimental data. The total mass of the burned gas to be transferred ($m_{b\to u,0}$) can be predetermined at the start of the combustion from

$$m_{b->u,0} = m_{f,0}\frac{1 + Ff_s}{Ff_s} \tag{4.10}$$

The first law can be written for each zone as

$$\begin{aligned} dU_u &= dQ_b - dW_b + dm_{in}h_{in} - dm_{out}h_{out} - dm_{uc}h_u + dm_{b\to u}h_b \\ dU_b &= dQ_b - dW_b + dm_{uc}h_u - dm_{b\to u}h_b + dm_f h_f \\ dU_{cyl} &= dU_u + dU_b \end{aligned} \tag{4.11}$$

The specific enthalpy should be calculated from the previous state. The heat transfer to the cylinder wall is assumed to be proportional to the volume of the zone. This is rather a rough estimation since the temperature will be different in each zone. More detailed study of heat transfer model is out of scope in this thesis. Therefore, only indeterminate energy quantity is the work done by each volume whereas the sum of the works is known as an input variable. It is rather complicated to calculate this analytically but can be solved in iteration by adjusting the volume of the each zone so that the sum of work of each zone is equal to the work done by the cylinder and resulting pressure is uniform. The initial value of the work done by each volume is calculated as in ratio of the number of moles of each gas. This will result in the convergence in a step or two during the compression phase. The detailed calculation routine will be described later.

The charge and the combustion gas is assumed to be ideal gas and, therefore follows the ideal gas law as depicted as

$$\begin{aligned} pV_u &= m_u R_u T_u \\ pV_b &= m_b R_b T_b \end{aligned} \tag{4.12}$$

Calculation Procedure

1. Changes in mass of transferred mass is calculated by subtracting the mass at the previous time step from the current time step. This is done for m_{in}, m_{out}, m_f and $m_{b\to u}$ by the equation 4.6

2. Changes in mass of the zones are calculated using the equation 4.7, 4.8 and 4.9.

3. The equivalent ratio of the zones are updated according to the mass transfer and fuel injection and the equivalent ratios from the previous time step.

$$
\begin{aligned}
m_{f,u} &= (m_{u,prev} - dm_{out})\frac{F_{u,prev}f_s}{1 + F_{u,prev}f_s} + dm_{bx}\frac{F_{b,prev}f}{(1 + F_{b,prev}f_s)} \\
m_{a,u} &= (m_{u,prev})\frac{1}{(1 + F_{b,prev}f_s)} - \frac{dm_f}{Ff_s} + dm_{bx}\frac{1}{(1 + F_{b,prev}f_s)} + dm_{in} \\
m_{f,b} &= (m_{b,prev} - dm_{bx})\frac{F_{b,prev}f_s}{1 + F_{b,prev}f_s} + dm_f \\
m_{a,b} &= (m_{b,prev} - dm_{bx})\frac{1}{(1 + F_{b,prev}f_s)} + \frac{dm_f}{Ff_s} \\
F_u &= \frac{m_{f,u}}{m_{a,u}f_s} \qquad F_b = \frac{m_{f,b}}{m_{a,b}f_s}
\end{aligned}
\tag{4.13}
$$

4. The composition and number of moles of the gas specie in the unburned zone is calculated.

$$
\begin{aligned}
d\mathbf{n}_u &= \frac{dm_{in}}{\mathbf{M}^T \cdot \mathbf{x}_{air}}\mathbf{x}_{air} - \frac{dm_{out}}{\mathbf{M}^T \cdot \mathbf{x}_u}\mathbf{x}_u - \frac{dm_f}{Ff_s\mathbf{M}^T \cdot \mathbf{x}_{u0}}\mathbf{x}_{u0} + \frac{dm_{b\to u}}{\mathbf{M}^T \cdot \mathbf{x}_b}\mathbf{x}_b \\
\mathbf{n}_{u,k+1} &= \mathbf{n}_{u,k} + d\mathbf{n}_{u,k+1} \\
\mathbf{x}_u &= \frac{\mathbf{n}_u}{|\mathbf{n}_u|_1}
\end{aligned}
\tag{4.14}
$$

5. The changes in energy states (Q,W,H_{in}, H_{out}, H_{f}) and the change in volume of the cylinder(V_{cyl}) are calculated as in the procedure 1.

6. Initially it is assumed that $T_{u,k+1} = T_{u,k}$ and $\mathbf{x}_{b,k+1} = \mathbf{x}_{b,k}$. Then the volume change of each zone is initially calculated by ratio of the number of moles of gases. Volume of the zones can be calculated by adding these volume changes to the corresponding volumes in the previous time step.

$$
\begin{aligned}
dV_u &= dV_{cyl}\frac{M_b m_u}{M_b m_u + M_u m_b} \qquad & dV_b &= dV_{cyl} - dV_u \\
V_{u,k+1} &= V_{u,k} + dV_{u,k+1} & V_{b,k+1} &= V_{b,k} + dV_{b,k+1}
\end{aligned}
\tag{4.15}
$$

7. The work done by each zone is proportional to the volume change and calculated.

$$dW_u = dW_{cyl}\frac{dV_u}{dV_{cyl}} \qquad dW_b = dW_{cyl} - dW_u \tag{4.16}$$

8. Calculate the internal energy of the zones according the equation 4.11

9. Calculate pressure and temperature of the zones using the routine.

$$\begin{aligned}[p_{u,temp} \;\; T_{u,temp}] &= \Phi_{PT}\left(m_u, n_u, U_u, V_u\right) \\ [p_{b,temp} \;\; T_{b,temp}] &= \Phi_{PT}\left(m_b, n_b, U_b, V_b\right)\end{aligned} \tag{4.17}$$

10. Now with the new temperature and pressure in the burned zone and the equivalent ratio calculated in the procedure 3, the composition can be calculated by equilibrium or complete combustion scheme depending on the temperature.

$$\mathbf{x}_{b,temp} = \Phi_{\mathbf{x}_b}\left(p_{b,temp}, T_{b,temp}, F_b\right) \tag{4.18}$$

11. $\mathbf{x}_{b,\text{temp}}$is compared to the one before. This can be effectively done by comparing the average molecular weight of the gas. If the error is large then one should repeat procedure 6 to 10 with updated $\mathbf{x}_b$ and T_b. Unless, one can proceed to the next procedure.

12. Procedure 6 to 11 should be repeated until the difference between p_b and p_u are sufficiently small. The volume of the zones should be adjusted in each iteration in the way that the difference is reduced.

In order to achieve the convergence, the change in pressure due to the volume change must be carefully examined because they are not in the monotonous relation. When volume increases by a certain amount, it is uncertain if the pressure will increase or decrease. However, it is possible to derive the analytical equation for approximate estimation. From the idea gas law,

$$\Delta p = \frac{mR(T+\Delta T)}{V+\Delta V} - \frac{mRT}{V} = \frac{mR(V\Delta T - T\Delta V)}{V(V+\Delta V)} \tag{4.19}$$

The change in temperature can be also expressed as a function of the change in volume since the change in the internal energy is only dependent on the volume change provided that the other changes due to mass exchange, heat loss and combustion are fixed and the temperature is dominantly dependent on the internal energy. The internal energy in the function of temperature is given by the NASA polynomials but analytical function for the inverse does not exist. Therefore, the approximate function is found by the curve fitting.

First, internal energy is calculated in the following range of temperature (T), equivalent ratio (F) and pressure (p) presuming the composition of air ($\mathbf{x}_{\text{air}}$) and fuel (n, m, l, k) fixed:

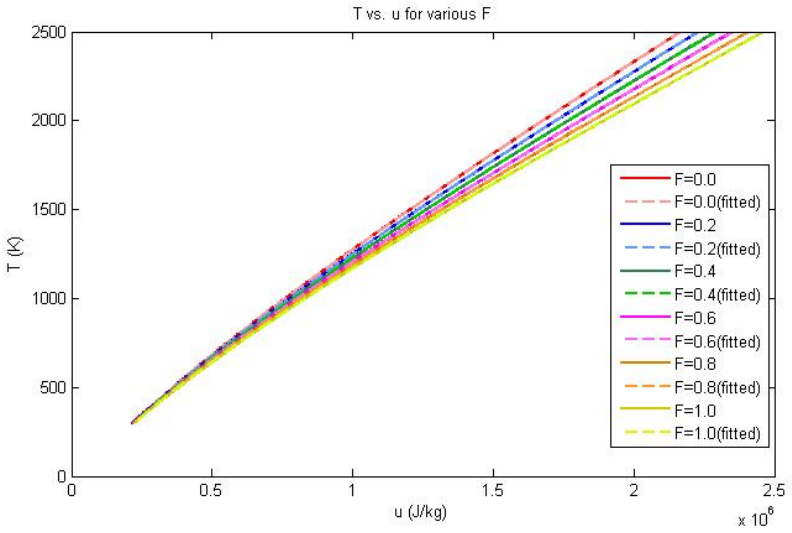

Figure 4.5: Temperature vs. Specific internal energy for various F and curve fitting

$$
\begin{aligned}
T &\in \{T : 300K \leqslant T \leqslant 2500K\} \\
p &\in \{p : 1bar \leqslant p \leqslant 100bar\} \\
F &\in \{F : 0 \leqslant p \leqslant 1\} \\
\mathbf{x}_{air} &= \left[0\ 0\ 0\ 0\ 0\ 0\ 0\ 2.095 \cdot 10^{-1}\ 0\ 2.933 \cdot 10^{-4}\ 7.809 \cdot 10^{-1}\ 9.302 \cdot 10^{-3}\right]^T \\
n &= 1,\ m = 1.8,\ l = 0,\ k = 0\ (C_n H_m O_l N_k)
\end{aligned}
$$

It is found that the pressure has negligible influence on the internal energy. Then the curve is fitted for each equivalent ratio value with the equation given

$$T(u) = a \cdot u^{0.5} + b \cdot u + c \tag{4.20}$$

The result is shown in the figure 4.5.

Having observed the curves, it is fair to assume that the change in temperature is linearly dependent on the change in specific internal energy when the change is small. In this regards, ΔT can be expressed as :

$$\Delta T = \frac{dT}{du}\frac{\Delta U}{m} \tag{4.21}$$

The derivative of the equation 4.21 yields

$$\frac{dT}{du} = 0.5a \cdot u^{-0.5} + b = a' u^{-0.5} + b \tag{4.22}$$

where the coefficients in the equation 4.22 vary with the equivalent ratio. Functions for the coefficients in the equivalent ratio can be also found by curve fitting. The result is

given in the equation 4.23 and the figure 4.6 and 4.7.

$$\begin{aligned} a' &= \text{ - } 1.428 \cdot 10^{-2} F^3 + 1.455 \cdot 10^{-4} F^2 + 2.816 \cdot 10^{-2} F + 0.3570 \\ b &= 5.102 \cdot 10^{-5} F^2 - 1.928 \cdot 10^{-4} F + 7.608 \cdot 10^{-4} \end{aligned} \tag{4.23}$$

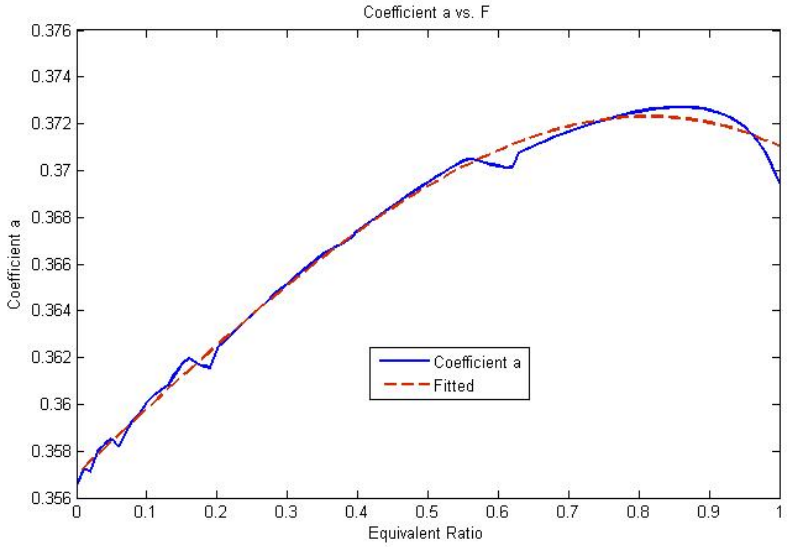

Figure 4.6: Curve fitting of the coefficient a' for dU/dt

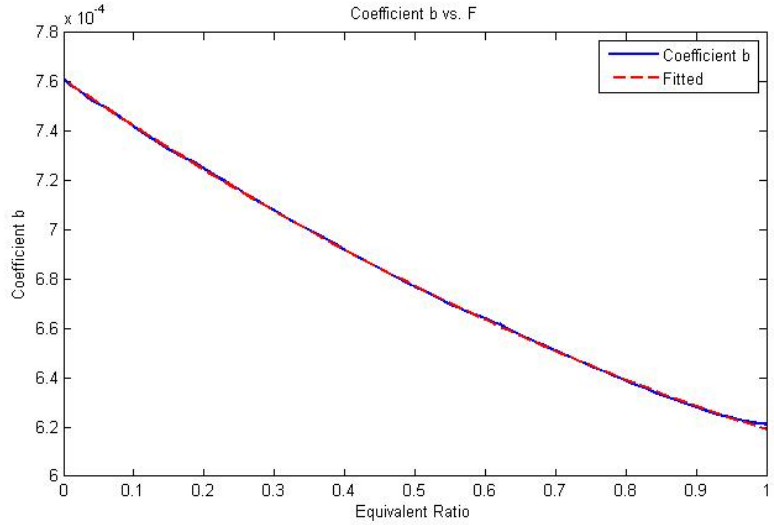

Figure 4.7: Curve fitting of the coefficient b for dU/dt

The change in the internal energy is caused by the change in volume determining the work

done by the control volume, that is:

$$\Delta U = -\Delta W = -\frac{dW_{cyl}}{dV_{cyl}}\Delta V \tag{4.24}$$

Substituting the equation 4.21 and 4.24 in the equation 4.19 :

$$\Delta p = \frac{-R\Delta V\left(V\frac{dT}{du}dW_{cyl} + TdV_{cyl}m\right)}{V(V+\Delta V)dV_{cyl}} \tag{4.25}$$

The equation 4.25 can be solved for ΔV.

$$\Delta V = -\frac{V^2\Delta p\, dV_{cyl}}{V\Delta p\, dV_{cyl} + R\left(\frac{dT}{du}V\, dW_{cyl} + T\, dV_{cyl}\, m\right)} \tag{4.26}$$

The equation 4.26 can be used for the update law by knowing the pressure difference in calculation between the zones and put the half the value of the difference as in order to prevent overshooting in iteration.

This method has proven that it converges very fast in most cases. The average number of iteration steps for the converges is within 1.05 over all engine cycles when the error bound is given $|(p_u - p_b)/p_u| < 0.001$.

It is often observed that the routine fails to converge and leading to negative pressure and temperature. This rises from the numerical problem where more than one model calculations are performed during a single time step prescribed. In such step, there may be a case where the work done for the time step and the volume difference have an opposite sign, that is:

$$\frac{dW_{cyl}}{dV_{cyl}} < 0 \tag{4.27}$$

This deteriorate the assumption that

$$dW_{cyl} = p \cdot dV_{cyl} \tag{4.28}$$

and hence the relation in the equation 4.24. A quick way to solve this would be modifying the equations 4.16 and 4.24 to

$$dW_u = \left|\frac{dW_{cyl}}{dV_{cyl}}\right| dV_u \qquad\qquad dW_b = dW_{cyl} - dW_u \tag{4.29}$$

$$\Delta U = -\Delta W = -\left|\frac{dW_{cyl}}{dV_{cyl}}\right| \Delta V \tag{4.30}$$

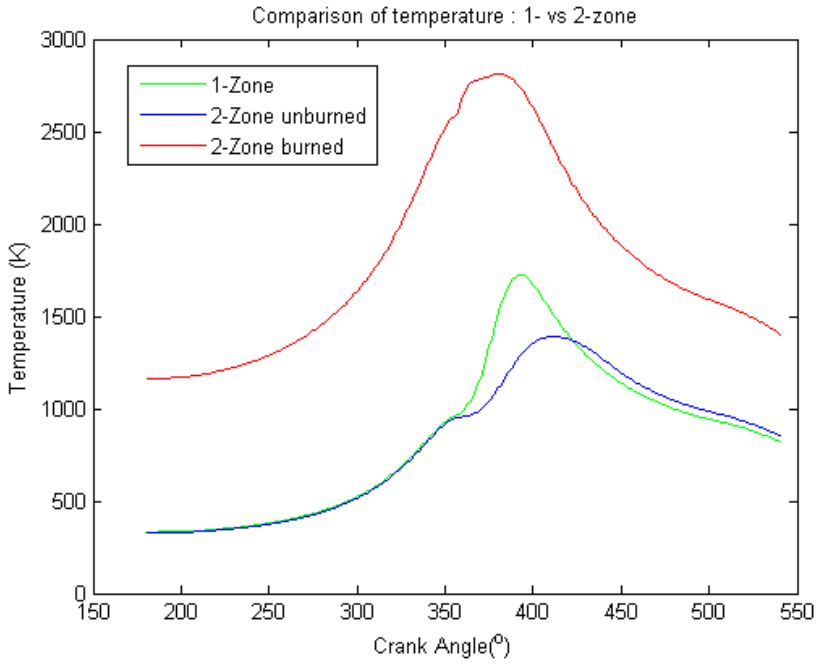

Figure 4.8: Comparison of temperature : 1- vs. 2-zone

4.2.2 Comparison with single zone

From the single zone model where the temperature is uniform in the cylinder, the prediction of NO_x was not really possible as the temperature is too low. In contrast, the prediction from the two-zone approach shows much more sensible result. A simulation was run for the laboratory engine, SCANIA DC1102 as described in the table tab:EngineSpec for the case of 1797RPM and BMEP 16.7 bar. From the single zone model, the prediction came out to be 3.87e-4 which is far lower than the measured value 6.13 g/kWh. In contrast, the two zone model resulted in 6.59 g/kWh which is reasonably accurate. This result justifies the use of the multi-zone, at least two-zone model, for the prediction of NO_x emission. The figure 4.8 shows the prediction of in-cylinder temperature of the single zone and the two-zone model.

Chapter 5

Engine Test and Comparison with the Simulation

As a model of the physical process intrinsically contains the uncertainty, it is important to validate the model with the real measurement from the controlled laboratory result. The uncertainty rises due to the limited range of application of main assumptions, oversimplification of the process and different environmental factors not accounted by the model. The uncertainty is the price to pay for the efficient modeling but the balance with the accuracy and defining the range of application is necessary.

In the thesis, the test setup, the measurement from the diesel engine connected to a hydraulic dynamometer and analysis of the data to represent the performance and emission data of the engine is presented.

5.1 Test setup

A steady state measurement of the test engine located in the machinery laboratory in NTNU is performed. Unfortunately the dynamometer in the laboratory was not capable of producing controllable load suitable for transient measurement. Also the sensors for temperature, pressure and emission were not designed for the full dynamic measurement in general. In this regard, the goal of the test was set to validate the engine model in the steady state operation.

The test setup used for the measurement is schematically shown in the figure 5.1.

The engine to be tested has the specifications given in the table 5.1

The cases of the tests has been set up so that they cover the most of the operation range of the engine. In this way, one can build a performance and emission map in different operation points. The test cases are given in the table 5.2

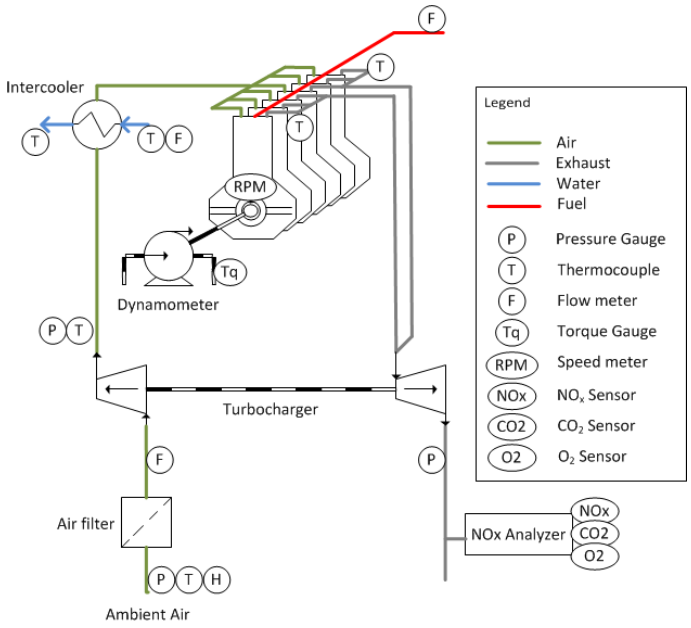

Figure 5.1: Engine Test Setup

For the steady state measurements, it is necessary to make sure that all the transient effects are stabilized. The transient effect due to turbo-lag and rotating inertia vanishes relatively shortly, in the order of several to tens of seconds. However, thermal loading of the engine attributes to the slow convergence to the steady state which is in the order of tens of minutes depending on the size step change in operation points applied. Therefore, some criteria should be set up in order to get rid of the transient influence. The criteria used in the test was $\pm 0.5\%$ for 4 minutes. This was verified by performing the linear regression on the acquired data. Then the average value of the time series of measurements can be taken as a representative value for the case.

In addition, dynamic in-cylinder pressure is also measured and recorded every 0.5 degree of crank angle. The full dynamic pressure data allows to monitor the pressure change in the cylinder through various cycles and enables to perform ROHR analysis. The ROHR analysis had been implemented in the data acquisition system and produced ROHR curve directly. The thesis uses the result of automated calculation for ROHR analysis.

From the raw measurements, some performance and emission parameters are to be calculated according to the ISO standard. This will be explained in the next section.

5.2 Analysis of the test result

The analysis of the test results must be carried out by the recognized standard so that the performance parameters calculated can be accepted as valid. The performance parameters interested in the thesis are BMEP, BSFC, Power, mass of fuel per cycle, mass flow of air

	Specifications
Model	Scania DC1102
Cylinder configuration	In-line engine
Number of cylinders	6
Cylinder bore	127.0 mm
Stroke	140 mm
Displacement Volume	10.64 dm3
Moment of inertia	2.8 kgm2
Firing sequence	1-5-3-6-2-4
Injection	4-stroke
Principle of operation	4-stroke
Maximum power	280 kW at 1800 RPM
Maximum torque	1750 Nm
Maximum speed	1800 RPM
Speed for maximum torque	1080 1500 RPM
Minimum BSFC	191g/kWh at 1300 RPM

Table 5.1: Specifications of the test engine

and exhaust and emission factors of NO_{x} and CO_2

Firstly, the composition of fuel and the composition of the air should be defined. The available information for the fuel is that it is MGO according to ISO 8217(2012). However, it doesn't give much information of the properties of interest such as the density, fuel composition, ignition point and viscosity. This is due to the large variance of the characteristics within the certain range specified in the standard. Also the term, MGO, is a little bit vague in defining the characteristics of the fuel. Therefore, the fuel data provided by a reference will be used for the analysis as given in the table 5.4 [29].

Also the dry air is assumed to be standard air which consists of oxygen, nitrogen, argon and carbon dioxide and their mole fraction is given 0.20950, 0.78090, 0.0093019 and 0.00029330 respectively. With the humidity measurement considered, the actual air containing water vapor can be calculated. The formula for such calculation are available from ISO 8178(2012).

As the ventury flow meter is used to measure the air flow, the measured value is the differential pressure across the ventury. This has to be converted to the mass flow according to the characteristic curve of the ventury.

The mass flow of exhaust can be calculated according to either the mass balance or the atomic balance. As the information of fuel flow is available, the mass balance method is used in the thesis. The mass of exhaust is then the sum of mass flow of air and fuel.

The emission from the exhaust gas was measured by the portable gas analyzer (PG-250) manufactured by Horiba. The response time of the analyzer is 45 seconds which is not suitable for transient measurement. Measurement of gas emission provides the volume

Table 5.2: Add caption

		Torque (Nm)						
BMEP (bar)		18.5	16.5	14.5	12.5	10.5	8.5	6.5
RPM	1800		1397		1058			550
	1600	1567		1228		889		550
	1400	1567		1228			720	550
	1200	1567	1397			889		550
	1000	1567			1058		720	
	800					889		550

Table 5.3: Cases of test for steady state engine operation

Viscosity at 50 ° C (mm2/s)			3.1
Density at 15 ° C (kg/m3)			0.852
Effective heating value (MJ/kg)			42.65
Composition	Wt%(%)	M(g/mol)	Mol%
Carbon	86.39	12.001	0.354751
Hydrogen	13.18	1.00794	0.644239
Sulphur	0.23	32.065	0.000352
Nitrogen	0.10	14.0067	0.00035
Oxygen	0.10	15.9994	0.000307

Table 5.4: Fuel Characteristics of Marine Gas Oil

fraction of the emission to the exhaust gas. For better comprehension of the level of emission, the specific values of the measurements should be calculated. These specific values are called the emission factor in unit of mass per kWh. This calculation can be done by the method specified in ISO 8178-1(2006).

Finally the performance parameters are calculated as

$$\begin{aligned} \dot{m}_f &= \rho_f \dot{V}_f && \text{Fuel flow (g/s)} \\ P &= \frac{\pi T q n_{\text{RPM}}}{30000} && \text{Shaft Power (kW)} \\ BSFC &= \frac{\dot{m}_f}{3600P} && \text{Brake Specific Fuel Consumption (g/kWh)} \\ m_{f_{\text{cyc}}} &= \frac{120\dot{m}_f}{n_{\text{RPM}} k_{\text{cyl}}} && \text{Mass of fuel injected per cycle (g/cyc)} \end{aligned} \tag{5.1}$$

With the performance and emission parameters calculated, the performance and emission

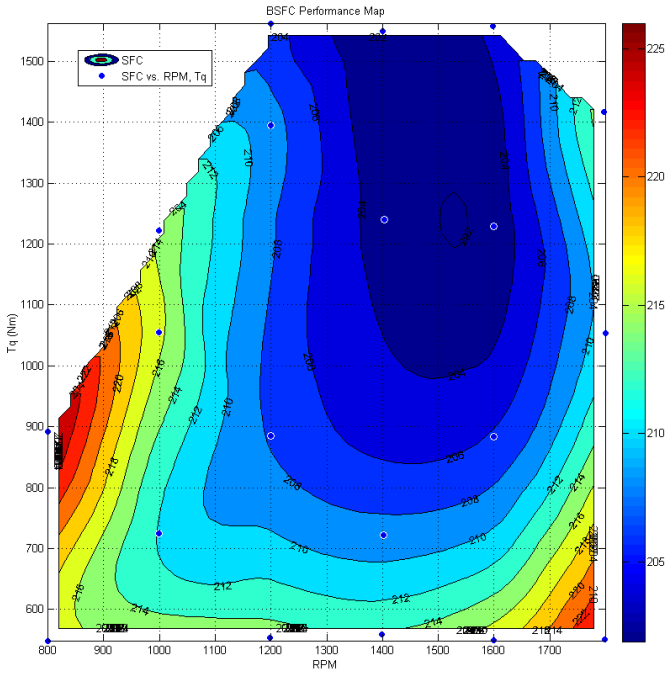

Figure 5.2: BSFC Performance Map

map can be constructed using curve fitting. The result is shown in the figure 5.2 and 5.3.

5.3 Comparison with the simulation result and tuning the model

5.3.1 Adaptation of the model to the specific engine

The engine is modeled with the complete model described in the chapter 3. The specific information required for modeling should contain

- Engine specification as in the table 5.1
- Valve profile
- Turbocharger performance map
- Intercooler effectivity curves
- ROHR curve from the measurement
- Injection timing of the fuel

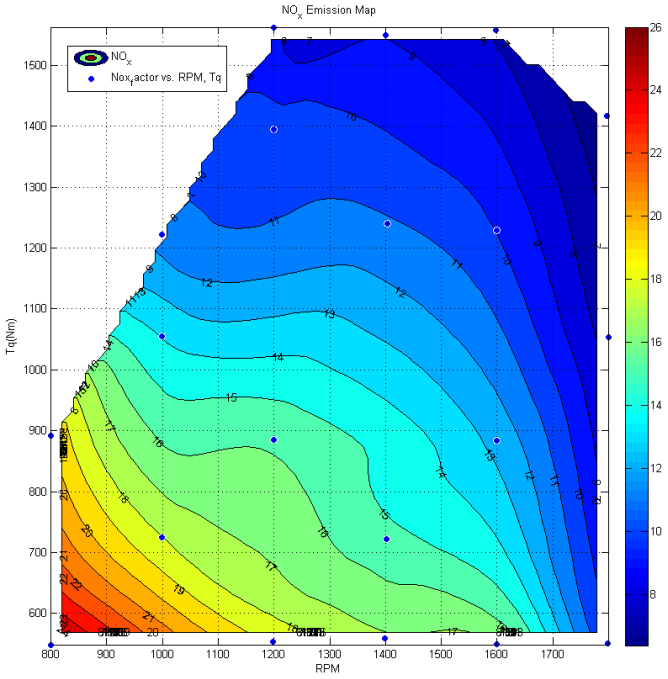

Figure 5.3: NO_x Emission Map

- Maximum mass of fuel injected per cycle
- Fuel composition
- Temperature of the cylinder head, wall and piston

Unfortunately, the turbocharger performance map could not be obtained from the manufacturer. The speed pickup for the rotational speed of the turbocharger was also unavailable from the current laboratory setup. Therefore, the turbocharger and intercooler component could not be modeled with reasonable accuracy. As the measurements to be compared is done at the steady state, the model excluded these parts and the constant manifold pressure and temperature at air inlet has been assumed instead. The constant manifold pressure and temperature can be obtained by averaging the measured values.

ROHR curve could be obtained from the dynamic cylinder pressure measurement. The pressure in the cylinder number 1 is measured every 0.5 crank angle and the pressure trace is can be analyzed to produce the rate of heat release. However, there are a great extent of uncertainty with regard to this analysis. Firstly, the heat transfer from the engine is not measured and, therefore, the net heat release rate was obtained only by the assumed heat transfer profile during the combustion. Secondly the accuracy of the crank angle for the corresponding pressure is a challenging and affects greatly on the ROHR analysis. Lastly the accuracy of pressure contributes to the uncertainty since the measurements are in gauge and converted to absolute value to be used for the analysis. These systematic

error was observed in the ROHR analysis obtained from the automated routine used in the lab. Having obtained the ROHR curves, the parameters of the three-Wiebe functions can be found by manual curve fitting for each case of the test and be used in the model. The injection timing has to be manually tuned while running the simulation as the injection profile was not available in the test setup.

Maximum mass of fuel injected per cycle can be found from the performance curve from the manufacturer of the engine where BSFC, maximum torque and power is available for a range of the engine speed. The mass of fuel mass injected per cycle is calculated as

$$m_{f\,cyc} = \frac{BSFC \cdot P_e}{30 i_{\text{cyl}} n_{\text{RPM}}} \tag{5.2}$$

The maximum value is then 0.203825g at 1080 RPM. The fuel composition is assumed as presented in the table /reftab:FuelChar.

The temperature of the cylinder head, wall and piston was assumed to be fixed during simulation and also for all cases. The value used in the thesis are $T_{\text{head}} = 550$, $T_{\text{wall}} = 550$ and $T_{\text{piston}} = 530$

For the simulation run, proper integration method should be selected with appropriate time step. In the thesis, Runge-Kutta 4 method is selected with time step of 0.0001 second. This would ensure a stable simulation with reasonable accuracy and computation time.

5.3.2 Result of the simulation and comparison

Having the parameters input for the model, the a set of 20 simulation cases shown in the table 5.5 were run and compared with the measurements. The first set of the simulation cases was done with the assumption that $F = 1$ in the burned zone. The result is shown in the figure 5.4. Also the performance and emission map for the simulation cases are presented in the figure 5.5.

The comparison shows that the prediction is not quite correct without any tuning of the model. However, it shows the similar trend at the same level of RPM for most of data except a few cases in NO_{x} factor especially in the low torque cases below 1000 Nm. Also the NO_{x} prediction doesn't vary as much as in the measured cases for different cases. The main reason for this is because the F value in the burned gas is fixed. The influence of the value of F with regard to the prediction of NO_{x} will be discussed in the next section. Also the air flows deviate too much for some cases. By simple calculation, the flow and the pressure doesn't match in most cases. Having discussed with the technician at the laboratory, it was found the accuracy of the flow meter haven't been verified or calibrated for a long time. Therefore, the air and exhaust flow data couldn't be compared in the thesis.

Prediction of BSFC from the simulation model has a significant deviation in the values. There are number of factors contributing to those errors. The primary cause of the error

Table 5.5: Add caption

case	RPM	Torque (Nm)	p_{in}	p_{exh}
1	799	549	1.087	1.065
2	799	891	1.187	1.163
3	999	724	1.243	1.218
4	999	1055	1.421	1.392
5	999	1222	1.565	1.533
6	1199	554	1.216	1.192
7	1199	886	1.441	1.412
8	1199	1395	1.867	1.830
9	1199	1563	2.065	2.024
10	1399	559	1.290	1.264
11	1401	722	1.429	1.401
12	1404	1240	1.924	1.885
13	1400	1549	2.305	2.258
14	1599	549	1.361	1.334
15	1599	883	1.708	1.674
16	1599	1229	2.105	2.063
17	1599	1558	2.540	2.490
18	1799	551	1.478	1.449
19	1799	1054	2.097	2.055
20	1797	1417	2.604	2.552

Table 5.6: Simulation Cases for $F_b = 1$

is expected to come from the error in the ROHR analysis of the measured in-cylinder pressure. As ROHR analysis is out of scope in the thesis, this couldn't be verified in depth. However, the shape of ROHR curve obtained from the laboratory suggests that there are potential errors. The systematic errors in ROHR analysis are caused by the following [24]:

- Signal processing error : The analogue pressure signal is converted to the digital numeric values with limited numerical accuracy
- Pressure reference error : As the in-cylinder pressure transducer is measuring the pressure relative to some arbitrary level, the absolute pressure may be incorrect.
- Crank angle error : The angle is measured using a code disk that gives a pulse signal at every 0.5 degree. The error due to the deformation of the crank mechanism or the pulse itself is difficult to adjust to the true value
- The pressure pulse : During combustion, the pressure waves are present in the cylinder and, therefore, it is difficult to find the representative value.
- Thermodynamic property error : In the analysis, heat capacity ratio is used for

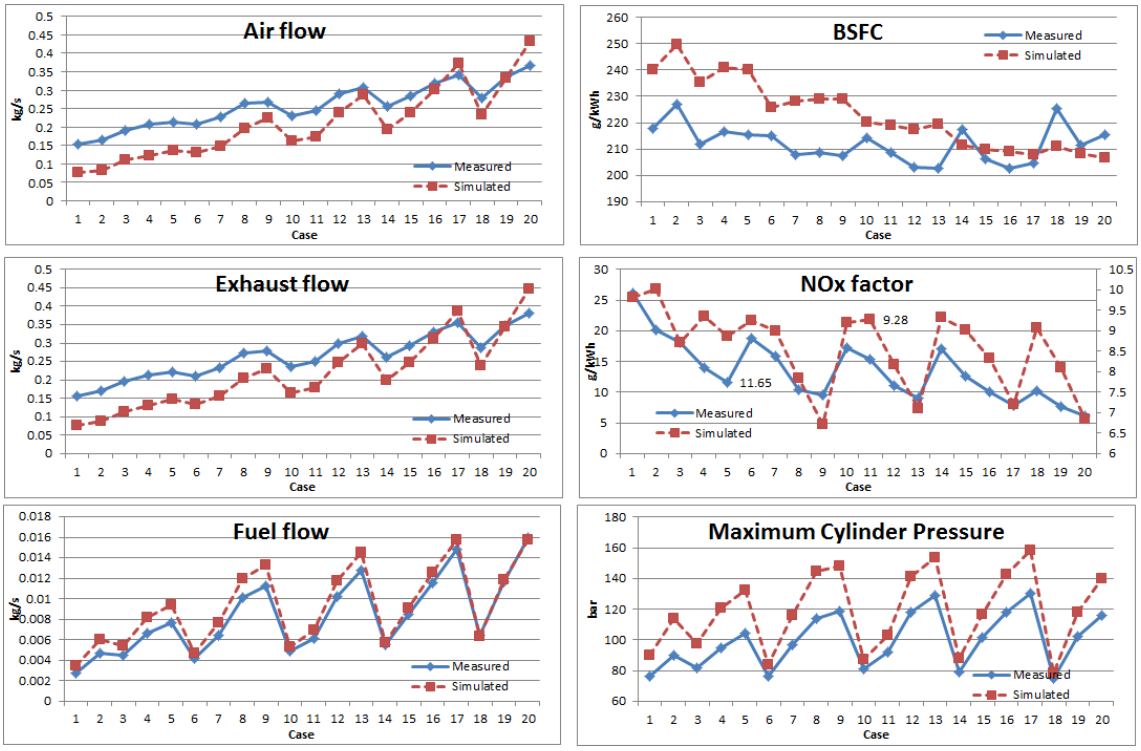

Figure 5.4: Comparison of simulation with test results

prediction of ROHR. As the ratio changes over combustion progress depending on the p, T and F, using static values for different operating cases may lead to an error.

As ROHR is the main key information for the prediction of performance and emission, this has to be improved with better accuracy over different operating conditions.

Another reason for the error in BSFC is the incorrect prediction of the friction loss. In the thesis, the friction loss is modeled using a simple quadratic function. However, it may deviate significantly from the real engine's characteristics. Also heat transfer model may contribute some as the static temperature is used for all cases.

5.3.3 Parametric study of the model

As mentioned in the previous section, the prediction of NO_x is not fairly accurate if the related parameters are not tuned. In the thesis, possible tuning parameters for the NO_x combustion without affecting the performance are the fuel-air equivalent ratio (F) in the burned zone and the mixing parameters determining the rate of mass transfer from the burned zone back to the unburned.

The most affective parameter is the fuel-air equivalent ratio F in the burned zone. Physically, F in the burned zone will vary over the combustion progress starting high in the beginning and low at the end. This may be modeled by varying F value in time in the

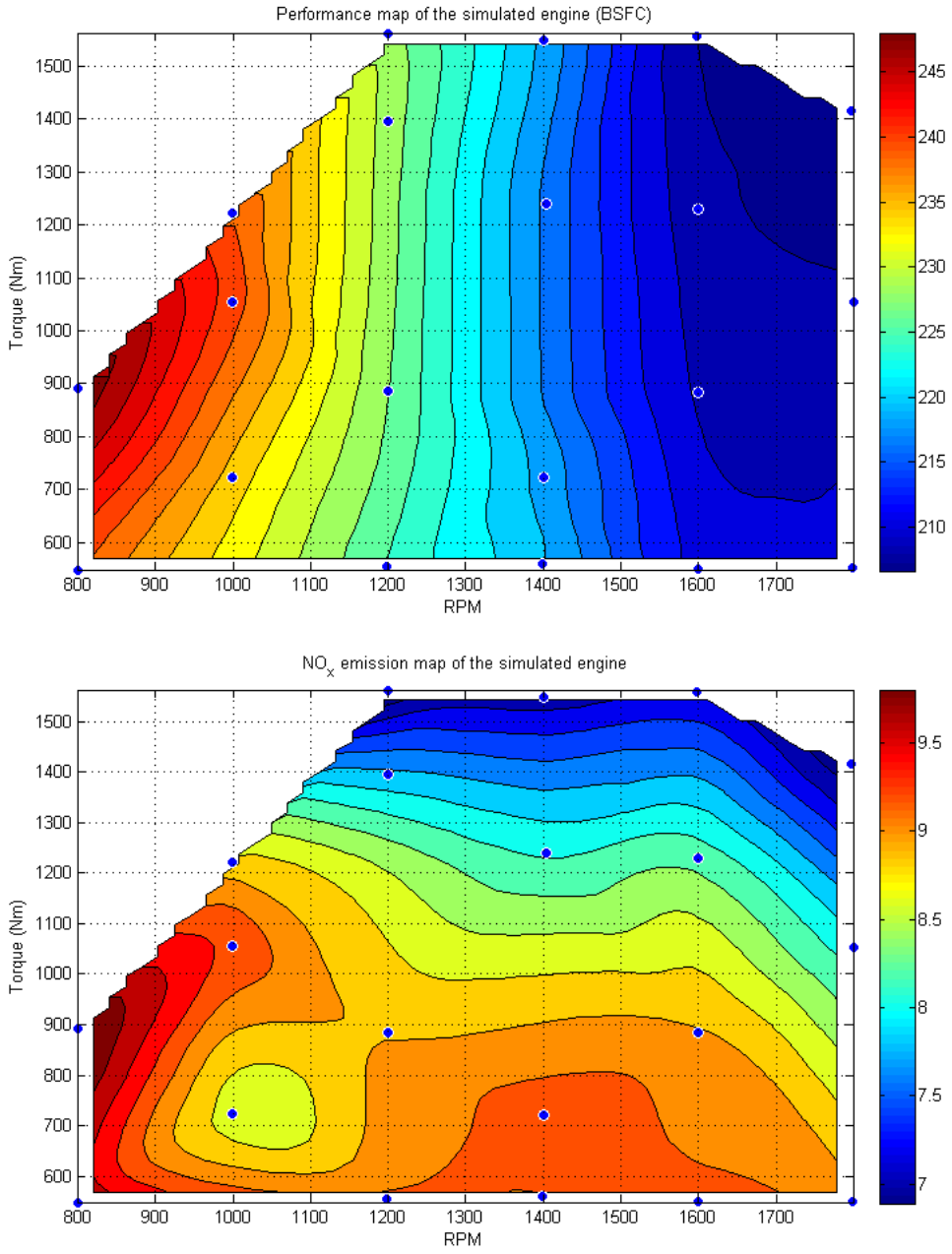

Figure 5.5: Performance and emission map of the simulated engine

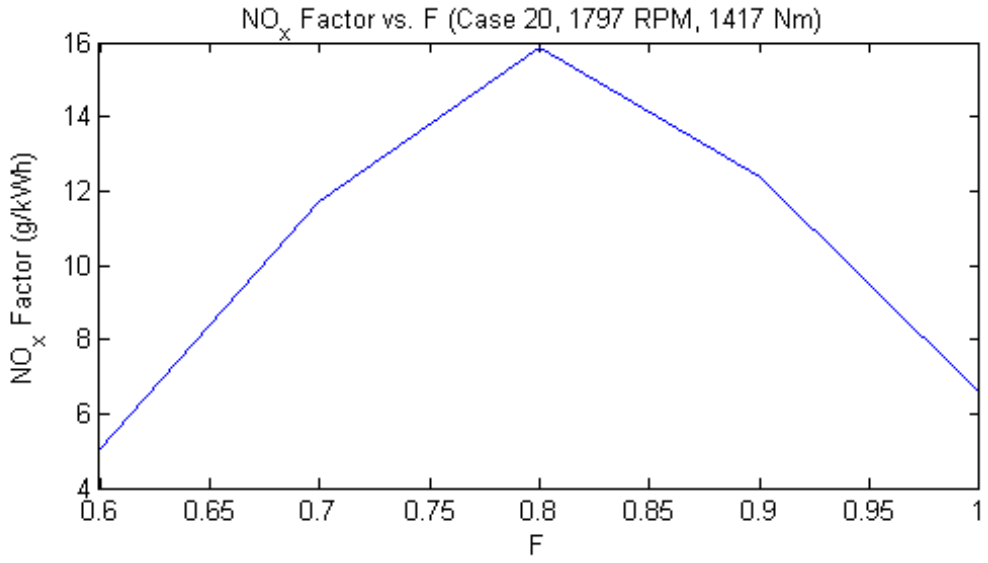

Figure 5.6: NO_x factor for different F_b

model or simply applying the effective mean value of it. This mean value would be in the range between the global F and 1. In the thesis, the affect of the different effective mean value of F was investigated. Case 20 (1797RPM, 1417Nm) from the simulation from the table 5.5 was taken for this sensitivity analysis.

The result is shown in the figure 5.6. It is found that the formation of NO_x both depends on the temperature and the concentration of the gas species involved in the Zeldovich mechanism. The figure 5.7 and figure 5.8 shows the concentration of the gas in the cylinder during the combustion. As F increases, the temperature of the gas increases because the total mass of the zone decreases proportionally to F causing the rate of formation to increase. However, as F increases, the concentration of main reactants such as N_2 and O_2 decreases resulting in decrease in the rate of formation. The combination of both results the figure 5.6. Tuning F_b to match the measurement should be manually done for each case so far in the thesis. Thus, the model is not predictive. This may be improved by correlating the physical parameters to the temporary F_b.

Another parameter is the mixing parameters which specifies the mass of the burned gas transfered to the unburned zone. The simulation case 1 (799 RPM, 549 Nm) was selected for the sensitivity analysis. There are two parameters defining the mixing function given in 4.9 : the crank angle at the start of the mixing (φ_{start} and the mixing duration $\Delta\varphi_{\text{mix}}$. F_b is set to be 1 in this analysis. The result is shown in the figure 5.9

As the both parameters increase, formation of NO_x increases. The Formation of NO_x is most vigorous in the beginning of the combustion as the gas is hottest. As the mixing duration is shortened, the more mass is transferred from the burned zone and reduces the total mass of NO_x formed. In contrast, as the start of mixing is delayed, the more burned gas remains in the burned zone and increases the formation of NO_x. This can be

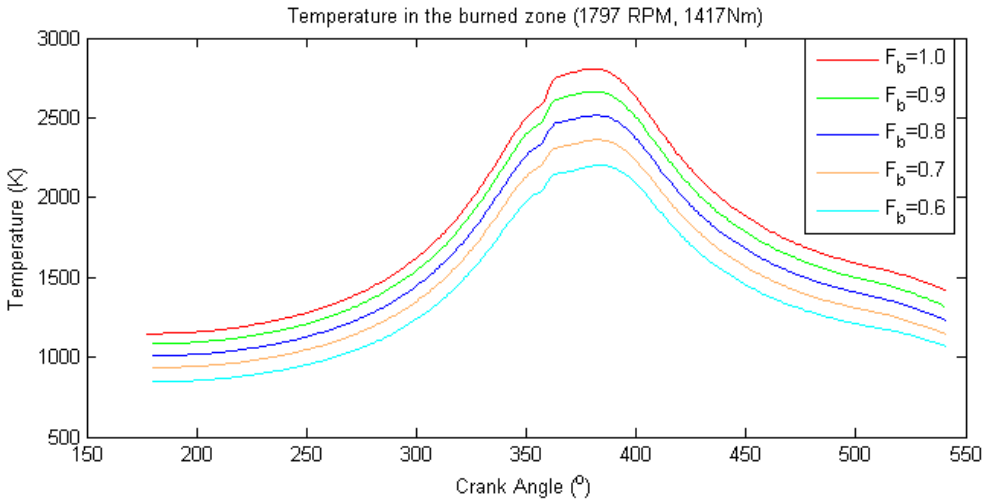

Figure 5.7: Temperature of the burned zone during combustion

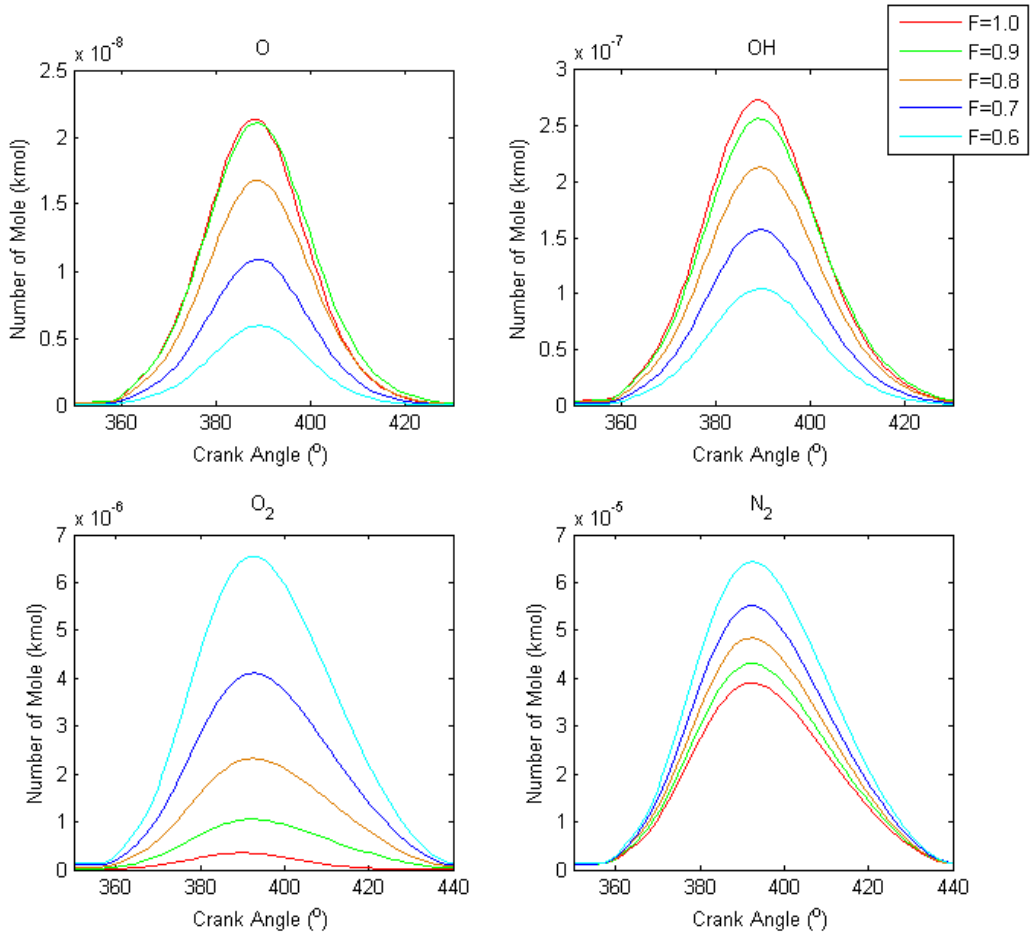

Figure 5.8: Concentration of the gas species during combustion

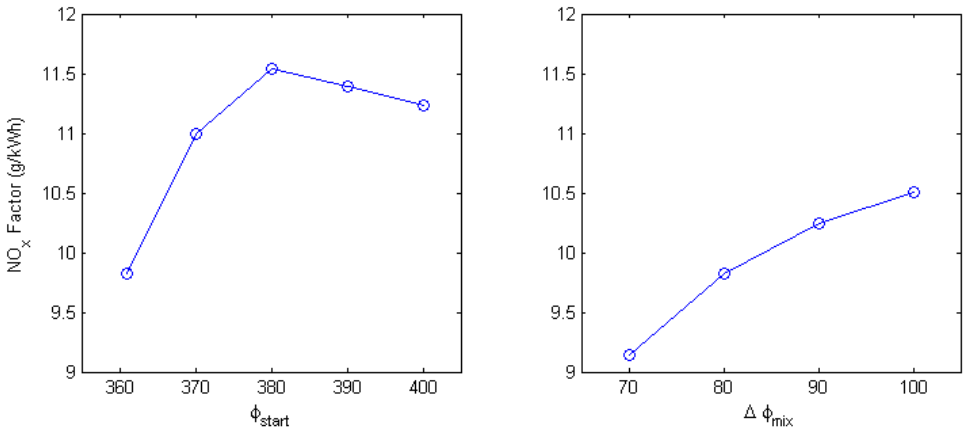

Figure 5.9: NO_x factor for different mixing parameters

understood based on the assumption of the model. However, it is not physically inspiring because the mass is transferred to the burned zone in the actual process and affects the temperature and the composition as seen in the previous sensitivity analysis. The mixing scheme used in the thesis was meant for the simplification of the model but reformulation may be required to reflect the physical process better.

Chapter 6

Conclusion

In the thesis, a overall process of building the dynamic mathmatical model of the diesel engine was reviewed and implemented. It covers most of the building blocks for the overall engine system from the thermodynamic calculation to the calculation of states of the components of the diesel engine. A majority of the effort is given to the improvement of the model in terms of computational efficiency and it was mainly achieved by implementing Grill's method for the calculation of the equilibrium composition of the combustion gas. The bond graph model based on the multi-component of gas species in the combustion gases was successfully constructed and it founded a ground for adaptation of the emission reduction strategy such as exhaust gas recirculation. The overall model was built with component libraries which can be reused in the future project. Full description of the components libraries are given in the chapter 3 so that potential users may have the easy access to the model when it is used.

Also the emission from the diesel engine was reviewed and the formation of NO_{x} was implemented as a mathmatical model and coupled with the dynamic engine model together with the two-zone model approach. The calculation of the two-zone model in the absence of the pressure profile was achieved with an effective method so that calculation time has not increased significantly from the single zone model as described in the chapter 4.

The simulation results of the model was compared with the test results in the laboratory to validate the model. Even though the accuracy of the model was not good enough to the expectation, it was capable to capture the trend of the performance and the emission in various operating points under steady-state conditions. The sensitivity analysis of prediction of NO_{x} formation was performed to see how the related parameters can be tuned to match the prediction to the measurement. Explanation of underlying physical process of this analysis was also presented to provide the background understanding of the tuning process.

However, the model misses certain parts to be used in the transient conditions. Firstly, the combustion model is purely empirical model requiring the static ROHR data from the laboratory analysis. This is the major part that made the model diagnostic, not predictive in

case of the rapid change in the cylinder conditions. Also the mixing phenomena between the burned and unburned zone was modeled with an ad hoc mixing function and actual physical process is missing in the model. Two-zone approach for the prediction of correct temperature may not be good enough for the diesel combustion where the continuous turbulent mixing process of the fuel and air governs the combustion process. In addition, the turbocharger could not be properly modeled in the process of adaptation of the real engine due to the lack of information, i.e. turbocharger performance map. This leads to the model to lack the one of the most critical part in regard to the transient performance.

In this regards, the following works are recommended to improve the model in the future:

- The current ROHR analysis used in the laboratory should be investigated and improved by using model based analysis. The thermal cycle model from this thesis may be used for such purpose.
- Predictive combustion model should be developed by understanding the physical process of diesel combustion better. This will include the understanding of the spray formation and mass transfer in the cylinder and mixing process in deeper depth and draw a model containing such characteristics of the combustion. This will also bring about implementing physically inspired mixing process of the zones.
- Multi-zone approach where the number of zones are greater than 3 should be implemented for better prediction with the diesel combustion. This may be easily extended from the current two-zone model.
- Heat transfer plays a significant role in the transient load and, therefore, more predictive model for it should be developed.
- A method to predict the performance of the turbocharger in the case of absence of the performance map should be developed. This may be done by using the available performance map and adjusting it to match the performance of the engine measured in the laboratory. Or a simple and effective experimental setup to evaluate the performance of the turbocharger may be developed.
- A laboratory setup for the measurements of performance and emission under the transient load should be developed to verify the transient model. Firstly, the important parameters for the transient operation the method to measure them should be investigated and implemented.

References

[1] A. Albrecht, O. Grondin, F. Le Berr, and G. Le Solliec. Towards a stronger simulation support for engine control design: a methodological point of view. *Oil and Gas Science and Technology - Rev. IFP*, 62(4):437–456, 2007.

[2] Dennis N. Assanis, Zoran S. Filipi, Scott B. Fiveland, and Michalis Syrimis. A methodology for cycle-by-cycle transient heat release analysis in a turbocharged direct injection diesel engine. *SAE Technical Paper*, 2000-01-1185, 2000.

[3] Charles E. Baukal. *Industrial combustion pollution and control*. M. Dekker, New York, 2004.

[4] C.T. Bowman. Kinetics of pollutant formation and destruction in combustion. *Prog. Energy Combust. Sci.,*, 1:13, 1975.

[5] A. Burcat and B. Ruscic. *Third millenium ideal gas and condensed phase thermochemical database for combustion with updates from active thermochemical tables*. Argonne National Laboratory Argonne, IL, 2005.

[6] M. W. Chase. *NIST-JANAF thermochemical tables*, volume no. 9 of *Journal of physical and chemical reference data, Monograph*. American Chemical Society and the American Institute of Physics for the National Institute of Standards and Technology, Washington, D.C., 1998.

[7] M.W. Chase, Jr. C.A. Davies, J.R. Downey, Jr. D.J. Frurip, R.A. McDonald, and A.N. Syverud. Nist-janaf thermochemical tables @ONLINE, July 12 2012.

[8] J. S. Coursey, D. J. Schwab, J. J. Tsai, and R. A. Dragoset. Atomic weights and isotopic compositions with relative atomic masses@ONLINE, April 4 2012.

[9] J. E. et al. Dec. Diesel combustion: An integrated view combining laser diagnostics, chemical kinetics, and empirical validation. 1999.

[10] DieselNet. International: Imo marine engine regulations@ONLINE, September 26 2011.

[11] R. Egnell. Combustion diagnostics by means of multizone heat release analysis and no calculation. 1998.

[12] C A Finol and K Robinson. Thermal modelling of modern engines: A review of empirical correlations to estimate the in-cylinder heat transfer coefficient. *Proceedings of the Institution of Mechanical Engineers, Part D: Journal of Automobile Engineering*, 220(12):1765–1781, 2006.

[13] L. Goldsworthy. Exhaust emissions from ship engines - significance, regulations, control technologies. *Australian and New Zealand Maritime Law Journal*, 24(No.1):30, 2010.

[14] M. Grill, A. Schmid, M. Chiodi, H. J. Berner, and M. Bargende. Calculating the properties of user-defined working fluids for real working-process simulations. SAE International, April 16-19, 2007 2007.

[15] J.B. Heywood. *Internal Combustion Engine Fundamentals*. McGraw Hill, 1988.

[16] IMO. Regulations for the prevention of air pollution from ships, 2010.

[17] Dean Karnopp. State variables and pseudo bond graphs for compressible thermofluid systems. *National Conference Publication - Institution of Engineers, Australia*, pages 861–865, 1979.

[18] Dean Karnopp, Donald L. Margolis, and Ronald C. Rosenberg. *System dynamics*. Wiley, Hoboken, 2012. 5th ed.

[19] D.I. Lee. Combustion simulations of direct injection diesel engine having 'm' type combustion chamber. Technical report.

[20] C. Olikara and G. Borman. A computer program for calculating properties of equilibrium combustion products with some applications to i.c. engines. *SAE Technical Paper 750468*, 1975.

[21] E. Pedersen. Modelling thermodynamic systems with changing gas mixtures. In J. J. Granda and F. E. Cellier, editors, *Proceedings of the 1999 International Conference on Bond Graph Modeling and Simulation*, volume 31 of *Simulation Series*, pages 189–195. Soc Computer Simulation.

[22] E. Pedersen and H. Engja. A bond graph model library for modelling diesel engine transient performance. In *ISME Tokyo 2000*, volume 2 of *Proc. of the Sixth International Symposium on Marine Engineering*, pages 447–455.

[23] Gamma Technology. Gt-suite engine performance application manual ver 7.1. 2010.

[24] Harald Valland. Dynamic cylinder pressure and rate of heat release. Technical report, Department of Marine Technology, NTNU, 2010.

[25] Harald Valland. Computation of thermodynamic properties of combustion products and fuel-air processes. Technical report, Department of Marine Technology, NTNU, 2012.

[26] S. Verhelst and C. G. W. Sheppard. Multi-zone thermodynamic modelling of spark-ignition engine combustion âĂŞ an overview. *Energy Conversion and Management*, 50(5):1326–1335, 2009.

[27] A. Westlund. *Measuring and Predicting Transient Diesel Engine Emissions*. Licentiate thesis, 2009.

[28] A Westlund. *Simplified Models for Emission Formation in Diesel Engines during Transient Operation*. Academic, 2011.

[29] Chris Whall, David Cooper, Karen Archer, Layla Twigger, Neil Thurston, David Ockwell, Alun McIntyre, and Alistair Ritchie. Quantification of emissions from ships associated with ship movements between ports in the european community. Technical report, European Commission, 2002.

[30] N. D. Whitehouse and R. Way. Rate of heat release in diesel engines and its correlation with fuel injection data. *Proceedings of the Institution of Mechanical Engineers, Conference Proceedings*, 184(10):17–27, 1969.

[31] J. Xi and BJ Zhong. Review: soot in diesel combustion systems. *Chemical Engineering Technology*, 29(6), 2006.

[32] F. Zacharias. Analytical representation of the thermodynamic properties of combustion gases. *SAE Technical Paper*, 670930, 1967.